รายงานวิจัยฉบับสมบูรณ์

โครงการการศึกษาและตรวจสอบความแตกต่างในกระบวนการจับกินเชื้อแบคทีเรียที่มีสายพันธุ์แตกต่างกันที่ก่อให้เกิดโรควัณโรคของเซลล์เจ้าบ้าน

โดย ผศ.ดร.มาริสา พลพวก

มิถุนายน 2558

สัญญาเลขที่ MRG5480181

รายงานวิจัยฉบับสมบูรณ์

โครงการการศึกษาและตรวจสอบความแตกต่างในกระบวนการจับกินเชื้อแบคทีเรียที่มีสายพันธุ์แตกต่างกันที่ก่อให้เกิดโรควัณโรคของเซลล์เจ้าบ้าน

ผศ.ดร.มาริสา พลพวก
ภาควิชาจุลชีววิทยา คณะวิทยาศาสตร์ มหาวิทยาลัยมหิดล

สนับสนุนโดยสำนักงานกองทุนสนับสนุนการวิจัย

Abstract

Project Code: MRG5480181

Project Title: Variation in autophagic control to different genotypic families of *Mycobacterium tuberculosis* in host macrophages.

Investigator: Assist. Prof. Marisa Ponpuak, Mahidol University

E-mail Address: marisa.pon@mahidol.ac.th

Project Period: 2 years with extension

Project Aims: As autophagy has been demonstrated as a key pathway in innate immune defense to restrict *Mycobacterium tuberculosis* growth inside host macrophages. Induction of autophagy has been shown to promote mycobacterial phagosome acidification and acquisition of lysosomal hydrolases resulting in the elimination of intracellular *M. tuberculosis* reference strains such as H37Rv and the vaccine strain BCG. However, the role of autophagy against *M. tuberculosis* clinical strains such as those belong to the Beijing genotype found to be hyper-virulent as demonstrated by their higher ability to survive in host macrophages, to cause higher bacterial load and mortality in animal models, and to cause heavy AFB smear-positive sputum in patients has never been examined. Therefore, we sought out to determine whether there is an alteration in autophagic control against strains of the Beijing genotype which may explain the hyper-virulence possessed by this family.

Methods: Here, we obtained *M. tuberculosis* clinical strains belonging to the Beijing genotype associated with hyper-virulence prevalent in Thailand and East Asia regions and the East African Indian genotype associated with low-virulence. We then compared the autophagic restriction by host macrophages against these strains comparing to that of the laboratory *M. tuberculosis* reference strain H37Rv. We then characterized the underlying autophagy resistant mechanism utilized by the Beijing strains.

Results: Our results showed that the Beijing strains display greater ability to resist autophagic killing as compared to that of the reference strain H37Rv and a strain belonging to the East African Indian genotype. In addition, we revealed a possible underlying mechanism in which the resistance of the Beijing strains to autophagic restriction is not simply achieved by blocking autophagy-mediated acidification of their phagosomes or by inhibiting the autophagic flux in host cells but achieved by preventing autophagolysosome biogenesis as demonstrated by their ability to inhibit the increased acquisition of cathepsin D, an enzyme of lysosomal acid hydrolases and a marker of lysosome, into mycobacterial compartments upon autophagy induction.

Conclusions: In this study, we discovered a previously unrecognized ability of the *M. tuberculosis* Beijing strains to evade host autophagy. In addition, we have characterized the associated underlying mechanism in which the Beijing strains can inhibit autophagolysosome biogenesis upon autophagy induction. Our work may have important implications for tuberculosis treatment especially in regions prevalent by the Beijing genotype.

Discussions and Future Directions: Our study showed that the *M. tuberculosis* Beijing strains possess the ability to resist autophagic elimination by host macrophages. Interestingly, *H. pylori* was also shown to evade autophagic killing by inhibiting autophagolysosome biogenesis in which the bacteria can do so through the use of the *H. pylori* vacuolating toxin (VacA). Whether *M. tuberculosis* Beijing strains possess similar or equivalent toxin/protein is not known. As a recent whole-genome sequencing of strains belonging to the *M. tuberculosis* Beijing family has been conducted, mining and comparing sequencing data between Beijing and non-Beijing strains may give insight into potential candidate genes that may play a role in the autophagic evasion. Their subsequent characterization will also provide a novel drug target. This is utmost important as it was recently reported that two of the first-line tuberculosis drugs, isoniazid and pyrazinamide, require autophagy pathway for their actions and thus the Beijing strains may have greater ability to resist these first-line tuberculosis treatment.

Keywords: Autophagy, Beijing strains, *M. tuberculosis*, Mycobacteria, Tuberculosis

บทคัดย่อ

รหัสโครงการ : MRG5480181

ชื่อโครงการ : การศึกษาและตรวจสอบความแตกต่างในกระบวนการจับกินเชื้อแบคทีเรียที่มีสายพันธุ์แตกต่างกัน ที่ก่อให้เกิดโรควัณโรคของเซลล์เจ้าบ้าน

ชื่อนักวิจัย : ผศ.ดร.มาริสา พลพวก มหาวิทยาลัยมหิดล

อีเมลล์: marisa.pon@mahidol.ac.th

ระยะเวลาโครงการ : 2 ปี และ ขยายเวลา

วัตถุประสงค์: เนื่องจากกระบวนการออโตฟาจีถูกค้นพบว่าเป็นกระบวนการทางภูมิคุ้มกันที่สำคัญของโฮสต์ที่ใช้ในการกำจัดเชื้อวัณโรค การกระตุ้นกระบวนการออโตฟาจีในเซลล์โฮสต์ก่อให้เกิดความเป็นกรดและการได้มาของไลโซโซมเอนไซม์ ในฟาโกโซมของเชื้อมัยโคแบคทีเรีย ซึ่งทำให้เชื้อถูกฆ่าตายในที่สุด แต่การศึกษาที่ผ่านมา ล้วนแต่ใช้มัยโคแบคทีเรียสายพันธุ์อ้างอิงเท่านั้น และยังไม่เคยมีการศึกษาถึงความสัมพันธ์ระหว่างกระบวนการออโตฟาจีต่อการฆ่าเชื้อมัยโคแบคทีเรียสายพันธุ์อื่น โดยเฉพาะสายพันธุ์ไบจิงที่ระบาดมากในไทยและภูมิภาคเอเชียตะวันออก ซึ่งมีความรุนแรงของเชื้อที่สูง สามารถที่จะทนต่อกลไกการกำจัดเชื้อของเซลล์โฮสต์ และ มีความรุนแรงที่จะก่อโรคในสัตว์ทดลองได้สูงกว่าสายพันธุ์อื่น ตลอดจนก่อให้เกิดจำนวนเชื้อในเสมหะคนไข้ที่มากกว่า ด้วยเหตุนี้ คณะผู้วิจัยในโครงการนี้จึงได้ศึกษาว่าเชื้อมัยโคแบคทีเรียสายพันธุ์ไบจิง ซึ่งเป็นสายพันธุ์ที่ก่อโรคได้รุนแรงกว่าสายพันธุ์อื่นนี้ มีความสามารถที่จะต้านทานกระบวนการฆ่าเชื้อออโตฟาจีได้หรือไม่

วิธีทดลอง: คณะผู้วิจัยได้นำเชื้อมัยโคแบคทีเรียสายพันธุ์ไบจิง และ สายพันธุ์อีสแอฟริกันอินเดียนซึ่งเป็นสายพันธุ์ที่มีความรุนแรงของเชื้อที่ต่ำ มาทำการทดลองเปรียบเทียบกับเชื้อมัยโคแบคทีเรียสายพันธุ์อ้างอิง ถึงความสามารถในการต้านทานกระบวนการฆ่าเชื้อออโตฟาจีในเซลล์มาโครฟาจ นอกจากนั้นคณะผู้วิจัยยังได้ทำการศึกษาเชิงลึกเพื่อหากลไกที่เชื้อมัยโคแบคทีเรียสายพันธุ์ไบจิง ใช้ในการต่อต้านกระบวนการฆ่าเชื้อออโตฟาจี

ผลการทดลอง: คณะผู้วิจัยค้นพบว่า เชื้อมัยโคแบคทีเรียสายพันธุ์ไบจิง ที่ระบาดมากในไทย สามารถที่จะต่อต้านกระบวนการฆ่าเชื้อออโตฟาจีของเซลล์โฮสต์ได้ ซึ่งกลไกที่สายพันธุ์ไบจิงใช้ในการต่อต้านกระบวนการฆ่าเชื้อออโตฟาจีคือการสกัดกั้นการรวมกันของไลโซโซมกับออโตฟาโกโซม ทำให้ไลโซ

โซมเอนไซม์ ไม่สามารถเข้าไปย่อยเชื้อมัยโคแบคทีเรียสายพันธุ์ไบจิงได้ สายพันธุ์ไบจิงจึงรอดพ้นจากกระบวนการฆ่าเชื้อออโตฟาจี

สรุปและวิจารณ์ผลการทดลอง: คณะผู้วิจัยได้ค้นพบว่าเชื้อมัยโคแบคทีเรียสายพันธุ์ไบจิงมีความสามารถในการต้านการฆ่าโดยกระบวนการออโตฟาจี นอกจากนี้คณะผู้วิจัยยังค้นพบเชิงลึกถึงกลไกที่ทำให้สายพันธุ์ไบจิงสามารถต่อต้านการฆ่าเชื้อโดยกระบวนการออโตฟาจีได้ ซึ่งองค์ความรู้ที่ได้มีความสำคัญต่อการรักษาผู้ที่ติดเชื้อวัณโรคสายพันธุ์ไบจิง ซึ่งเป็นสายพันธุ์ที่ระบาดมากในประเทศไทย โดยเฉพาะได้มีการเผยแพร่งานวิจัยเมื่อไม่นานมานี้ว่า กลไกการทำงานของยา Isoniazid (ไอโซไนอะซิด) และ Pyrazinamide (ไพราซินาไมด์) ซึ่งเป็น 2 ตัวยา ในยาอันดับแรก (First line) ที่ใช้ในการรักษาวัณโรคนั้น ขึ้นอยู่กับการทำงานของกระบวนการออโตฟาจี ดังนั้นถ้าสายพันธุ์ไบจิงสามารถสกัดกั้นกระบวนการออโตฟาจีได้ สายพันธุ์ไบจิงก็น่าที่จะต่อต้านการทำงานของยาทั้ง 2 ตัวนี้ได้ ซึ่งก็มีข้อมูลบ่งชี้ว่าสายพันธุ์ไบจิง มีความสามารถในการดื้อยามากกว่ามัยโคแบคทีเรียสายพันธุ์อื่น

ข้อเสนอแนะสำหรับงานวิจัยในอนาคต: จากการค้นพบของคณะผู้วิจัยในโครงการนี้ ว่าเชื้อมัยโคแบคทีเรียสายพันธุ์ไบจิงสามารถที่จะต่อต้านกระบวนการฆ่าเชื้อออโตฟาจีได้นั้น คณะผู้วิจัยขอเสนองานวิจัยในอนาคตเพื่อต่อยอดดังนี้ เนื่องจากได้มีการเผยแพร่ข้อมูลจีโนมของสายพันธุ์ไบจิงเมื่อไม่นานมานี้ ดังนั้นการเปรียบเทียบจีโนมของเชื้อมัยโคแบคทีเรียสายพันธุ์อื่นกับสายพันธุ์ไบจิง จะสามารถทำให้ทราบถึงจีนที่มีความแตกต่างกันระหว่างสายพันธุ์ ซึ่งก็น่าจะมีจีนที่เป็นตัวก่อให้เกิดความต้านทานของสายพันธุ์ไบจิงต่อกระบวนการฆ่าเชื้อออโตฟาจีอยู่ การศึกษาในเชิงลึกว่าจีนหรือโปรตีนตัวไหนมีความสำคัญต่อการต้านกระบวนการออโตฟาจีในสายพันธุ์ไบจิง จะทำให้เราค้นพบเป้าหมายของยาตัวใหม่เพื่อการพัฒนาต่อยอดต่อไป ซึ่งจะมีความสำคัญมากโดยเฉพาะถ้าสายพันธุ์ไบจิง มีความสามารถในการดื้อยา Isoniazid (ไอโซไนอะซิด) และ Pyrazinamide (ไพราซินาไมด) ที่มากกว่าสายพันธุ์อื่น

คำหลัก : ออโตฟาจี, สายพันธุ์ไบจิง, เชื้อวัณโรค, มัยโคแบคทีเรีย, วัณโรค

Introduction

Autophagy (macroautophagy) is an evolutionary conserved cellular homeostatic process for qualitative and quantitative control of cytoplasmic biomass by removing long-lived proteins, cytosolic toxic aggregates, and defunct organelles [1-4]. In addition, autophagy has been increasingly appreciated for its role as a primordial form of cellular innate immunity against invading pathogens [1, 2, 5]. Autophagy can be initiated when cells encounter stresses such as nutritional and immune insults resulted from i.e. starvation, change in the level of immune mediators, and the presence of structural components of microbes and their products [1-4]. Upon responding to an upstream stress signal, Atg proteins are organized into complexes and collaborate to generate a specialized double-membrane autophagosome [3, 4]. These complexes include (i) the protein kinase complexes ULK1 and AMPK to activate Beclin-1, (ii) the class III phosphatidylinositol 3-kinase complexes VPS34 and Beclin-1 to generate PI3P for recruitment of downstream effectors, and (iii) the Atg5/Atg12/Atg16 conjugation complexes that act as an E3 ligase for LC3 lipidation required for elongation and closure of autophagosome [1, 3, 4]. Cytosolic substrates can be either non-selectively engulfed into autophagosome or alternatively selectively recognized and collected into autophagosome by different types of cargo receptors/adaptors [6-8]. Upon closure, autophagosome fuses with lysosome resulting in the delivery of lysosomal acid hydrolases which then degrade the enclosed contents. The resulting digested molecules such as amino acids are then released and recycled back into the cytoplasm [1, 3, 4].

Autophagy has been shown to play important roles in cell autonomous defense against intracellular bacteria, parasites, and viruses [1, 9-11]. In the context of *M. tuberculosis* infection,

induction of autophagy by starvation or other autophagy inducers results in the killing of the tubercle bacilli by overcoming the block in phagolysosomal biogenesis as demonstrated by the acidification and acquisition of lysosomal hydrolases into compartments harboring the mycobacteria [12-17], even when they have survived in phagocytes by evading immunological mechanisms [18]. The proposed mechanistic details for autophagy-mediated mycobacterial elimination include (i) the direct engulfment of mycobacteria into autophagosomes and subsequent delivery to lysosomes for degradation and, (ii) the generation of killing peptides converted from innocuous cytosolic substrates engulfed and partially digested in autophagosomes/autophagolysosomes and subsequent delivery of these killing peptides to mycobacteria via fusion of autophagic vacuoles with mycobacterial phagosomes [19]. The importance of autophagy pathway in antimycobacterial defense was substantiated by the findings that mice deficient in Atg5 expression in macrophages display a high susceptibility to mycobacterial infection [20, 21]. Furthermore, autophagy was shown to be required for effective antimycobacterial drug action of isoniazid and pyrazinamide, two of the first-line tuberculosis drugs, in an animal model of tuberculosis [22]. In addition, a genome-wide siRNA screen to identify host factors that regulate mycobacterial load in macrophages infected with different strains of *M. tuberculosis* revealed autophagy as the main host cell functional module that is perturbed by the pathogen [23]. Moreover, polymorphisms in the human autophagy and autophagy-related genes *IRGM* and *P2X7*, are found to be associated with susceptibility to tuberculosis [24-28]. All of these data underscore the importance of autophagic process in mycobacterial control and indicate that the magnitude of autophagic elimination of mycobacteria may be the key determinant of their virulence and pathogenesis.

M. tuberculosis can be subdivided into several distinct genotypic families/lineages [29], among which the Beijing genotype, regarded as the highly successful lineage of *M. tuberculosis* often associated with multidrug resistance, was shown to be globally distributed representing around 50% of strains in East Asia and more than 13% of strains worldwide [30]. The success of the Beijing family was thought to stem from its associated hyper-virulent phenotypes as demonstrated by their higher ability to survive in host macrophages, to cause higher bacterial load and mortality in animal models, and to cause heavy AFB smear-positive sputum in patients [31-36]. However, the mechanism attributing to the greater ability of *M. tuberculosis* Beijing genotype to survive in host cells remains unclear. As autophagy has been shown to be important for controlling *M. tuberculosis* growth inside host cells but the characterization of this pathway has been conducted using *M. tuberculosis* laboratory reference strains such as H37Rv and the vaccine strain BCG [12-17, 37] but not with the clinical strains such as those belong to the Beijing genotype, we set out to determine whether there is an alteration in autophagic control against strains of the Beijing genotype which may explain the hyper-virulence possessed by this family. Our results showed that the Beijing strains display greater ability to resist autophagic killing as compared to that of the reference strain H37Rv and a strain belonging to the East African Indian (EAI) genotype [29, 38]. In addition, we revealed a possible underlying mechanism in which the resistance of the Beijing strains to autophagic restriction is not simply achieved by blocking autophagy-mediated acidification of their phagosomes or by inhibiting the autophagic flux in host cells but achieved by preventing autophagolysosome biogenesis as demonstrated by their ability to inhibit the increased acquisition of cathepsin D, an enzyme of lysosomal acid hydrolases and a marker of lysosome, into mycobacterial compartments upon autophagy induction.

Materials and Methods

Cell and bacterial culture

Mouse macrophage RAW 264.7 cells (ATCC) were maintained in DMEM (Hyclone), 10% FBS (Hyclone), and 4 mM *L*-glutamine (Hyclone) (full media). Earle's Balanced Salt Solution (EBSS) (Sigma) (starve media) was used to induce autophagy. Cells were cultured at 37^{o}C and 5% CO_2. *M. tuberculosis* reference strain H37Rv and the previously described *M. tuberculosis* EAI and Beijing strains [39, 40] were cultured in Middlebrook 7H9 broth supplemented with 0.05% Tween 80, 0.2% glycerol, and 10% oleic acid, albumin, dextrose, and catalase (OADC; BD Biosciences) at 37^{o}C and homogenized to generate single-cell suspension. For infection experiments, number of bacteria was adjusted to 3 x 10^6 colony forming unit (CFU) per 1 mL (CFU/mL) in complete DMEM by measuring the OD at 600 nm. CFU was calculated from the precalibrated standard curve. For bacterial survival assays, bacilli were plated onto Middlebrook 7H11 agar supplemented with 0.05% Tween 80, 0.2% glycerol, and 10% OADC (BD Biosciences) and grown at 37^{o}C.

Fluorescent dye, antibodies, DNA construct, and siRNAs

LysoTracker Red (Invitrogen) was used at 1:4000. For immunofluorescence assays, monoclonal antibody against Cathepsin D (R&D Systems) was used at 1:200. For immunoblotting, polyclonal antibodies against Beclin-1 (Santa Cruz) were used at 1:500 and monoclonal antibody against Actin (Abcam) was used at 1:2000. Plasmid construct used in this study was previously described [41]. All siRNAs used in this study were from Dharmacon.

Macrophage transfection

RAW264.7 cells were transfected with 5 μg of cDNAs or 1.5 μg of siRNAs as previously described [42]. In brief, 10-15 × 10^6 cells were resuspended in 100 μL of Nucleofector solution kit V (Amaxa). Plasmid DNAs or siRNAs were then added to the cell suspension and cells were nucleoporated using Amaxa Nucleofector apparatus with program D-032. Cells were then transferred into a new flask containing 12 mL complete media and incubated at 37 °C followed by a medium change at 6 hr of incubation. Cells were then used in assays after 24 hr of transfection with plasmid DNAs or 48 hr of transfection with siRNAs.

Macrophage infection, mycobacterial survival, and immunofluorescence microscopy

Infection of RAW264.7 cells with mycobacteria and quantification of mycobacterial survival after autophagy induction were carried out as previously described [15]. In brief, 3 × 10^5 cells of RAW264.7 macrophages were plated onto each well of 12-well plates 12 hr before infections. Cells were then infected with single cell suspension of mycobacteria in complete media at MOI of 10:1 for 1 hr. Cells were then washed three times with PBS to remove uninternalized mycobacteria and autophagy was then induced by treatment with starvation media for 4 hr. Cells were then lyzed and survival of bacteria was determined by plating for CFU. For immunofluorescence microscopy, 3 × 10^5 cells of Raw264.7 macrophages were plated onto coverslips in 12-well plates 12 hr before infections. Cells were then infected with 3 × 10^6 Alexa 488- or Alexa 405-labeled mycobacteria per well in complete media at 37^{o}C for 15 min, washed three times in PBS, and chased for 1 hr in complete media as previously

described [42]. Cells were then washed three times with PBS and autophagy was then induced by treatment with starvation media for 2 hr. Cells were then fixed with 4% paraformaldehyde/PBS for 15 min followed by permeabilization with 0.1% Triton X-100/PBS for 5 min. Coverslips were then blocked in PBS containing 3% BSA and then stained with primary antibodies according to manufacturer's recommendation. Cells were washed three times with PBS and then incubated with appropriate secondary antibodies (Invitrogen) for 1 hr at room temperature. Coverslips were then mounted using ProLong Gold Antifade Mountant (Invitrogen) and analyzed by confocal microscopy using the Zeiss LSM-700 Laser Scanning Microscope. For LysoTracker Red staining, cells were prestained in complete media containing LysoTracker Red for 2 hr at 37^{o}C before infections. Subsequent steps were carried out as described above but in the presence of LysoTracker Red until the cells were fixed. For analysis of RFP-GFP-LC3 transfected cells, cells were fixed and mounted as described above. The numbers of $RFP^{+}GFP^{+}$-LC3 puncta (autophagosomes) and $RFP^{+}GFP^{-}$-LC3 puncta (autolysosomes) were determined in cells that contain mycobacteria in infection conditions and compared to those of the uninfected control. At least 50 phagosomes per experimental condition in three independent experiments were quantified. For quantification, % mycobacteria-marker colocalization was fraction of total mycobacterial phagosomes examined counted as positive when one or more puncta were observed on or in contact with the mycobacterial phagosomes.

Immunoblotting

Cells were lysed in lysis buffer containing 20 mM Tris, 100 mM NaCl, and 1% NP-40. Cell lysates were then separated by 10% SDS-PAGE and proteins were transferred onto a

nitrocellulose membrane (Amersham Biosciences). Membranes were then blocked with 5% blocking solution (Roche Diagnostics) for 1 hr before incubation with appropriate primary antibodies at 4 ^{0}C overnight. Membranes were then washed three times with PBS containing 0.1% Tween 20 (0.1% PBST) followed by incubation with appropriate horseradish peroxidase-conjugated secondary antibody (Pierce) at room temperature for 1 hr. Membranes were then washed four times with 0.1% PBST followed by incubation with a chemiluminescence substrate (Roche Diagnostics) at room temperature for 2 min. Proteins were then detected by the enhanced chemiluminescence method.

Statistical analysis

Unless indicated otherwise, all experiments were independently conducted at least three times and data were pooled for presentation as means ± SEM. All data were analyzed with Prism software (GraphPad) using two-tailed unpaired Student's t tests. *p* values less than 0.05 were considered significant.

Results

The Beijing strains resist autophagic killing of mycobacteria by host cells

It has been well documented that induction of autophagy by starvation or other autophagy inducers in host macrophages results in the killing of mycobacteria reference strains such as *M. tuberculosis* H37Rv and the vaccine strain BCG [12, 14, 16, 43-45]. However, the autophagic killing capacity of host cells against *M. tuberculosis* clinical strains has not been characterized in detail. Therefore, we set out to evaluate whether different *M. tuberculosis* strains possess differential ability to alter host autophagic killing capacity. As a control, we observed no variation in the infection of RAW264.7 macrophages by different *M. tuberculosis* strains when compared to that of the reference strain H37Rv (Figure 1A). Our results showed that similarly to what has previously been observed [14, 15, 37, 46], induction of autophagy in RAW264.7 macrophages by starvation, a classical method to stimulate autophagy, for 4 hr can efficiently kill intracellular *M. tuberculosis* reference strain H37Rv by around 50% (Fig. 1B). In addition, autophagy induction in RAW264.7 macrophages is able to comparably restrict an *M. tuberculosis* strain belonging to the East African Indian genotype (EAI) (Fig. 1B). In contrast, autophagy induction by starvation cannot promote the elimination of the strains belonging to the Beijing genotype (BJY and BJN) (Fig. 1B). It should be noted that the viability of cells infected with different strains of *M. tuberculosis* is more than 90%. This is also consistent with previous reports using MOI of 10 of *M. tuberculosis* to infect RAW264.7 macrophages for short term incubation of 4 hr [13-15, 42, 46]. In addition, to confirm that the observed mycobacterial control is mediated through autophagy pathway, we targeted Beclin-1 by siRNAs in RAW264.7 macrophages and determined *M. tuberculosis* survival by CFU analysis. Beclin-1 targeting was

verified by immunoblotting (Fig. 1C). Depletion of Beclin-1 resulted in a decrease in starvation-induced elimination of *M. tuberculosis* reference strain H37Rv and the EAI strain confirming the role of autophagy in the killing of these mycobacteria (Fig. 1D). In addition, Beclin-1 knockdown does not alter the resistance of the Beijing strains to starvation-induced elimination (Fig. 1D). Altogether, these results indicated that autophagic control capacity of host cells against different strains of *M. tuberculosis* is not identical and unlike what has previously been observed with the laboratory reference strains which are effectively killed by autophagy induction, the Beijing strains are able to resist autophagic restriction by host cells. The observed alteration in autophagic killing capacity against different strains of *M. tuberculosis* was not related to the presence of intact *pks 15/1*, a gene encoding a polyketide synthase required for the synthesis of phenolic glycolipid, a known virulence factor of mycobacteria [47], as both the BJY (*pks 15/1* present) and BJN (*pks 15/1* absent) can similarly resist autophagic killing by host cells while the EAI (*pks 15/1* present) is efficiently eliminated by autophagy induction (Fig. 1B and D).

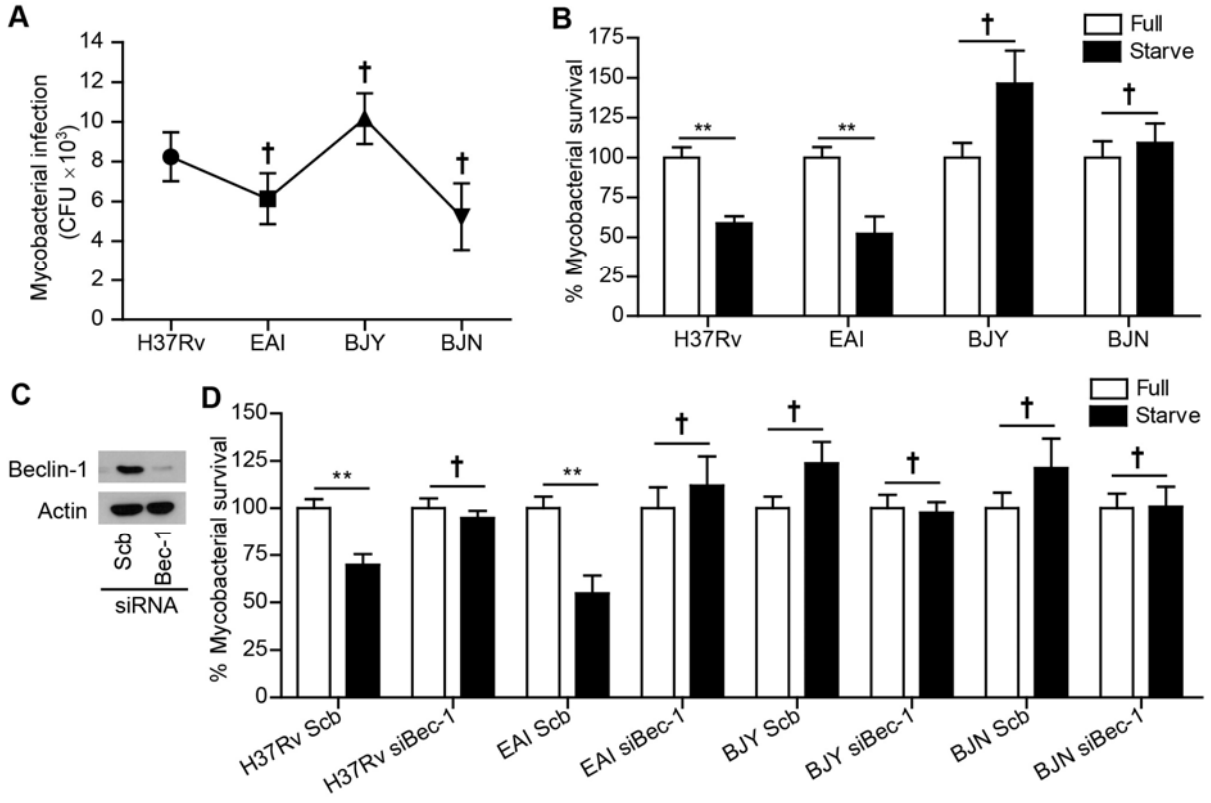

FIG 1. The Beijing strains of *M. tuberculosis* possess greater ability to resist starvation-induced autophagic killing in host macrophages. *(A)* RAW264.7 macrophages were infected with different *M. tuberculosis* strains at MOI of 10 for 1 hr. After washing the cells multiple times to remove uninternalized mycobacteria, cells were then lyzed and the number of mycobacteria that infected host cells was determined by plating for CFU. *(B)* RAW264.7 macrophages were infected with different *M. tuberculosis* strains at MOI of 10 for 1 hr. After washing the cells multiple times to remove uninternalized mycobacteria, cells were then induced to undergo autophagy by starvation for 4 hr. Cells were then harvested and the number of viable mycobacteria was determined by plating for CFU. *(C)* RAW264.7 macrophages were transfected with siRNAs against Beclin-1 or scramble (Scb) control. After 48 hr of transfection, RAW264.7 cells were collected and processed for immunoblot analysis to estimate the efficacy of Beclin-1 depletion. *(D)* RAW264.7 macrophages were transfected with siRNAs as in (C). At 48 hr after transfection, cells were infected with different strains of *M. tuberculosis* and then subjected to autophagy induction by starvation and CFU analysis as in (B). Data are means ± SEM from at least three independent experiments. $^{**}p < 0.01$ and $^{\dagger}p \geq 0.05$, all relative to the full control set to 100%. EAI, the East African Indian strain with intact *pks15/1*; BJY, the Beijing strain with intact *pks15/1*; BJN, the Beijing strain without intact *pks15/1*.

The Beijing strains avoid autophagic elimination not by inhibiting autophagy-mediated acidification of their phagosomes

As our results showed the greater ability of the Beijing strains to resist starvation-induced autophagic killing by host cells (Fig. 1), we set out to determine the molecular mechanism involved. We first examined whether the ability of the Beijing strains to evade autophagic restriction is due to their ability to inhibit autophagy-mediated acidification of their phagosomes. To determine this, we performed the confocal microscopy analysis for colocalization of mycobacteria with the LysoTracker Red (LTR) dye. The results showed that acidification of *M. tuberculosis* H37Rv phagosomes is enhanced upon autophagy induction by starvation as previously reported for reference strains [14, 15, 37, 46] (Fig. 2A and B). In addition, induction of autophagy by starvation increases the phagosomal acidification of the EAI strain albeit not statistically significant (Fig. 2A and B). Surprisingly, the acidification of the Beijing strains (BJY and BJN) also appeared to be substantially enhanced upon autophagy induction by starvation (Fig. 2A and B). Thus, these results indicated that even though the Beijing strains are able to inhibit the autophagic control by host cells, these bacteria do so not by simply inhibiting the autophagy-mediated acidification of their phagosomes but through another mechanism.

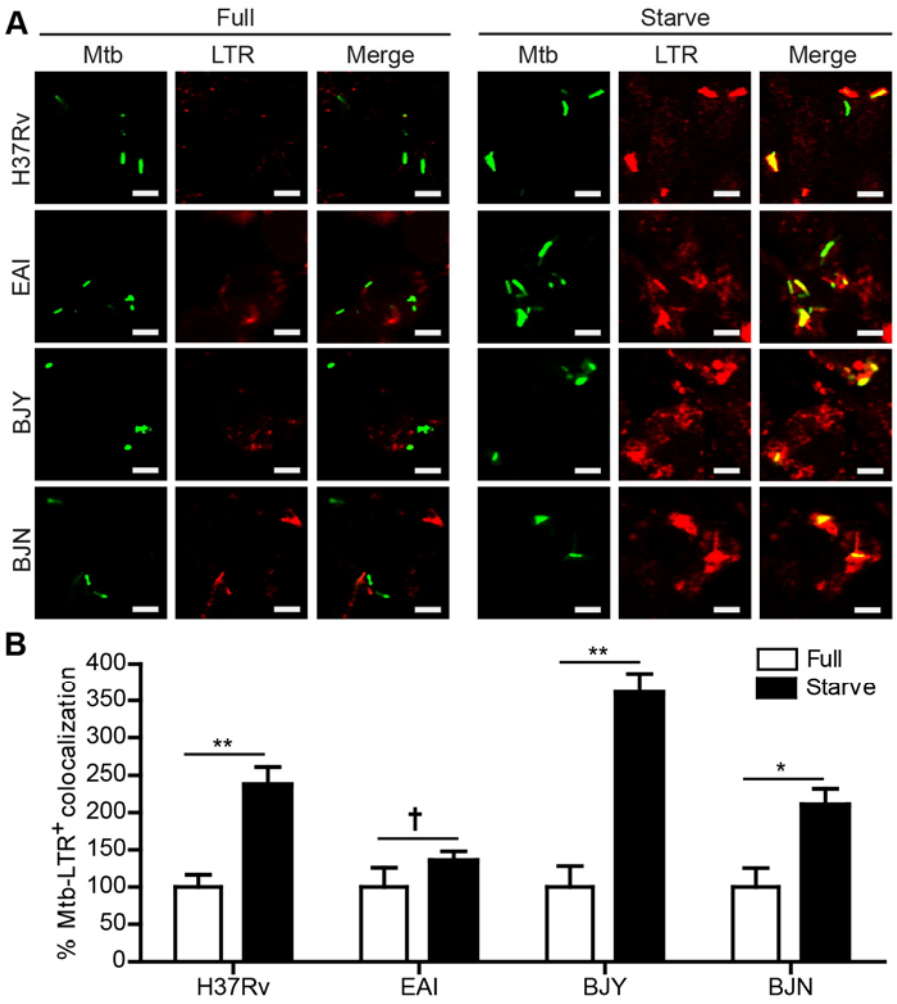

FIG 2. The Beijing strains inhibit starvation-induced autophagic killing not by blocking autophagy-mediated acidification of their phagosomes. (*A and B*) RAW264.7 macrophages were infected with Alexa-488-labeled mycobacteria at MOI of 10 for 15 min and subsequently chased for 1 hr in complete media. LysoTracker Red (LTR) dye was used to stain acidic compartments. Cells were then induced to undergo autophagy by starvation for 2 hr. Cells were then processed for confocal microscopy analysis for the colocalization of mycobacteria with LTR. Data are means ± SEM from at least three independent experiments. At least 50 phagosomes per condition per independent experiment were quantified. $^{**}p < 0.01$, $^{*}p < 0.05$, $^{\dagger}p \geq 0.05$, all relative to the full control set to 100%. EAI, the East African Indian strain with intact *pks15/1*; BJY, the Beijing strain with intact *pks15/1*; BJN, the Beijing strain without intact *pks15/1*.

The ability of the Beijing strains to escape autophagic restriction is not conferred by their capacity to block host autophagic flux

In addition to the direct killing mechanism mediated by autophagy whereby mycobacteria are captured into autophagosomes and then delivered into acidic lysosomes, autophagy can eliminate mycobacteria using another indirect mechanism whereby the innocuous cytosolic precursors are captured into autophagosomes which during the process of maturation into autolysosomes partially digest these precursors into killing peptides that are subsequently delivered to mycobacteria via fusion of the autophagosomes/autolysosomes with *M. tuberculosis* phagosomes [15]. Thus, the Beijing strains may evade autophagic killing through their differential ability to block the maturation of other population of cytosolic autophagosomes not containing mycobacteria. To test this possibility, autophagic flux in host cells was measured by fluorescent microscopy analysis for the conversion of $RFP^{+}GFP^{+}$-LC3 puncta (autophagosomes) to $RFP^{+}GFP^{-}$-LC3 puncta (autolysosomes). The results showed that the maturation of autophagosomes into autolysosomes is similarly inhibited in host macrophages infected with different *M. tuberculosis* strains when compared to that of the uninfected cells (Fig. 3A and B; white bar) as demonstrated by an increase in the number of $RFP^{+}GFP^{+}$-LC3 puncta in conjunction with no increase in the number of $RFP^{+}GFP^{-}$-LC3 puncta. The block in autophagic flux upon infection was further demonstrated when cells are subjected to autophagy induction by starvation (Fig. 3A and B; black bar). These results indicated that all of the tested strains and the reference *M. tuberculosis* H37Rv possess comparable ability to retard autophagic flux in host macrophages. Thus, the greater ability of the Beijing strains to resist

autophagic elimination cannot be attributed to their ability to inhibit autophagic maturation in host cells.

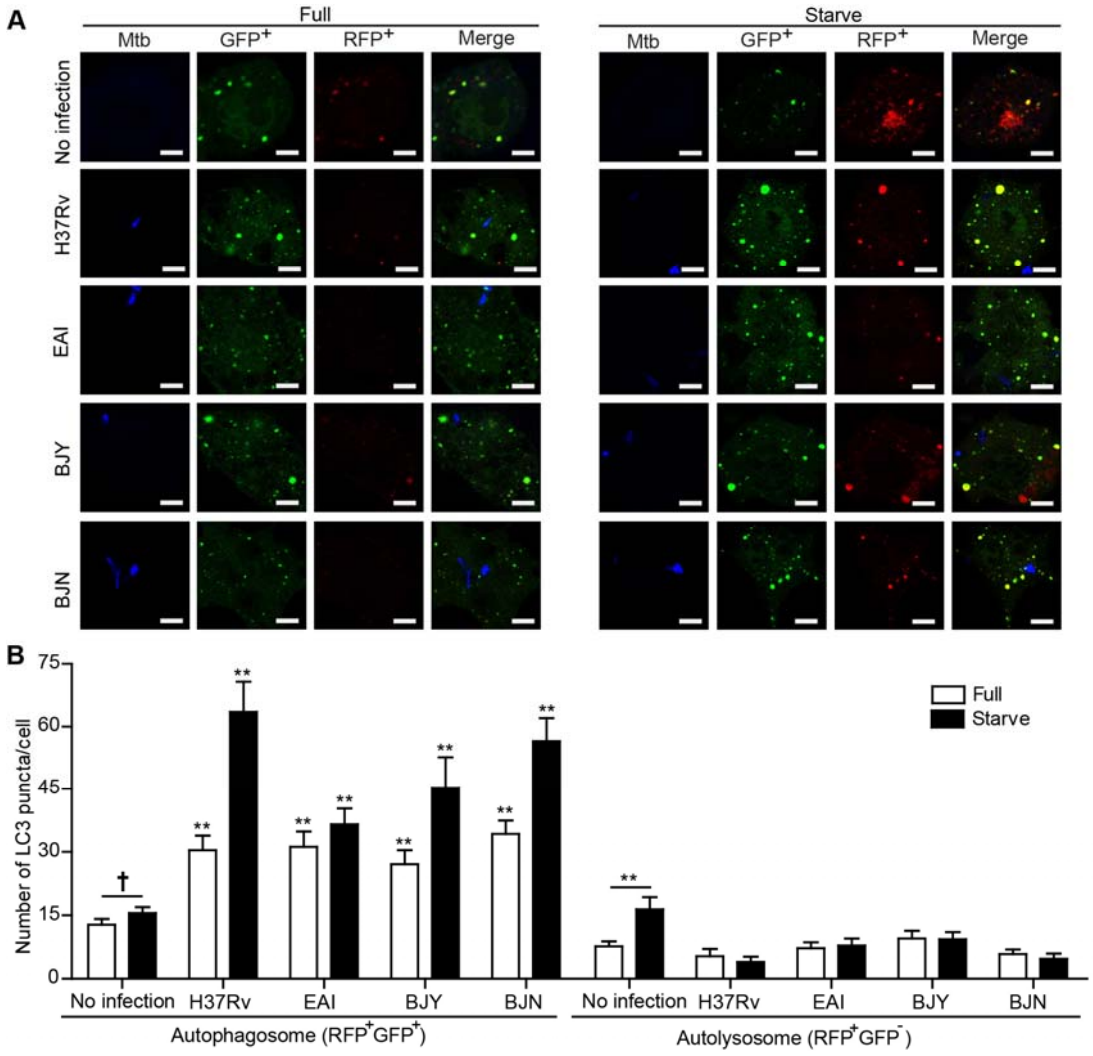

FIG 3. Evasion of starvation-induced autophagic elimination by the Beijing strains is not a result of their differential ability to block autophagic flux in host cells. (*A and B*) RAW264.7 cells were transfected with cDNAs encoding RFP-GFP-LC3. Transfected cells were then infected with Alexa-405-labeled mycobacteria for 15 min and subsequently chased for 1 hr in complete media. Cells were induced to undergo autophagy by starvation for 2 hr. Cells were then processed for confocal microscopy (Z-Stacks) analysis for the number of LC3 puncta per cell. Data are means ± SEM pooled from two independent experiments. The number of RFP^+GFP^+-LC3 (autophagosomes) and RFP^+GFP^--LC3 (autolysosomes) were quantified in Z-Stacks images of 30 cells per condition per independent experiment. $^{**}p < 0.01$ and $^{\dagger}p \geq 0.05$, all relative to full and starvation of uninfected control. EAI, the East African Indian strain with intact *pks15/1*; BJY, the Beijing strain with intact *pks15/1*; BJN, the Beijing strain without intact *pks15/1*.

The Beijing strains evade starvation-induced autophagic control by suppressing autophagolysosome biogenesis

Some bacteria such as *Helicobacter pylori* and *Mycobacterium marinum* were shown to reside in compartments that are acidified but lack a lysosomal marker cathepsin D in response to autophagy [48-50], indicating a defect in autophagolysosome biogenesis and thus sparing these bacteria from elimination. Therefore, we sought out to determine whether the Beijing strains may possess a similar ability. As a result, we analyzed the colocalization of different *M. tuberculosis* strains with LysoTracker Red and cathepsin D upon autophagy induction by starvation. Confirming our results in Fig. 2, acidification of phagosomes containing different *M. tuberculosis* strains are substantially augmented (LTR^+) upon treatment of cells with starvation (Fig. 4A and C). However, while there was an enhance in colocalization of the reference strain H37Rv and the EAI strain with cathepsin D ($CathD^+$) in response to autophagy induction by starvation (Fig. 4B and D), there was no increase in the colocalization of the Beijing strains (BJY and BJN) with cathepsin D ($CathD^+$) observed upon starvation treatment (Fig. 4B and D). These data indicated that even though their phagosomes are efficiently acidified, the Beijing strains possess an ability to suppress autophagolysosome biogenesis in response to autophagy induction. Note that the anti-cathepsin D antibody used can recognize both the immature and mature forms of cathepsin D and hence the lack of increased colocalization of the Beijing phagosomes with cathepsin D may include both the mature and immature forms. To further confirm autophagy involvement in this process, we depleted Beclin-1 in RAW264.7 macrophages and assess the colocalization of different mycobacteria with LysoTracker Red and cathepsin D. Our results showed that autophagy is required for the increased phagosome

acidification of all *M. tuberculosis* strains (LTR^+) upon starvation (Fig. 5A and B). However, while there was an enhance in the colocalization of *M. tuberculosis* reference strain H37Rv and the EAI strain with cathepsin D ($CathD^+$) upon starvation treatment and that this process depends on autophagy (Fig. 6A and B), there was no increase in $CathD^+$ colocalization with the Beijing strains upon starvation treatment even in autophagy efficient cells (Fig. 6A and B). Altogether, these data indicated that the Beijing strains possess greater ability to evade starvation-induced autophagic killing by their higher capacity to inhibit autophagolysosome biogenesis as demonstrated by their suppression of the enhanced acquisition of cathepsin D into their phagosomes upon autophagy induction in host cells.

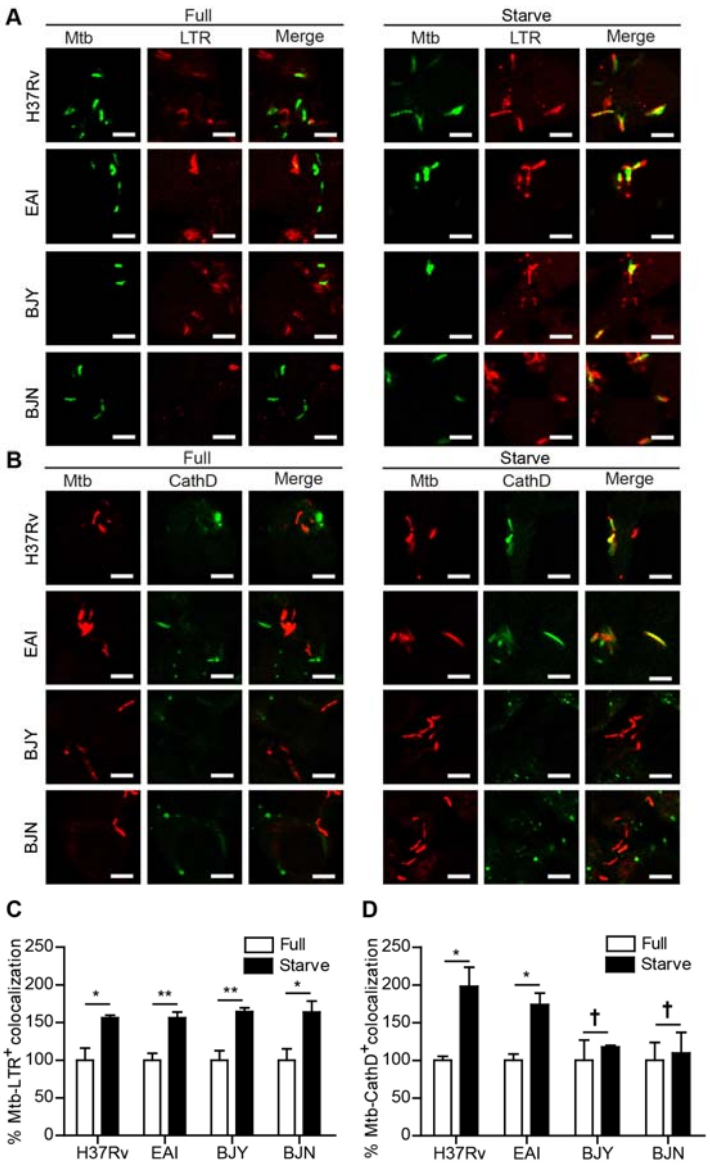

FIG 4. The Beijing strains escape from starvation-induced autophagic elimination by suppressing autophagolysosome biogenesis. (*A and C*) RAW264.7 cells were infected with Alexa 405-labeled mycobacteria (pseudocolored green) for 15 min and subsequently chased for 1 hr in complete media. Acidic compartments were stained with LysoTracker Red. Cells were then induced to undergo autophagy by starvation for 2 hr. Cells were then fixed and processed for confocal microscopy analysis. *(B and D)* RAW264.7 cells were infected with Alex 405-labeled mycobacteria (pseudocolored red) and processed as described above. Cells were then fixed and stained for cathepsin D. Data are means ± SEM from at least 3 independent experiments. At least 50 phagosomes per condition per independent experiment were quantified. $^{**}p < 0.01$, $^{*}p < 0.05$, $^{\dagger}p \geq 0.05$, all relative to the full control set to 100%. EAI, the East African Indian strain with intact *pks15/1*; BJY, the Beijing strain with intact *pks15/1*; BJN, the Beijing strain without intact *pks15/1*.

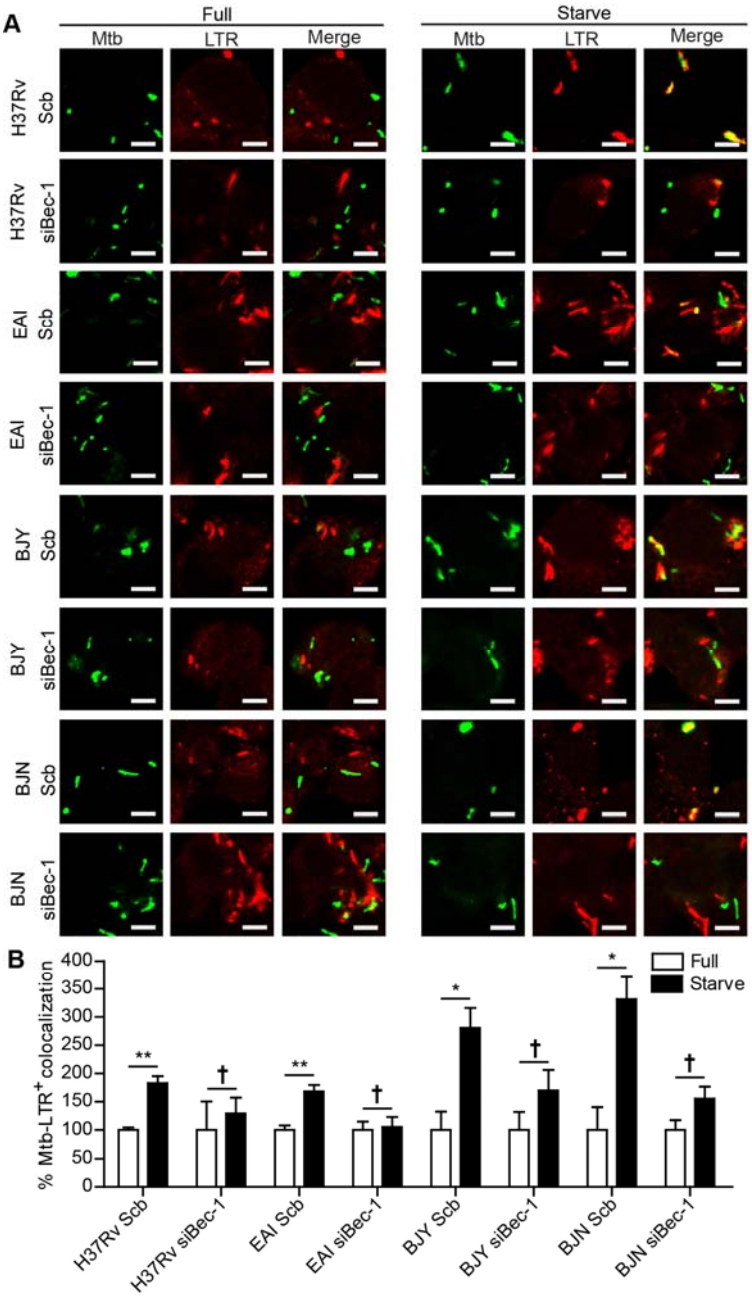

FIG 5. Autophagy is required for the starvation-enhanced acidification of the *M. tuberculosis* reference strain H37Rv and the EAI strain phagosomes. (*A-B*) RAW264.7 cells were transfected with siRNAs against Beclin-1 or scramble (Scb) control. After 48 hr of transfection, cells were infected with Alexa 405-labeled mycobacteria (pseudocolored green) and processed as in Fig. 4A and C. Data are means ± SEM from at least 3 independent experiments. At least 50 phagosomes per condition per independent experiment were quantified. $^{**}p < 0.01$, $^{*}p < 0.05$, and $^{\dagger}p \geq 0.05$, all relative to the full control set to 100%. EAI, the East African Indian strain with intact *pks15/1*; BJY, the Beijing strain with intact *pks15/1*; BJN, the Beijing strain without intact *pks15/1*.

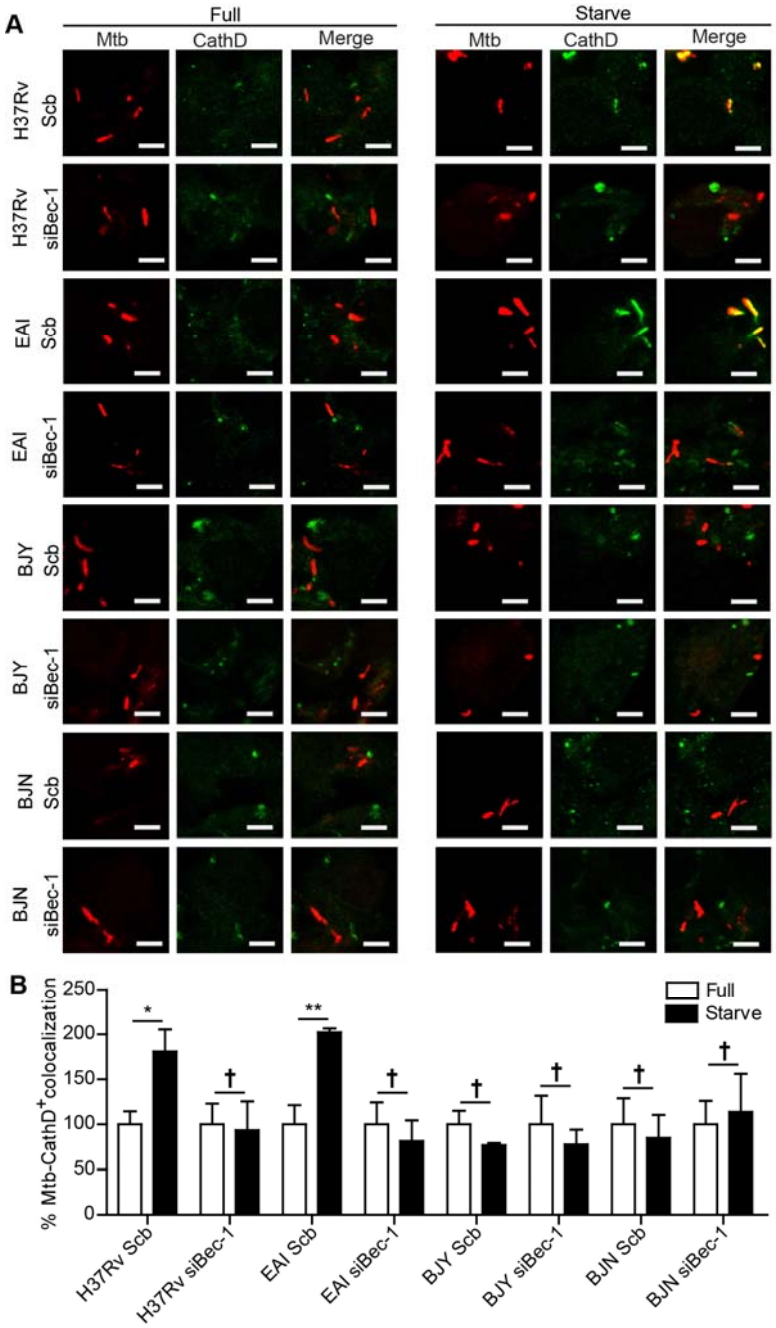

FIG 6. The increased cathepsin D acquisition in response to starvation observed with the *M. tuberculosis* reference strain H37Rv and the EAI strain depends on autophagy. (*A-B*) RAW264.7 cells were transfected with siRNAs against Beclin-1 or scramble (Scb). After 48 hr of transfection, cells were then infected with Alexa 405-labeled mycobacteria (pseudocolored red) and processed for cathepsin D staining as in Fig. 4B and D. Data are means ± SEM from at least 3 independent experiments. At least 50 phagosomes per condition per independent experiment were quantified. $^{**}p < 0.01$, $^{*}p < 0.05$, and $^{\dagger}p \geq 0.05$, all relative to the full control set to 100%. EAI, the East African Indian strain with intact *pks15/1*; BJY, the Beijing strain with intact *pks15/1*; BJN, the Beijing strain without intact *pks15/1*.

Taken together our results showed that there is a variation in the capacity of different *M. tuberculosis* strains to resist starvation-induced autophagic killing in host macrophages of which the Beijing strains possess unique capability to evade autophagic elimination upon autophagy induction. The Beijing strains do so not by simply inhibiting the autophagy-mediated acidification of their phagosomes or by blocking the autophagic flux in host cells, but by inhibiting autophagolysosome biogenesis as demonstrated by their ability to suppress the increased acquisition of cathepsin D into their compartments upon autophagy induction by starvation and thus escape from autophagic restriction.

Discussion

Autophagy has been demonstrated as an important innate immune defense mechanism utilized by host cells for the elimination of various intracellular bacteria, parasites, and viruses [1, 9-11]. In addition, induction of autophagy by starvation or other autophagy inducers has been extensively shown to result in the killing of *M. tuberculosis* by disabling the block in phagolysosomal biogenesis imposed by the tubercle bacilli [12-17]. As the ability of autophagy in the restriction of *M. tuberculosis* has been observed in studies using the laboratory reference strains but has not been characterized in detail in cells infected with the clinical strains especially those belonging to the Beijing family previously shown to be hyper-virulent associated with their higher ability to survive in host macrophages and cause higher bacterial load and mortality in animal models [31-36], we set out to examine autophagic killing capacity of host cells against different strains of *M. tuberculosis*. In our present study, we have uncovered the previously unrecognized ability of the *M. tuberculosis* Beijing strains to evade starvation-induced autophagic elimination. In addition, we have determined a possible underlying mechanism in which the Beijing strains can escape starvation-induced autophagic killing by inhibiting autophagolysosome biogenesis as demonstrated by their ability to suppress the enhanced acquisition of cathepsin D into their compartments. As autophagy was previously shown to be a key determinant of host resistance against mycobacterial infection [20, 21, 23-28], our findings may explain the hyper-virulent phenotypes associated with the Beijing family [31-36] thought to be resulted from their higher ability to survive in host macrophages but the underlying mechanism was previously unknown.

Consistent with previous findings that showed the effect of starvation-induced autophagy in the elimination of *M. tuberculosis* reference strains [12-17], we also observed that starvation treatment of infected RAW macrophages results in the restriction of the laboratory reference strain *M. tuberculosis* H37Rv. In contrast to that of the reference strains, we observed a previously unrecognized ability of *M. tuberculosis* Beijing strains to avoid autophagic killing by blocking autophagolysosome biogenesis. The ability to interfere with autophagy pathway of host macrophages possessed by the Beijing strains is similar to those possessed by and previously reported for *H. pylori* and *M. marinum* [48-50]. These bacteria were also found to escape from autophagic elimination by inhibiting autophagolysosome biogenesis in host cells in response to autophagy induction as determined by a decrease in enhanced cathepsin D acquisition into their compartments. Cathepsin D, an aspartic endopeptidase, is synthesized in the rough endoplasmic reticulum as preprocathepsin D and then being targeted to various compartments such as phagosomes, autophagosomes, endosomes, and lysosomes as procathepsin D [51-53]. Upon transport, inactive procathepsin D is converted into active form of cathepsin D by acidic pH and thus the presence of cathepsin D precursors (and other lysosomal acid hydrolases) in acidified compartments is necessary for their degradative function. Our results showed that although the acidification of *M. tuberculosis* Beijing phagosomes are efficiently increased upon autophagy induction by starvation, these was no increase in the acquisition of cathepsin D into their phagosomes upon starvation treatment indicating a defect in autophagolysosome biogenesis.

The mechanism by which the Beijing strains inhibit autophagolysosome biogenesis is under investigation by our laboratory. Among several mycobacterial factors previously shown to be involved in *M. tuberculosis* survival in host cells, phenolic glycolipid (PGL) synthesized by a

polyketide synthase encoded by the intact *pks15/1* gene was demonstrated for its activity to reduce the production of Th1-type cytokines [47, 54], some of which have been shown to induce autophagy [1]. However, our data showed no significant relationship between the presence of intact *pks15/1* gene and the ability of mycobacteria to resist starvation-induced autophagic elimination and thus indicating that PGL is not the factor that renders the Beijing strains to escape autophagic restriction. Interestingly, in the case of *H. pylori* which was also shown to evade autophagic killing by residing in acidic compartments that lack cathepsin D in response to autophagy [48-50], it was previously reported that the maturation of procathepsin D into the mature form as well as its sorting in mammalian cells can be impaired by *H. pylori* vacuolating toxin (VacA) [55]. Whether *M. tuberculosis* Beijing strains possess similar or equivalent protein is not known. As a recent whole-genome sequencing of strains belonging to the *M. tuberculosis* Beijing family has been conducted [56], mining and comparing sequencing data between Beijing and non-Beijing strains may give insight into potential candidate genes that may play a role in the autophagic evasion. In addition to the bacterial factor, two host proteins, Rab8b and its downstream effector TANK-binding kinase 1 (TBK1), have been shown to play prominent roles in autophagy-mediated mycobacterial phagosome maturation as demonstrated by decreased mycobacterial phagosome acidification and cathepsin D acquisition upon siRNA-mediated depletion of Rab8b or pharmacological inhibition of TBK1 [37]. Whether the Beijing strains are able to interfere with Rab8b and TBK1 functions in autophagy-mediated mycobacterial phagosome maturation is a subject of our study.

Besides our principle finding discussed above, our data also showed that the acquisition of cathepsin D into the EAI phagosomes is substantially enhanced upon autophagy induction similar to what has previously been observed with *M. tuberculosis* reference strains [12-17].

Interestingly, previous studies showed that the EAI strains possess a higher ability to stimulate TNF-α synthesis in infected host cells when compared to that of the Beijing strains [40, 57]. As TNF-α has been shown to be a potent autophagic inducer [1], the enhanced production of TNF-α upon EAI strain infection may augment autophagy induction level in our system and thus may help increase the acquisition of cathepsin D into the EAI phagosomes. Whether the EAI strain possesses greater ability to induce host autophagy as a result of increased TNF-α production awaits further examination. If the EAI strain is found to enhance host autophagy, this may in turn explain the low-virulent phenotypes associated with this *M. tuberculosis* family as demonstrated by their reduced transmissibility, low level of growth inside macrophages, and decreased bacterial burden (100-fold lower when compared to that of the Beijing strains) and mortality in mouse models [29, 38]. In addition, we also observed an enhanced growth of the Beijing strains inside host cells upon autophagy induction albeit not statistically significant and this effect was decreased in cells deficient of Beclin-1 (Figure 1B and D). Whether the Beijing strains can, in addition to resisting autophagic killing by host cells, subvert autophagy pathway for their own growth inside macrophages await further investigation.

References

1. Deretic V, Saitoh T and Akira S. Autophagy in infection, inflammation and immunity. *Nat Rev Immunol*. 2013; 13: 722-37.

2. Levine B, Mizushima N and Virgin HW. Autophagy in immunity and inflammation. *Nature*. 2011; 469: 323-35.

3. Mizushima N, Yoshimori T and Ohsumi Y. The role of Atg proteins in autophagosome formation. *Annu Rev Cell Dev Biol*. 2011; 27: 107-32.

4. Yang Z and Klionsky DJ. Mammalian autophagy: core molecular machinery and signaling regulation. *Current opinion in cell biology*. 2010; 22: 124-31.

5. Randow F and Munz C. Autophagy in the regulation of pathogen replication and adaptive immunity. *Trends in immunology*. 2012; 33: 475-87.

6. Boyle KB and Randow F. The role of 'eat-me' signals and autophagy cargo receptors in innate immunity. *Current opinion in microbiology*. 2013; 16: 339-48.

7. Johansen T and Lamark T. Selective autophagy mediated by autophagic adapter proteins. *Autophagy*. 2011; 7: 279-96.

8. Mandell MA, Jain A, Arko-Mensah J, et al. TRIM proteins regulate autophagy and can target autophagic substrates by direct recognition. *Dev Cell*. 2014; 30: 394-409.

9. Deretic V and Levine B. Autophagy, immunity, and microbial adaptations. *Cell host & microbe*. 2009; 5: 527-49.

10. Gomes LC and Dikic I. Autophagy in antimicrobial immunity. *Molecular cell*. 2014; 54: 224-33.

11. Huang J and Brumell JH. Bacteria-autophagy interplay: a battle for survival. *Nature reviews Microbiology*. 2014; 12: 101-14.

12. Alonso S, Pethe K, Russell DG and Purdy GE. Lysosomal killing of Mycobacterium mediated by ubiquitin-derived peptides is enhanced by autophagy. *Proceedings of the National Academy of Sciences of the United States of America*. 2007; 104: 6031-6.

13. Delgado MA, Elmaoued RA, Davis AS, Kyei G and Deretic V. Toll-like receptors control autophagy. *The EMBO journal*. 2008; 27: 1110-21.

14. Gutierrez MG, Master SS, Singh SB, Taylor GA, Colombo MI and Deretic V. Autophagy is a defense mechanism inhibiting BCG and Mycobacterium tuberculosis survival in infected macrophages. *Cell*. 2004; 119: 753-66.

15. Ponpuak M, Davis AS, Roberts EA, et al. Delivery of cytosolic components by autophagic adaptor protein p62 endows autophagosomes with unique antimicrobial properties. *Immunity*. 2010; 32: 329-41.

16. Singh SB, Davis AS, Taylor GA and Deretic V. Human IRGM induces autophagy to eliminate intracellular mycobacteria. *Science*. 2006; 313: 1438-41.

17. Xu Y, Jagannath C, Liu XD, Sharafkhaneh A, Kolodziejska KE and Eissa NT. Toll-like receptor 4 is a sensor for autophagy associated with innate immunity. *Immunity*. 2007; 27: 135-44.

18. Vergne I, Chua J, Singh SB and Deretic V. Cell biology of mycobacterium tuberculosis phagosome. *Annu Rev Cell Dev Biol*. 2004; 20: 367-94.

19. Ponpuak M and Deretic V. Autophagy and p62/sequestosome 1 generate neo-antimicrobial peptides (cryptides) from cytosolic proteins. *Autophagy*. 2011; 7: 336-7.

20. Castillo EF, Dekonenko A, Arko-Mensah J, et al. Autophagy protects against active tuberculosis by suppressing bacterial burden and inflammation. *Proceedings of the National Academy of Sciences of the United States of America*. 2012; 109: E3168-76.

21. Watson RO, Manzanillo PS and Cox JS. Extracellular M. tuberculosis DNA targets bacteria for autophagy by activating the host DNA-sensing pathway. *Cell*. 2012; 150: 803-15.

22. Kim JJ, Lee HM, Shin DM, et al. Host cell autophagy activated by antibiotics is required for their effective antimycobacterial drug action. *Cell host & microbe*. 2012; 11: 457-68.

23. Kumar D, Nath L, Kamal MA, et al. Genome-wide analysis of the host intracellular network that regulates survival of Mycobacterium tuberculosis. *Cell*. 2010; 140: 731-43.

24. Bahari G, Hashemi M, Taheri M, Naderi M, Eskandari-Nasab E and Atabaki M. Association of IRGM polymorphisms and susceptibility to pulmonary tuberculosis in Zahedan, Southeast Iran. *TheScientificWorldJournal*. 2012; 2012: 950801.

25. Che N, Li S, Gao T, et al. Identification of a novel IRGM promoter single nucleotide polymorphism associated with tuberculosis. *Clinica chimica acta; international journal of clinical chemistry*. 2010; 411: 1645-9.

26. Intemann CD, Thye T, Niemann S, et al. Autophagy gene variant IRGM -261T contributes to protection from tuberculosis caused by Mycobacterium tuberculosis but not by M. africanum strains. *PLoS pathogens*. 2009; 5: e1000577.

27. King KY, Lew JD, Ha NP, et al. Polymorphic allele of human IRGM1 is associated with susceptibility to tuberculosis in African Americans. *PloS one*. 2011; 6: e16317.

28. Li CM, Campbell SJ, Kumararatne DS, et al. Association of a polymorphism in the P2X7 gene with tuberculosis in a Gambian population. *The Journal of infectious diseases*. 2002; 186: 1458-62.

29. Reiling N, Homolka S, Walter K, et al. Clade-specific virulence patterns of Mycobacterium tuberculosis complex strains in human primary macrophages and aerogenically infected mice. *mBio*. 2013; 4.

30. Brudey K, Driscoll JR, Rigouts L, et al. Mycobacterium tuberculosis complex genetic diversity: mining the fourth international spoligotyping database (SpolDB4) for classification, population genetics and epidemiology. *BMC microbiology*. 2006; 6: 23.

31. Dormans J, Burger M, Aguilar D, et al. Correlation of virulence, lung pathology, bacterial load and delayed type hypersensitivity responses after infection with different Mycobacterium tuberculosis genotypes in a BALB/c mouse model. *Clin Exp Immunol*. 2004; 137: 460-8.

32. Hanekom M, van der Spuy GD, Streicher E, et al. A recently evolved sublineage of the Mycobacterium tuberculosis Beijing strain family is associated with an increased ability to spread and cause disease. *Journal of clinical microbiology*. 2007; 45: 1483-90.

33. Portevin D, Gagneux S, Comas I and Young D. Human macrophage responses to clinical isolates from the Mycobacterium tuberculosis complex discriminate between ancient and modern lineages. *PLoS pathogens*. 2011; 7: e1001307.

34. Tsenova L, Ellison E, Harbacheuski R, et al. Virulence of selected Mycobacterium tuberculosis clinical isolates in the rabbit model of meningitis is dependent on phenolic glycolipid produced by the bacilli. *The Journal of infectious diseases*. 2005; 192: 98-106.

35. van der Spuy GD, Kremer K, Ndabambi SL, et al. Changing Mycobacterium tuberculosis population highlights clade-specific pathogenic characteristics. *Tuberculosis*. 2009; 89: 120-5.

36. Zhang M, Gong J, Yang Z, Samten B, Cave MD and Barnes PF. Enhanced capacity of a widespread strain of Mycobacterium tuberculosis to grow in human macrophages. *The Journal of infectious diseases*. 1999; 179: 1213-7.

37. Pilli M, Arko-Mensah J, Ponpuak M, et al. TBK-1 promotes autophagy-mediated antimicrobial defense by controlling autophagosome maturation. *Immunity*. 2012; 37: 223-34.

38. Albanna AS, Reed MB, Kotar KV, et al. Reduced transmissibility of East African Indian strains of Mycobacterium tuberculosis. *PloS one*. 2011; 6: e25075.

39. Yorsangsukkamol J, Chaiprasert A, Prammananan T, Palittapongarnpim P, Limsoontarakul S and Prayoonwiwat N. Molecular analysis of Mycobacterium tuberculosis from tuberculous meningitis patients in Thailand. *Tuberculosis*. 2009; 89: 304-9.

40. Yorsangsukkamol J, Chaiprasert A, Palaga T, et al. Apoptosis, production of MMP9, VEGF, TNF-alpha and intracellular growth of M. tuberculosis for different genotypes and different pks5/1 genes. *Asian Pac J Allergy Immunol*. 2011; 29: 240-51.

41. Kimura S, Noda T and Yoshimori T. Dissection of the autophagosome maturation process by a novel reporter protein, tandem fluorescent-tagged LC3. *Autophagy*. 2007; 3: 452-60.

42. Ponpuak M, Delgado MA, Elmaoued RA and Deretic V. Monitoring autophagy during Mycobacterium tuberculosis infection. *Methods in enzymology*. 2009; 452: 345-61.

43. Floto RA, Sarkar S, Perlstein EO, Kampmann B, Schreiber SL and Rubinsztein DC. Small molecule enhancers of rapamycin-induced TOR inhibition promote autophagy, reduce toxicity in Huntington's disease models and enhance killing of mycobacteria by macrophages. *Autophagy*. 2007; 3: 620-2.

44. Yuk JM, Shin DM, Lee HM, et al. Vitamin D3 induces autophagy in human monocytes/macrophages via cathelicidin. *Cell host & microbe*. 2009; 6: 231-43.

45. Zullo AJ and Lee S. Mycobacterial induction of autophagy varies by species and occurs independently of mammalian target of rapamycin inhibition. *The Journal of biological chemistry*. 2012; 287: 12668-78.

46. Harris J, De Haro SA, Master SS, et al. T helper 2 cytokines inhibit autophagic control of intracellular Mycobacterium tuberculosis. *Immunity*. 2007; 27: 505-17.

47. Hanekom M, Gey van Pittius NC, McEvoy C, Victor TC, Van Helden PD and Warren RM. Mycobacterium tuberculosis Beijing genotype: a template for success. *Tuberculosis*. 2011; 91: 510-23.

48. Lerena MC and Colombo MI. Mycobacterium marinum induces a marked LC3 recruitment to its containing phagosome that depends on a functional ESX-1 secretion system. *Cell Microbiol*. 2011; 13: 814-35.

49. Terebiznik MR, Raju D, Vazquez CL, et al. Effect of Helicobacter pylori's vacuolating cytotoxin on the autophagy pathway in gastric epithelial cells. *Autophagy*. 2009; 5: 370-9.

50. Terebiznik MR, Vazquez CL, Torbicki K, et al. Helicobacter pylori VacA toxin promotes bacterial intracellular survival in gastric epithelial cells. *Infection and immunity*. 2006; 74: 6599-614.

51. Hasilik A and Neufeld EF. Biosynthesis of lysosomal enzymes in fibroblasts. Synthesis as precursors of higher molecular weight. *The Journal of biological chemistry*. 1980; 255: 4937-45.

52. Kornfeld S. Lysosomal enzyme targeting. *Biochem Soc Trans*. 1990; 18: 367-74.

53. Benes P, Vetvicka V and Fusek M. Cathepsin D--many functions of one aspartic protease. *Crit Rev Oncol Hematol*. 2008; 68: 12-28.

54. Reed MB, Domenech P, Manca C, et al. A glycolipid of hypervirulent tuberculosis strains that inhibits the innate immune response. *Nature*. 2004; 431: 84-7.

55. Satin B, Norais N, Telford J, et al. Effect of helicobacter pylori vacuolating toxin on maturation and extracellular release of procathepsin D and on epidermal growth factor degradation. *The Journal of biological chemistry*. 1997; 272: 25022-8.

56. Merker M, Blin C, Mona S, et al. Evolutionary history and global spread of the Mycobacterium tuberculosis Beijing lineage. *Nature genetics*. 2015.

57. Wang C, Peyron P, Mestre O, et al. Innate immune response to Mycobacterium tuberculosis Beijing and other genotypes. *PloS one*. 2010; 5: e13594.

เอกสารแนบหมายเลข 3

Output จากโครงการวิจัยที่ได้รับทุนจาก สกว.

1. ผลงานตีพิมพ์ในวารสารวิชาการนานาชาติ จำนวน 3 เรื่อง

1.1 Md Fazlul Haque, Rachasak Boonhok, Therdsak Prammananan, Angkana Chaiprasert, Pongsak Utaisincharoen, Jetsumon Sattabongkot, Prasit Palittapongarnpim, **Marisa Ponpuak***. Resistance to cellular autophagy by *Mycobacterium tuberculosis* Beijing strains. *Innate Immunity.* 2015. DOI: 10.1177/1753425915594245.

1.2 **Marisa Ponpuak**, Michael A. Mandell, Tomonori Kimura, Santosh Chauhan, Cédric Cleyrat, Vojo Deretic*. Secretory Autophagy. *Current Opinion in Cell Biology*. 2015. May 16;35:106-116.

1.3 Mark Kennedy, Matthew E Fishbaugher, Ashley M Vaughan, Rapatbhorn Patrapuvich, Rachasak Boonhok, Narathatai Yimamnuaychok, Nastaran Rezakhani, Peter Metzger, **Marisa Ponpuak**, Jetsumon Sattabongkot, Stefan H Kappe, Jen CC Hume, Scott E Lindner*. A rapid and scalable density gradient purification method for *Plasmodium* sporozoites. Malaria Journal. 2012. Dec 17;11:421.

2. การนำผลงานวิจัยไปใช้ประโยชน์

- เชิงวิชาการ สร้างนักศึกษาปริญญาเอก จำนวน 2 คน

2.1 Dr. Md Fazlul Haque

2.2 Dr. Rachasak Boonhok

3. อื่นๆ

-

ภาคผนวก

Page Proof Instructions and Queries

Journal Title: Innate Immunity (INI)

Article Number: 594245

Greetings, and thank you for publishing with SAGE. We have prepared this page proof for your review. Please respond to each of the below queries by digitally marking this PDF using Adobe Reader.

Click "Comment" in the upper right corner of Adobe Reader to access the mark-up tools as follows:

For textual edits, please use the "Annotations" tools. Please refrain from using the two tools crossed out below, as data loss can occur when using these tools.

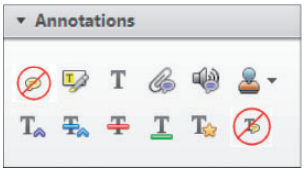

For formatting requests, questions, or other complicated changes, please insert a comment using "Drawing Markups."

Detailed annotation guidelines can be viewed at: http://www.sagepub.com/repository/binaries/pdfs/AnnotationGuidelines.pdf
Adobe Reader can be downloaded (free) at: http://www.adobe.com/products/reader.html.

No.	Query
	Please confirm that all author information, including names, affiliations, sequence, and contact details, is correct.
	Please review the entire document for typographical errors, mathematical errors, and any other necessary corrections; check headings, tables, and figures.
	Please confirm that the Funding and Conflict of Interest statements are accurate.
	Please ensure that you have obtained and enclosed all necessary permissions for the reproduction of artistic works, (e.g. illustrations, photographs, charts, maps, other visual material, etc.) not owned by yourself. Please refer to your publishing agreement for further information.
	Please note that this proof represents your final opportunity to review your article prior to publication, so please do send all of your changes now.
AQ: 1	Please provide the manufacturer location details for HyClone (city, state (if US) and country).
AQ: 2	Please check the editing of this sentence carefully as the original wording was unclear.
AQ: 3	Please provide the manufacturer location details for Roche Diagnostics (city, state (if US) and country).

Research Article

Innate Immunity

Innate Immunity
0(0) 1–13

DOI: 10.1177/1753425915594245
ini.sagepub.com

SAGE

Resistance to cellular autophagy by *Mycobacterium tuberculosis* Beijing strains

Md Fazlul Haque[1,2], Rachasak Boonhok[1,3], Therdsak Prammananan[4,5], Angkana Chaiprasert[5,6], Pongsak Utaisincharoen[1], Jetsumon Sattabongkot[3], Prasit Palittapongarnpim[1,4] and Marisa Ponpuak[1]

Abstract

Autophagy represents a key pathway in innate immune defense to restrict *Mycobacterium tuberculosis* growth inside host macrophages. Induction of autophagy has been shown to promote mycobacterial phagosome acidification and acquisition of lysosomal hydrolases, resulting in the elimination of intracellular *M. tuberculosis* reference strains such as H37Rv. The notorious Beijing genotype has been previously shown to be hyper-virulent and associated with increased survival in host cells and a high mortality rate in animal models, but the underlying mechanism that renders this family to have such advantages remains unclear. We hypothesize that autophagic control against *M. tuberculosis* Beijing strains may be altered. Here, we discovered that the Beijing strains can resist autophagic killing by host cells compared with that of the reference strain H37Rv and a strain belonging to the East African Indian genotype. Moreover, we have determined a possible underlying mechanism and found that the greater ability to evade autophagic elimination possessed by the Beijing strains stems from their higher capacity to inhibit autophagolysosome biogenesis upon autophagy induction. In summary, a previously unrecognized ability of the *M. tuberculosis* Beijing strains to evade host autophagy was identified, which may have important implications for tuberculosis treatment, especially in regions prevalent by the Beijing genotype.

Keywords

Autophagy, Beijing strains, *M. tuberculosis*, mycobacteria, tuberculosis

Date received: 6 May 2015;accepted: 10 June 2015

Introduction

Autophagy (macroautophagy) is an evolutionary conserved cellular homeostatic process for qualitative and quantitative control of cytoplasmic biomass by removing long-lived proteins, cytosolic toxic aggregates and defunct organelles.[1–4] In addition, autophagy has been increasingly appreciated for its role as a primordial form of cellular innate immunity against invading pathogens.[1,2,5] Autophagy can be initiated when cells encounter stresses such as nutritional and immune insults resulting from starvation, a change in the level of immune mediators, and the presence of structural components of microbes and their products.[1–4] Upon responding to an upstream stress signal, Atg proteins are organized into complexes and collaborate to generate a specialized double-membrane autophagosome.[3,4] These complexes include (i) the protein kinase complexes ULK1 and AMPK to activate Beclin-1, (ii) the class III phosphatidylinositol 3-kinase complexes VPS34 and Beclin-1 to generate PI3P for recruitment of downstream effectors, and (iii) the Atg5/Atg12/Atg16 conjugation complexes that act as an E3 ligase

[1]Department of Microbiology, Faculty of Science, Mahidol University, Bangkok, Thailand
[2]Department of Zoology, Faculty of Life and Earth Science, Rajshahi University, Rajshahi, Bangladesh
[3]Mahidol Vivax Research Center, Faculty of Tropical Medicine, Mahidol University, Bangkok, Thailand
[4]National Center for Genetic Engineering and Biotechnology, National Science and Technology Development Agency, Pratumthani, Thailand
[5]Drug-Resistance Tuberculosis Research Fund, Siriraj Foundation, Faculty of Medicine Siriraj Hospital, Mahidol University, Bangkok, Thailand
[6]Department of Microbiology, Faculty of Medicine Siriraj Hospital, Mahidol University, Bangkok, Thailand

Corresponding author:
Marisa Ponpuak, Department of Microbiology, Faculty of Science, Mahidol University, Rama VI Road, Bangkok 10400, Thailand.
Email: marisa.pon@mahidol.ac.th

for LC3 lipidation required for elongation and closure of an autophagosome.[1,3,4] Cytosolic substrates can be either non-selectively engulfed into an autophagosome or selectively recognized and collected into autophagosome by different types of cargo receptors/adaptors.[6–8] Upon closure, an autophagosome fuses with the lysosome resulting in the delivery of lysosomal acid hydrolases, which then degrade the enclosed contents. The resulting digested molecules, such as amino acids, are then released and recycled back into the cytoplasm.[1,3,4]

Autophagy has been shown to play important roles in cells' autonomous defense against intracellular bacteria, parasites and viruses.[1,9–11] In the context of *Mycobacterium tuberculosis* infection, induction of autophagy by starvation or other autophagy inducers results in the killing of the tubercle bacilli by overcoming the block in phagolysosomal biogenesis, as demonstrated by the acidification and acquisition of lysosomal hydrolases into compartments harboring the mycobacteria,[12–17] even when they have survived in phagocytes by evading immunological mechanisms.[18] The proposed mechanistic details for autophagy-mediated mycobacterial elimination include (i) the direct engulfment of mycobacteria into autophagosomes and subsequent delivery to lysosomes for degradation, and (ii) the generation of killing peptides converted from innocuous cytosolic substrates engulfed and partially digested in autophagosomes/autophagolysosomes and subsequent delivery of these killing peptides to mycobacteria via fusion of autophagic vacuoles with mycobacterial phagosomes.[19] The importance of the autophagy pathway in antimycobacterial defense was substantiated by the findings that mice deficient in Atg5 expression in macrophages display a high susceptibility to mycobacterial infection.[20,21] Furthermore, autophagy was shown to be required for effective antimycobacterial drug action of isoniazid and pyrazinamide, two of the first-line tuberculosis drugs, in an animal model of tuberculosis.[22] In addition, a genome-wide siRNA screen to identify host factors that regulate mycobacterial load in macrophages infected with different strains of *M. tuberculosis* revealed autophagy as the main host cell functional module that is perturbed by the pathogen.[23] Moreover, polymorphisms in the human autophagy and autophagy-related genes *IRGM* and *P2X7* are found to be associated with susceptibility to tuberculosis.[24–28] All of these data underscore the importance of autophagic process in mycobacterial control and indicate that the magnitude of autophagic elimination of mycobacteria may be the key determinant of their virulence and pathogenesis.

Mycobacterium tuberculosis can be subdivided into several distinct genotypic families/lineages,[29] among which the Beijing genotype, regarded as the highly successful lineage of *M. tuberculosis* often associated with multidrug resistance, was shown to be globally distributed, representing around 50% of strains in East Asia and more than 13% of strains worldwide.[30] The success of the Beijing family was thought to stem from its associated hyper-virulent phenotypes, as demonstrated by their higher ability to survive in host macrophages, to cause higher bacterial load and mortality in animal models, and to cause heavy AFB smear-positive sputum in patients.[31–36] However, the mechanism attributing to the greater ability of *M. tuberculosis* Beijing genotype to survive in host cells remains unclear. As autophagy has been shown to be important for controlling *M. tuberculosis* growth inside host cells but the characterization of this pathway has been conducted using *M. tuberculosis* laboratory reference strains such as H37Rv and the vaccine strain BCG,[12–17,37] but not ~~with~~ the clinical strains such as those belong to the Beijing genotype, we set out to determine whether there is an alteration in autophagic control against strains of the Beijing genotype ~~that~~ may explain the hyper-virulence possessed by this family. Our results showed that the Beijing strains display greater ability to resist autophagic killing than that of the reference strain H37Rv and a strain belonging to the East African Indian (EAI) genotype.[29,38] In addition, we revealed a possible underlying mechanism in which the resistance of the Beijing strains to autophagic restriction is not simply achieved by blocking autophagy-mediated acidification of their phagosomes or by inhibiting the autophagic flux in host cells but achieved by preventing autophagolysosome biogenesis, as demonstrated by their ability to inhibit the increased acquisition of cathepsin D, an enzyme of lysosomal acid hydrolases and a marker of lysosome, into mycobacterial compartments upon the induction of autophagy.

Materials and methods

Cell and bacterial culture

Mouse macrophage RAW 264.7 cells (ATCC) were maintained in DMEM (~~HyClone~~), 10% FBS (~~HyClone~~) and 4 mM L-glutamine (~~HyClone~~) (full media). Earle's Balanced Salt Solution (Sigma, St. Louis, MO, USA) (starve media) was used to induce autophagy. Cells were cultured at 37°C and in 5% CO_2. *Mycobacterium tuberculosis* reference strain H37Rv, and the previously described *M. tuberculosis* EAI and Beijing strains,[39,40] were cultured in Middlebrook 7H9 broth supplemented with 0.05% Tween 80, 0.2% glycerol, and 10% oleic acid, albumin, dextrose and catalase (OADC; BD ~~Biosciences~~) at 37°C and homogenized to generate single-cell suspension. For infection experiments, the number of bacteria was adjusted to 3×10^6 CFU/ml in complete DMEM by measuring the OD at 600 nm. CFU was calculated from the precalibrated standard curve. For bacterial survival assays, bacilli were plated onto Middlebrook

7H11 agar supplemented with 0.05% Tween 80, 0.2% glycerol and 10% OADC (BD Biosciences), and grown at 37°C.

Fluorescent dye, Abs, DNA construct and siRNAs

LysoTracker Red (LTR; Invitrogen, Carlsbad, CA, USA) was used at 1:4000. For immunofluorescence assays, monoclonal Ab against Cathepsin D (R&D Systems, Minneapolis, MN, USA) was used at 1:200. For immunoblotting, polyclonal Abs against Beclin-1 (Santa Cruz, Santa Cruz, CA, USA) were used at 1:500 and monoclonal Ab against Actin (Abcam, Cambridge, UK) was used at 1:2000. The plasmid construct used in this study was as previously described.[41] All siRNAs used in this study were from Dharmacon (Lafayette, CO, USA).

Macrophage transfection

RAW264.7 cells were transfected with 5 μg cDNAs or 1.5 μg siRNAs as previously described.[42] In brief, $10–15 \times 10^6$ cells were re-suspended in 100 μl of Nucleofector solution kit V (Amaxa, London, UK). Plasmid DNAs or siRNAs were then added to the cell suspension and cells were nucleoporated using the Amaxa Nucleofector apparatus with the program D-032. Cells were then transferred into a new flask containing 12 ml complete media and incubated at 37°C followed by a medium change at 6 h of incubation. Cells were then used in assays after 24 h of transfection with plasmid DNAs or 48 h of transfection with siRNAs.

Macrophage infection, mycobacterial survival and immunofluorescence microscopy

Infection of RAW264.7 cells with mycobacteria and quantification of mycobacterial survival after autophagy induction were carried out as previously described.[15] In brief, 3×10^5 cells of RAW264.7 macrophages were plated onto each well of 12-well plates 12 h before infection. Cells were then infected with a single-cell suspension of mycobacteria in complete media at an MOI of 10:1 for 1 h. Cells were then washed three times with PBS to remove un-internalized mycobacteria and autophagy was then induced by treatment with starvation media for 4 h. Cells were then lyzed and survival of bacteria was determined by plating for CFU. For immunofluorescence microscopy, 3×10^5 Raw264.7 macrophages were plated onto coverslips in 12-well plates 12 h before infection. Cells were then infected with 3×10^6 Alexa 488- or Alexa 405-labeled mycobacteria per well in complete media at 37°C for 15 min, washed three times in PBS and chased for 1 h in complete media as previously described.[42] Cells were then washed three times with PBS and autophagy was then induced by treatment with starvation media for 2 h. Cells were then fixed with 4% paraformaldehyde/PBS for 15 min followed by permeabilization with 0.1% Triton X-100/PBS for 5 min. Coverslips were then blocked in PBS containing 3% BSA and stained with primary Abs according to the manufacturer's recommendation. Cells were washed three times with PBS and then incubated with appropriate secondary Abs (Invitrogen) for 1 h at room temperature (25°C). Coverslips were then mounted using ProLong Gold Antifade Mountant (Invitrogen) and analyzed by confocal microscopy using the Zeiss LSM-700 Laser Scanning Microscope (Carl Zeiss, Jena, Germany). For LTR staining, cells were prestained in complete media containing LTR for 2 h at 37°C before infection. Subsequent steps were carried out as described above but in the presence of LTR until the cells were fixed. For analysis of RFP–GFP–LC3 transfected cells, cells were fixed and mounted as described above. The numbers of RFP^+GFP^+–LC3 puncta (autophagosomes) and RFP^+GFP^-–LC3 puncta (autolysosomes) were determined in cells that contained mycobacteria in infection conditions and compared them with those of the uninfected control. At least 50 phagosomes per experimental condition in three independent experiments were quantified. For quantification, the percentage mycobacteria–marker colocalization was a fraction of total mycobacterial phagosomes examined and counted as positive when one or more puncta were observed on or in contact with the mycobacterial phagosomes.

Immunoblotting

Cells were lysed in lysis buffer containing 20 mM Tris, 100 mM NaCl and 1% NP-40. Cell lysates were then separated by 10% SDS-PAGE and proteins were transferred onto a nitrocellulose membrane (Amersham Biosciences, Little Chalfont, UK). Membranes were then blocked with 5% blocking solution (Roche Diagnostics) for 1 h before incubation with appropriate primary Abs at 4°C overnight (16 h). Membranes were then washed three times with PBS containing 0.1% Tween 20 (0.1% PBST) followed by incubation with appropriate HRP-conjugated secondary Ab (Pierce, Rockford, IL, USA) at room temperature for 1 h. Membranes were then washed four times with 0.1% PBST followed by incubation with a chemiluminescence substrate (Roche Diagnostics) at room temperature for 2 min. Proteins were then detected with the enhanced chemiluminescence method.

Statistical analysis

Unless indicated otherwise, all experiments were independently conducted at least three times and data were pooled for presentation as mean ± SEM. All data were

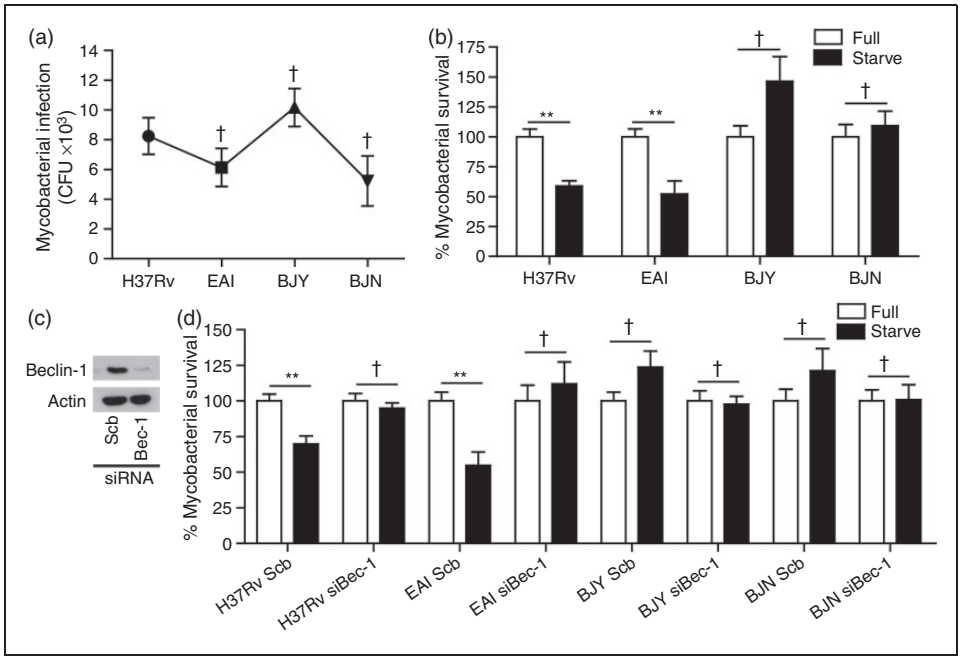

Figure 1. The Beijing strains of *M. tuberculosis* possess a greater ability to resist starvation-induced autophagic killing in host macrophages. (A) RAW264.7 macrophages were infected with different *M. tuberculosis* strains at an MOI of 10 for 1 h. After washing the cells multiple times to remove un-internalized mycobacteria, cells were then lyzed and the number of mycobacteria that infected host cells was determined by plating for CFU. (B) RAW264.7 macrophages were infected with different *M. tuberculosis* strains at MOI of 10 for 1 h. After washing the cells multiple times to remove un-internalized mycobacteria, cells were then induced to undergo autophagy by starvation for 4 h. Cells were then harvested and the number of viable mycobacteria was determined by plating for CFU. (C) RAW264.7 macrophages were transfected with siRNAs against Beclin-1 or scramble (Scb) control. After 48 h of transfection, RAW264.7 cells were collected and processed for immunoblot analysis to estimate the efficacy of Beclin-1 depletion. (D) RAW264.7 macrophages were transfected with siRNAs as in (C). At 48 h after transfection, cells were infected with different strains of *M. tuberculosis* and then subjected to autophagy induction by starvation and CFU analysis as in (B). Data are mean ± SEM from at least three independent experiments. $^{**}P < 0.01$ and $\dagger P \geq 0.05$, all relative to the full control set to 100%. EAI, the East African Indian strain with intact *pks15/1*; BJY, the Beijing strain with intact *pks15/1*; BJN, the Beijing strain without intact *pks15/1*.

analyzed with Prism software (GraphPad, La Jolla, CA, USA) using two-tailed unpaired Student's *t*-tests. *P*-values <0.05 were considered significant.

Results

The Beijing strains resist autophagic killing of mycobacteria by host cells

It has been well documented that induction of autophagy by starvation or other autophagy inducers in host macrophages results in the killing of mycobacteria reference strains such as *M. tuberculosis* H37Rv and the vaccine strain BCG.[12,14,16,43–45] However, the autophagic killing capacity of host cells against *M. tuberculosis* clinical strains has not been characterized in detail. Therefore, we set out to evaluate whether different *M. tuberculosis* strains possess differing abilities to alter host autophagic killing capacity. As a control, we observed no variation in the infection of RAW264.7 macrophages by different *M. tuberculosis* strains when compared with that of the reference strain H37Rv (Figure 1A). Our results showed that, similarly to what has previously been observed,[14,15,37,46] induction of autophagy in RAW264.7 macrophages by starvation, a classical method to stimulate autophagy, for 4 h can efficiently kill intracellular *M. tuberculosis* reference strain H37Rv by around 50% (Figure 1B). In addition, autophagy induction in RAW264.7 macrophages is able to restrict comparably an *M. tuberculosis* strain belonging to the EAI genotype (Figure 1B). In contrast, autophagy induction by starvation cannot promote the elimination of the strains belonging to the Beijing genotype (BJY and BJN) (Figure 1B). It should be noted that the viability of cells infected with different strains of *M. tuberculosis* is >90%. This is also consistent with previous studies that used an MOI of 10 of *M. tuberculosis* to infect RAW264.7 macrophages for short-term incubation (4 h).[13–15,42,46] In addition, to confirm that the observed mycobacterial control is mediated through the autophagy pathway, we targeted Beclin-1 by siRNAs in RAW264.7

macrophages and determined *M. tuberculosis* survival by CFU analysis. Beclin-1 targeting was verified by immunoblotting (Figure 1C). Depletion of Beclin-1 resulted in a decrease in starvation-induced elimination of *M. tuberculosis* reference strain H37Rv and the EAI strain confirming the role of autophagy in the killing of these mycobacteria (Figure 1D). In addition, Beclin-1 knockdown does not alter the resistance of the Beijing strains to starvation-induced elimination (Figure 1D). Altogether, these results indicate that autophagic control capacity of host cells against different strains of *M. tuberculosis* is not identical and, unlike what has previously been observed with the laboratory reference strains, which are effectively killed by autophagy induction, the Beijing strains are able to resist autophagic restriction by host cells. The observed alteration in autophagic killing capacity against different strains of *M. tuberculosis* was not related to the presence of intact *pks 15/1*, a gene encoding a polyketide synthase required for the synthesis of phenolic glycolipid, a known virulence factor of mycobacteria,[47] as both the BJY (pks 15/1 present) and BJN (pks 15/1 absent) can similarly resist autophagic killing by host cells while the EAI (pks 15/1 present) is efficiently eliminated by autophagy induction (Figure 1B, D).

The Beijing strains avoid autophagic elimination not by inhibiting autophagy-mediated acidification of their phagosomes

As our results showed the greater ability of the Beijing strains to resist starvation-induced autophagic killing by host cells (Figure 1), we set out to determine the molecular mechanism involved. We first examined whether the ability of the Beijing strains to evade autophagic restriction is due to their ability to inhibit autophagy-mediated acidification of their phagosomes. To determine this, we performed confocal microscopy analysis for colocalization of mycobacteria with LTR dye. The results showed that acidification of *M. tuberculosis* H37Rv phagosomes is enhanced upon autophagy induction by starvation, as previously reported for reference strains (Figure 2A, B).[14,15,37,46] In addition, the induction of autophagy by starvation increases the phagosomal acidification of the EAI strain, albeit not statistically significantly (Figure 2A, B). Surprisingly, the acidification of the Beijing strains (BJY and BJN) also appeared to be substantially enhanced upon autophagy induction by starvation (Figure 2A, B). Thus, these results indicated that even though the Beijing strains are able to inhibit the autophagic control by host cells, these bacteria do so not by simply inhibiting the autophagy-mediated acidification of their phagosomes but through another mechanism.

The ability of the Beijing strains to escape autophagic restriction is not conferred by their capacity to block host autophagic flux

In addition to the direct killing mechanism mediated by autophagy whereby mycobacteria are captured into autophagosomes and then delivered into acidic lysosomes, autophagy can eliminate mycobacteria using another indirect mechanism whereby the innocuous cytosolic precursors are captured into autophagosomes, which, during the process of maturation into autolysosomes, partially digest these precursors into killing peptides that are subsequently delivered to mycobacteria via fusion of the autophagosomes/autolysosomes with *M. tuberculosis* phagosomes.[15] Thus, the Beijing strains may evade autophagic killing through their differential ability to block the maturation of other population of cytosolic autophagosomes not containing mycobacteria. To test this possibility, autophagic flux in host cells was measured by fluorescent microscopy analysis for the conversion of RFP^+GFP^+–LC3 puncta (autophagosomes) to RFP^+GFP^-–LC3 puncta (autolysosomes). The results showed that the maturation of autophagosomes into autolysosomes is similarly inhibited in host macrophages infected with different *M. tuberculosis* strains when compared with that of the uninfected cells (Figure 3A, B, white bar) as demonstrated by an increase in the number of RFP^+GFP^+–LC3 puncta in conjunction with no increase in the number of RFP^+GFP^-–LC3 puncta. The block in autophagic flux upon infection was further demonstrated when cells were subjected to autophagy induction by starvation (Figure 3A, B, black bar). These results indicated that all of the tested strains and the reference *M. tuberculosis* H37Rv possess comparable ability to retard autophagic flux in host macrophages. Thus, the greater ability of the Beijing strains to resist autophagic elimination cannot be attributed to their ability to inhibit autophagic maturation in host cells.

The Beijing strains evade starvation-induced autophagic control by suppressing autophagolysosome biogenesis

Some bacteria such as *Helicobacter pylori* and *Mycobacterium marinum* were shown to reside in compartments that are acidified but lack a lysosomal marker cathepsin D in response to autophagy,[48–50] indicating a defect in autophagolysosome biogenesis and thus sparing these bacteria from elimination. Therefore, we sought out to determine whether the Beijing strains may possess a similar ability. As a result, we analyzed the colocalization of different strains of *M. tuberculosis* with LTR and cathepsin D upon autophagy induction by starvation. Confirming our results shown in Figure 2, acidification of

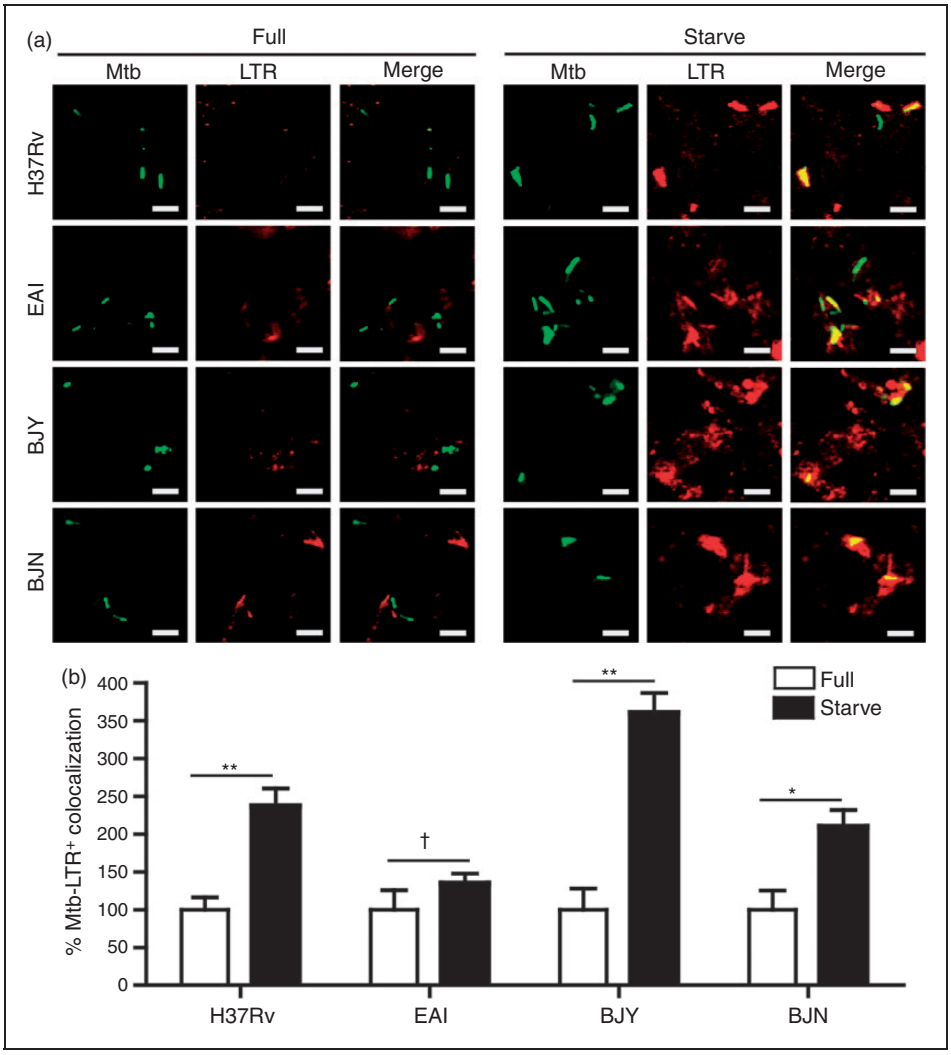

Figure 2. The Beijing strains inhibit starvation-induced autophagic killing not by blocking autophagy-mediated acidification of their phagosomes. (A, B) RAW264.7 macrophages were infected with Alexa-488-labeled mycobacteria at an MOI of 10 for 15 min and subsequently chased for 1 h in complete media. LTR dye was used to stain acidic compartments. Cells were then induced to undergo autophagy by starvation for 2 h. Cells were then processed for confocal microscopy analysis for the colocalization of mycobacteria with LTR. Data are mean ± SEM from at least three independent experiments. At least 50 phagosomes per condition per independent experiment were quantified. $^{**}P < 0.01$, $^{*}P < 0.05$, $\dagger P \geq 0.05$, all relative to the full control set to 100%. EAI, the East African Indian strain with intact *pks15/1*; BJY, the Beijing strain with intact *pks15/1*; BJN, the Beijing strain without intact *pks15/1*.

phagosomes containing different strains of *M. tuberculosis* are substantially augmented (LTR^+) upon treatment of cells with starvation (Figure 4A, C). However, while there was enhanced colocalization of the reference strain H37Rv and the EAI strain with cathepsin D ($CathD^+$) in response to autophagy induction by starvation (Figure 4B, D), there was no increase in the colocalization of the Beijing strains (BJY and BJN) with cathepsin D ($CathD^+$) observed upon starvation treatment (Figure 4B, D). These data indicated that even though their phagosomes are efficiently acidified, the Beijing strains possess an ability to suppress autophagolysosome biogenesis in response to autophagy induction. Note that the anti-cathepsin D Ab used can recognize both the immature and mature forms of cathepsin D and hence the lack of increased colocalization of the Beijing phagosomes with cathepsin D may include both the mature and immature forms. To further confirm autophagy involvement in this process, we depleted Beclin-1 in RAW264.7 macrophages and assessed the colocalization of different mycobacteria with LTR and cathepsin D. Our results showed that autophagy is required for the increased phagosome acidification of all *M. tuberculosis* strains (LTR^+) upon starvation (Figure 5A, B). However, while there was an increase in the colocalization of *M. tuberculosis* reference strain H37Rv and the EAI strain with cathepsin D ($CathD^+$) upon starvation treatment and that this process depends on autophagy (Figure 6A, B), there was no increase in $CathD^+$

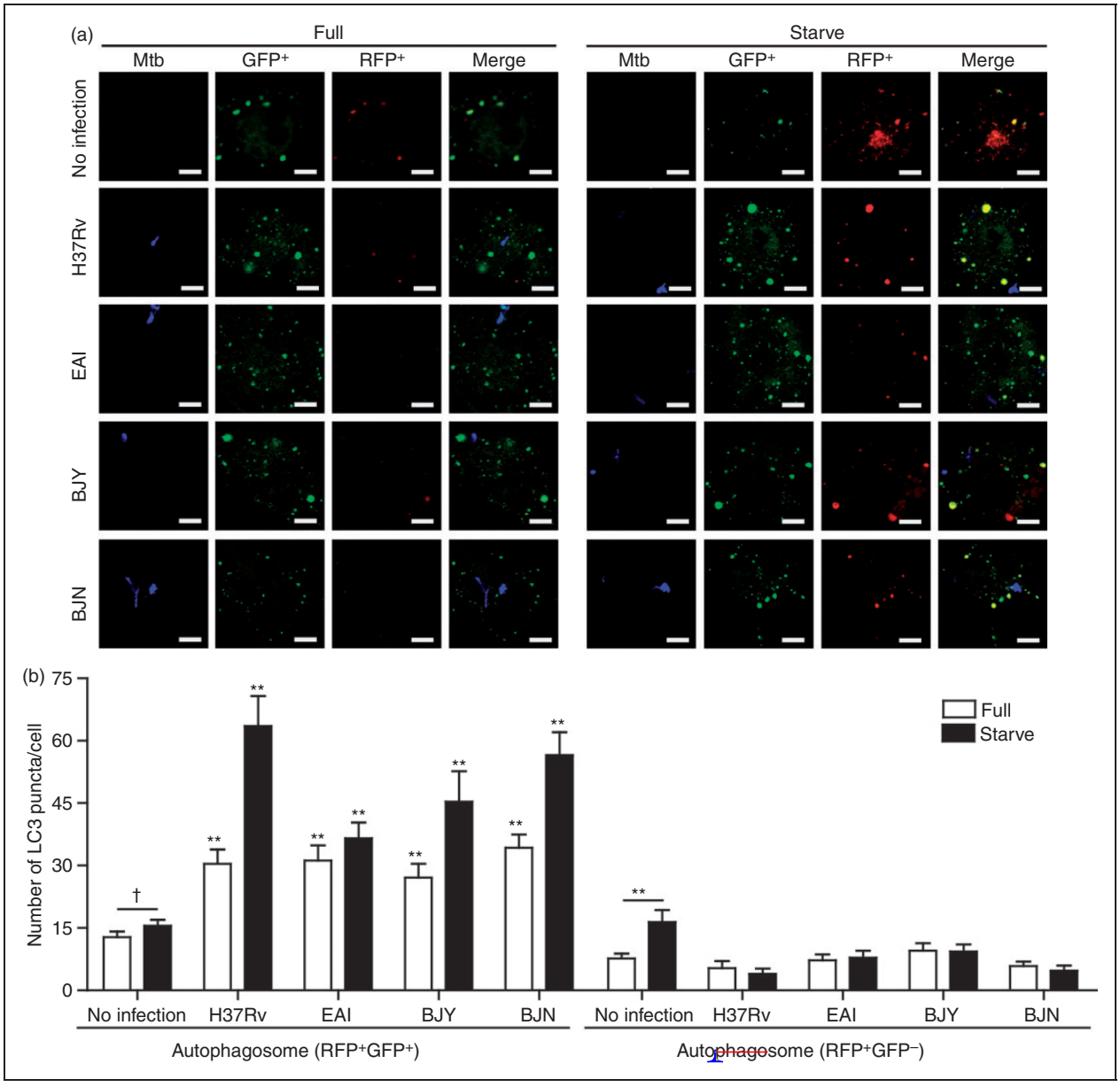

Figure 3. Evasion of starvation-induced autophagic elimination by the Beijing strains is not a result of their differential ability to block autophagic flux in host cells. (A, B) RAW264.7 cells were transfected with cDNAs encoding RFP–GFP–LC3. Transfected cells were then infected with Alexa-405-labeled mycobacteria for 15 min and subsequently chased for 1 h in complete media. Cells were induced to undergo autophagy by starvation for 2 h. Cells were then processed for confocal microscopy (Z-Stacks) analysis for the number of LC3 puncta per cell. Data are mean ± SEM combined from two independent experiments. The number of RFP^+GFP^+–LC3 (autophagosomes) and RFP^+GFP^-–LC3 (autolysosomes) were quantified in Z-Stacks images of 30 cells per condition per independent experiment. $^{**}P < 0.01$ and $\dagger P \geq 0.05$, all relative to full and starvation of uninfected control. EAI, the East African Indian strain with intact *pks15/1*; BJY, the Beijing strain with intact *pks15/1*; BJN, the Beijing strain without intact *pks15/1*.

colocalization with the Beijing strains upon starvation treatment, even in autophagy efficient cells (Figure 6A, B). Altogether, these data indicate that the Beijing strains possess a greater ability to evade starvation-induced autophagic killing by their higher capacity to inhibit autophagolysosome biogenesis as demonstrated by their suppression of the enhanced acquisition of cathepsin D into their phagosomes upon autophagy induction in host cells.

Taken together, our results show that there is a variation in the capacity of different *M. tuberculosis* strains to resist starvation-induced autophagic killing in host macrophages, of which the Beijing strains possess a unique capability to evade autophagic elimination upon autophagy induction. The Beijing strains do so not by simply inhibiting the autophagy-mediated acidification of their phagosomes or by blocking the autophagic flux in host cells, but by inhibiting

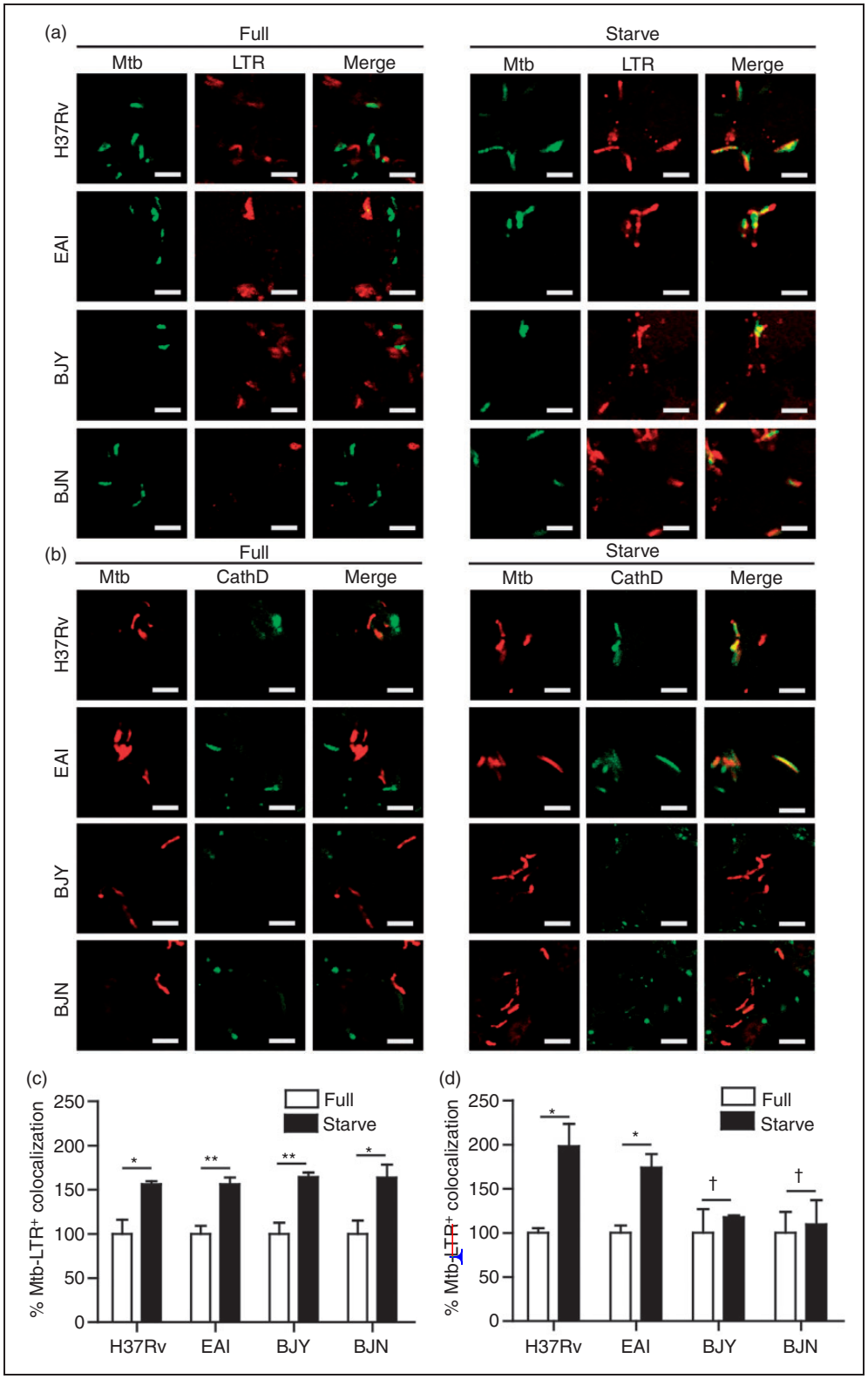

Figure 4. The Beijing strains escape from starvation-induced autophagic elimination by suppressing autophagolysosome biogenesis. (A, C) RAW264.7 cells were infected with Alexa 405-labeled mycobacteria (pseudocolored green) for 15 min and subsequently chased for 1 h in complete media. Acidic compartments were stained with LTR. Cells were then induced to undergo autophagy by starvation for 2 h. Cells were then fixed and processed for confocal microscopy analysis. (B, D) RAW264.7 cells were infected with Alex 405-labeled mycobacteria (pseudocolored red) and processed as described above. Cells were then fixed and stained for cathepsin D. Data are mean ± SEM from at least three independent experiments. At least 50 phagosomes per condition per independent experiment were quantified. $^{**}P < 0.01$, $^{*}P < 0.05$, $\dagger P \geq 0.05$, all relative to the full control set to 100%. EAI, the East African Indian strain with intact *pks15/1*; BJY, the Beijing strain with intact *pks15/1*; BJN, the Beijing strain without intact *pks15/1*.

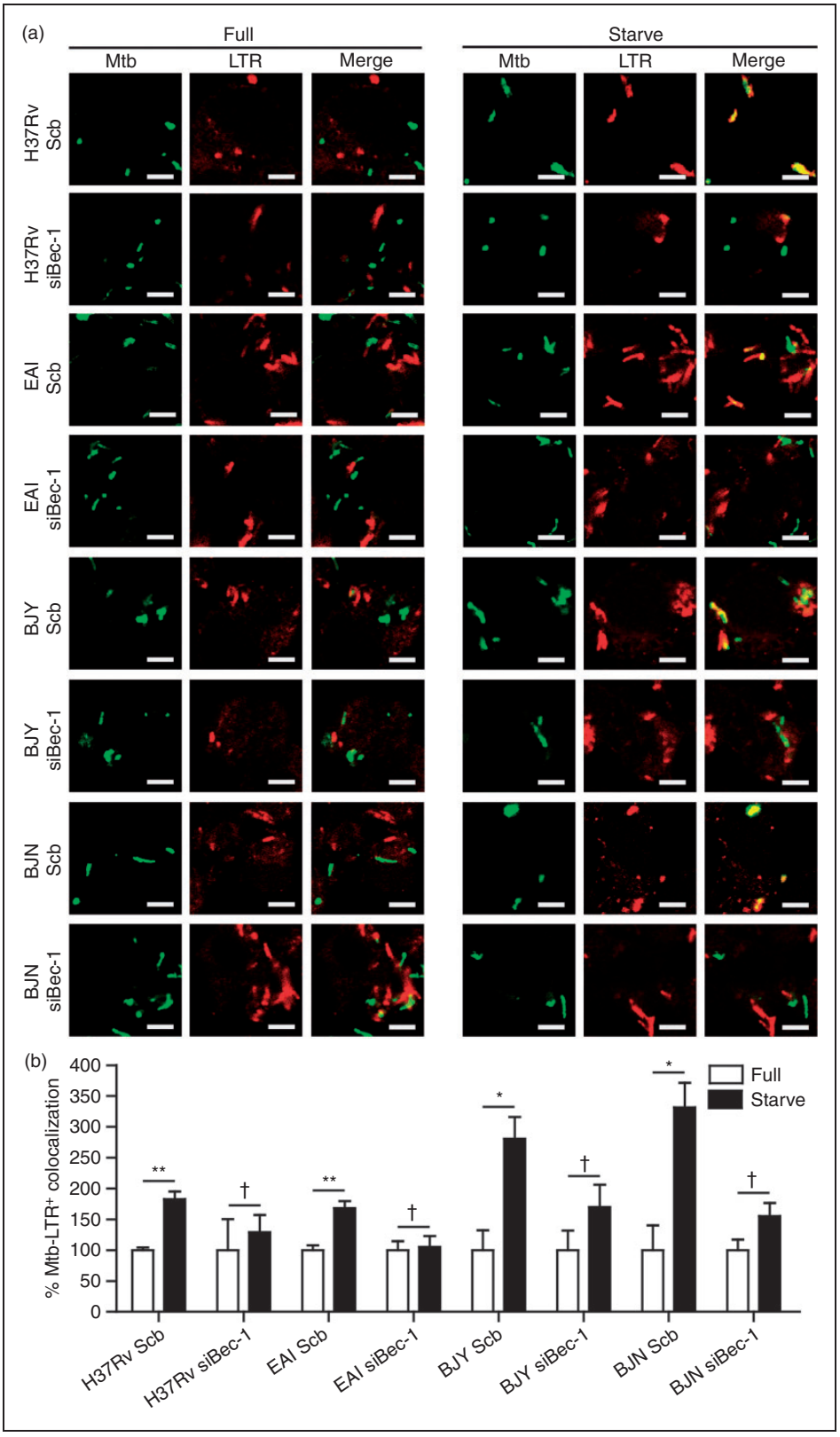

Figure 5. Autophagy is required for the starvation-enhanced acidification of the *M. tuberculosis* reference strain H37Rv and the EAI strain phagosomes. (A, B) RAW264.7 cells were transfected with siRNAs against Beclin-1 or scramble (Scb) control. After 48 h of transfection, cells were infected with Alexa 405-labeled mycobacteria (pseudocolored green) and processed as in Figure 4 (A, C). Data are means ± SEM from at least three independent experiments. At least 50 phagosomes per condition per independent experiment were quantified. $^{**}P < 0.01$, $^{*}P < 0.05$, and $\dagger P \geq 0.05$, all relative to the full control set to 100%. EAI, the East African Indian strain with intact *pks15/1*; BJY, the Beijing strain with intact *pks15/1*; BJN, the Beijing strain without intact *pks15/1*.

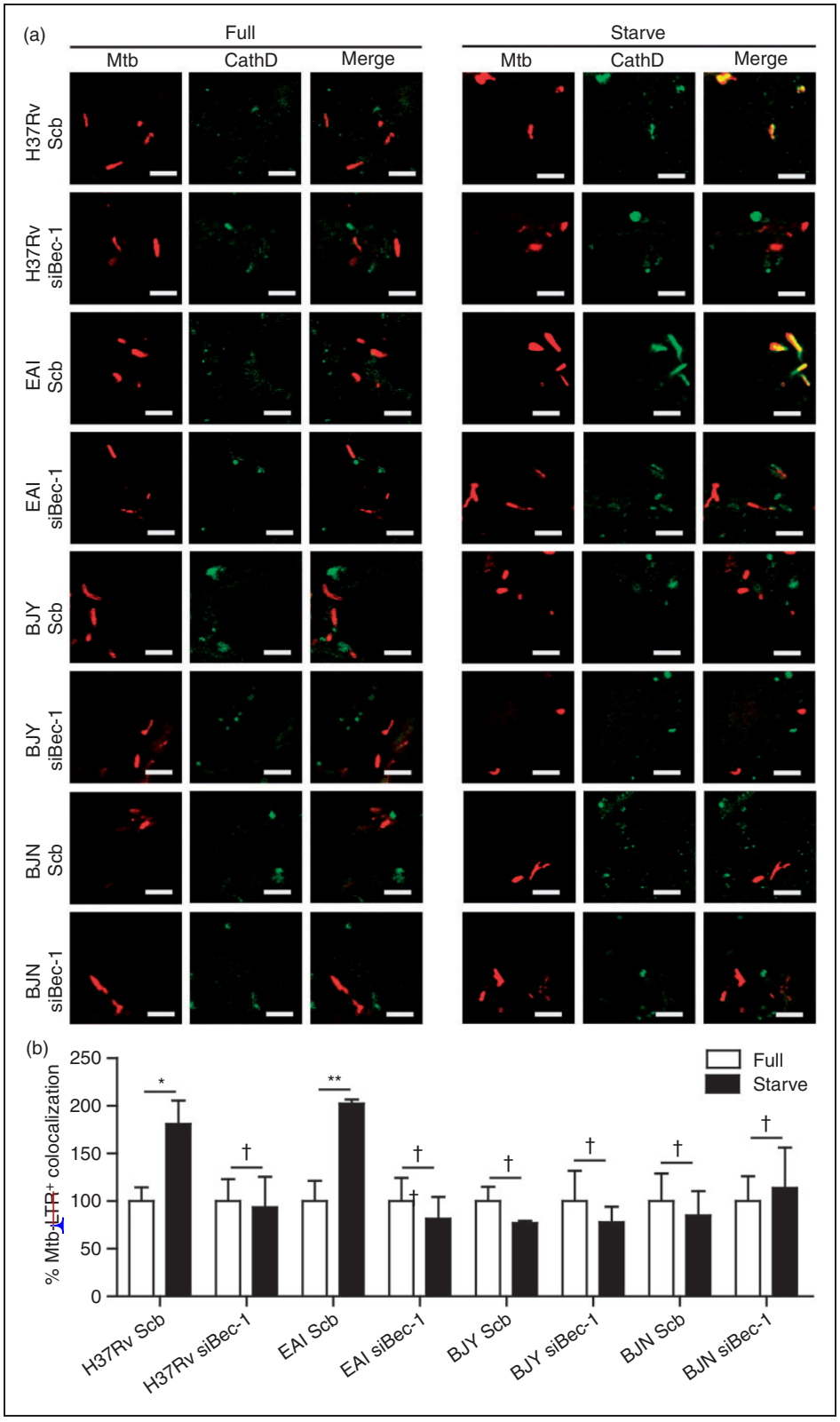

Figure 6. The increased cathepsin D acquisition in response to starvation observed with the *M. tuberculosis* reference strain H37Rv and the EAI strain depends on autophagy. (A, B) RAW264.7 cells were transfected with siRNAs against Beclin-1 or scramble (Scb). After 48 h of transfection, cells were then infected with Alexa 405-labeled mycobacteria (pseudocolored red) and processed for cathepsin D staining as in Figure 4 (B, D). Data are means ± SEM from at least three independent experiments. At least 50 phagosomes per condition per independent experiment were quantified. $^{**}P < 0.01$, $^{*}P < 0.05$, and $\dagger P \geq 0.05$, all relative to the full control set to 100%. EAI, the East African Indian strain with intact *pks15/1*; BJY, the Beijing strain with intact *pks15/1*; BJN, the Beijing strain without intact *pks15/1*.

autophagolysosome biogenesis, as demonstrated by their ability to suppress the increased acquisition of cathepsin D into their compartments upon autophagy induction by starvation and thus escape from autophagic restriction.

Discussion

Autophagy has been demonstrated as an important innate immune defense mechanism utilized by host cells for the elimination of various intracellular bacteria, parasites and viruses.[1,9–11] In addition, induction of autophagy by starvation or other autophagy inducers has been extensively shown to result in the killing of *M. tuberculosis* by disabling the block in phagolysosomal biogenesis imposed by the tubercle bacilli.[12–17] As the ability of autophagy in the restriction of *M. tuberculosis* has been observed in studies using laboratory reference strains but has not been characterized in detail in cells infected with the clinical strains, especially those belonging to the Beijing family, which has previously been shown to be hyper-virulent (associated with their higher ability to survive in host macrophages and cause higher bacterial load and mortality in animal models),[31–36] we set out to examine the autophagic killing capacity of host cells against different strains of *M. tuberculosis*. In our present study, we uncovered the previously unrecognized ability of *M. tuberculosis* Beijing strains to evade starvation-induced autophagic elimination. In addition, we have determined a possible underlying mechanism in which the Beijing strains can escape starvation-induced autophagic killing by inhibiting autophagolysosome biogenesis, as demonstrated by their ability to suppress the enhanced acquisition of cathepsin D into their compartments. As autophagy was previously shown to be a key determinant of host resistance against mycobacterial infection,[20,21,23–28] our findings may explain the hyper-virulent phenotypes associated with the Beijing family,[31–36] which are thought to have resulted from their higher ability to survive in host macrophages, but the underlying mechanism was previously unknown.

Consistent with previous findings that showed the effect of starvation-induced autophagy in the elimination of *M. tuberculosis* reference strains,[12–17] we also observed that starvation treatment of infected RAW macrophages results in the restriction of the laboratory reference strain *M. tuberculosis* H37Rv. In contrast to that of the reference strains, we observed a previously unrecognized ability of *M. tuberculosis* Beijing strains to avoid autophagic killing by blocking autophagolysosome biogenesis. The ability to interfere with the autophagy pathway of host macrophages possessed by the Beijing strains is similar to those possessed by and previously reported for *H. pylori* and *M. marinum*.[48–50] These bacteria were also found to escape from autophagic elimination by inhibiting autophagolysosome biogenesis in host cells in response to autophagy induction, as determined by a decrease in enhanced cathepsin D acquisition into their compartments. Cathepsin D, an aspartic endopeptidase, is synthesized in the rough endoplasmic reticulum as preprocathepsin D and then targeted to various compartments such as phagosomes, autophagosomes, endosomes and lysosomes as procathepsin D.[51–53] Upon transport, inactive procathepsin D is converted into active form of cathepsin D by acidic pH and thus the presence of cathepsin D precursors (and other lysosomal acid hydrolases) in acidified compartments is necessary for their degradative function. Our results showed that although the acidification of *M. tuberculosis* Beijing phagosomes are efficiently increased upon autophagy induction by starvation, these was no increase in the acquisition of cathepsin D into their phagosomes upon starvation treatment, indicating a defect in autophagolysosome biogenesis.

The mechanism by which the Beijing strains inhibit autophagolysosome biogenesis is under investigation by our laboratory. Among several mycobacterial factors previously shown to be involved in *M. tuberculosis* survival in host cells, phenolic glycolipid (PGL) synthesized by a polyketide synthase encoded by intact *pks15/1* was demonstrated to reduce the production of Th1-type cytokines,[47,54] some of which have been shown to induce autophagy.[1] However, our data showed no significant relationship between the presence of intact *pks15/1* and the ability of mycobacteria to resist starvation-induced autophagic elimination, thus indicating that PGL is not the factor that renders the Beijing strains to escape autophagic restriction. Interestingly, in the case of *H. pylori*, which was also shown to evade autophagic killing by residing in acidic compartments that lack cathepsin D in response to autophagy,[48–50] it was previously reported that the maturation of procathepsin D into the mature form, as well as its sorting in mammalian cells, can be impaired by *H. pylori* vacuolating toxin.[55] Whether *M. tuberculosis* Beijing strains possess a similar or equivalent protein is not known. As a recent whole-genome sequencing of strains belonging to the *M. tuberculosis* Beijing family has been conducted,[56] mining and comparing sequencing data between Beijing and non-Beijing strains may give insight into potential candidate genes that may play a role in the autophagic evasion. In addition to the bacterial factor, two host proteins, Rab8b and its downstream effector TANK-binding kinase 1 (TBK1), have been shown to play prominent roles in autophagy-mediated mycobacterial phagosome maturation, as demonstrated by decreased mycobacterial phagosome acidification and cathepsin D acquisition upon siRNA-mediated depletion of Rab8b or pharmacological inhibition of TBK1.[37] Whether the Beijing strains are able to interfere with Rab8b and TBK1 functions in

autophagy-mediated mycobacterial phagosome maturation is a subject of our study.

Besides our principle finding, discussed above, our data also showed that the acquisition of cathepsin D into the EAI phagosomes is substantially enhanced upon autophagy induction, similar to what has previously been observed with *M. tuberculosis* reference strains.[12–17] Interestingly, previous studies showed that the EAI strains possess a higher ability to stimulate TNF-α synthesis in infected host cells when compared with that of the Beijing strains.[40,57] As TNF-α has been shown to be a potent autophagic inducer,[1] the enhanced production of TNF-α upon EAI strain infection may augment the autophagy induction level in our system and may thus help increase the acquisition of cathepsin D into the EAI phagosomes. Whether the EAI strain possesses greater ability to induce host autophagy as a result of increased TNF-α production awaits further examination. If the EAI strain is found to enhance host autophagy, this may, in turn, explain the low virulence phenotypes associated with this *M. tuberculosis* family, as demonstrated by their reduced transmissibility, low level of growth inside macrophages, and decreased bacterial burden (100-fold lower when compared with that of the Beijing strains) and mortality in mouse models.[29,38] In addition, we also observed an enhanced growth of the Beijing strains inside host cells upon autophagy induction, albeit not a statistically significant increase, and this effect was decreased in cells deficient of Beclin-1 (Figure 1B, D). Whether the Beijing strains can, in addition to resisting autophagic killing by host cells, subvert autophagy pathway for their own growth inside macrophages await further investigation.

Funding

This work was supported by Thailand Research Fund, Office of the Higher Education Commission, and Mahidol University; National Science and Technology Development Agency; and Faculty of Science, Mahidol University.

Conflict of interest

The authors do not have any potential conflicts of interest to declare.

References

1. Deretic V, Saitoh T and Akira S. Autophagy in infection, inflammation and immunity. *Nat Rev Immunol* 2013; 13: 722–737.
2. Levine B, Mizushima N and Virgin HW. Autophagy in immunity and inflammation. *Nature* 2011; 469: 323–335.
3. Mizushima N, Yoshimori T and Ohsumi Y. The role of Atg proteins in autophagosome formation. *Annu Rev Cell Dev Biol* 2011; 27: 107–132.
4. Yang Z and Klionsky DJ. Mammalian autophagy: core molecular machinery and signaling regulation. *Curr Opin Cell Biol* 2010; 22: 124–131.
5. Randow F and Munz C. Autophagy in the regulation of pathogen replication and adaptive immunity. *Trends Immunol* 2012; 33: 475–487.
6. Boyle KB and Randow F. The role of 'eat-me' signals and autophagy cargo receptors in innate immunity. *Curr Opin Microbiol* 2013; 16: 339–348.
7. Johansen T and Lamark T. Selective autophagy mediated by autophagic adapter proteins. *Autophagy* 2011; 7: 279–296.
8. Mandell MA, Jain A, Arko-Mensah J, et al. TRIM proteins regulate autophagy and can target autophagic substrates by direct recognition. *Dev Cell* 2014; 30: 394–409.
9. Deretic V and Levine B. Autophagy, immunity, and microbial adaptations. *Cell Host Microbe* 2009; 5: 527–449.
10. Gomes LC and Dikic I. Autophagy in antimicrobial immunity. *Mol Cell* 2014; 54: 224–233.
11. Huang J and Brumell JH. Bacteria-autophagy interplay: a battle for survival. *Nat Rev Microbiol* 2014; 12: 101–114.
12. Alonso S, Pethe K, Russell DG and Purdy GE. Lysosomal killing of *Mycobacterium* mediated by ubiquitin-derived peptides is enhanced by autophagy. *Proc Natl Acad Sci U S A* 2007; 104: 6031–6036.
13. Delgado MA, Elmaoued RA, Davis AS, et al. Toll-like receptors control autophagy. *EMBO J* 2008; 27: 1110–1121.
14. Gutierrez MG, Master SS, Singh SB, et al. Autophagy is a defense mechanism inhibiting BCG and *Mycobacterium tuberculosis* survival in infected macrophages. *Cell* 2004; 119: 753–766.
15. Ponpuak M, Davis AS, Roberts EA, et al. Delivery of cytosolic components by autophagic adaptor protein p62 endows autophagosomes with unique antimicrobial properties. *Immunity* 2010; 32: 329–341.
16. Singh SB, Davis AS, Taylor GA and Deretic V. Human IRGM induces autophagy to eliminate intracellular mycobacteria. *Science* 2006; 313: 1438–1441.
17. Xu Y, Jagannath C, Liu XD, et al. Toll-like receptor 4 is a sensor for autophagy associated with innate immunity. *Immunity* 2007; 27: 135–144.
18. Vergne I, Chua J, Singh SB and Deretic V. Cell biology of *Mycobacterium tuberculosis* phagosome. *Annu Rev Cell Dev Biol* 2004; 20: 367–394.
19. Ponpuak M and Deretic V. Autophagy and p62/sequestosome 1 generate neo-antimicrobial peptides (cryptides) from cytosolic proteins. *Autophagy* 2011; 7: 336–337.
20. Castillo EF, Dekonenko A, Arko-Mensah J, et al. Autophagy protects against active tuberculosis by suppressing bacterial burden and inflammation. *Proc Natl Acad Sci U S A* 2012; 109: E3168–E3176.
21. Watson RO, Manzanillo PS and Cox JS. Extracellular *M. tuberculosis* DNA targets bacteria for autophagy by activating the host DNA-sensing pathway. *Cell* 2012; 150: 803–815.
22. Kim JJ, Lee HM, Shin DM, et al. Host cell autophagy activated by antibiotics is required for their effective antimycobacterial drug action. *Cell Host Microbe* 2012; 11: 457–468.
23. Kumar D, Nath L, Kamal MA, et al. Genome-wide analysis of the host intracellular network that regulates survival of *Mycobacterium tuberculosis*. *Cell* 2010; 140: 731–743.
24. Bahari G, Hashemi M, Taheri M, et al. Association of IRGM polymorphisms and susceptibility to pulmonary tuberculosis in Zahedan, Southeast Iran. ScientificWorldJournal. 2012; 2012: 950801.
25. Che N, Li S, Gao T, et al. Identification of a novel IRGM promoter single nucleotide polymorphism associated with tuberculosis. *Clin Chim Acta* 2010; 411: 1645–1649.
26. Intemann CD, Thye T, Niemann S, et al. Autophagy gene variant IRGM -261T contributes to protection from tuberculosis caused by *Mycobacterium tuberculosis* but not by *M. africanum* strains. *PLoS Pathog* 2009; 5: e1000577.

27. King KY, Lew JD, Ha NP, et al. Polymorphic allele of human IRGM1 is associated with susceptibility to tuberculosis in African Americans. *PloS One* 2011; 6: e16317.
28. Li CM, Campbell SJ, Kumararatne DS, et al. Association of a polymorphism in the P2X7 gene with tuberculosis in a Gambian population. *J Infect Dis* 2002; 186: 1458–1462.
29. Reiling N, Homolka S, Walter K, et al. Clade-specific virulence patterns of *Mycobacterium tuberculosis* complex strains in human primary macrophages and aerogenically infected mice. *mBio* 2013; 4.
30. Brudey K, Driscoll JR, Rigouts L, et al. *Mycobacterium tuberculosis* complex genetic diversity: mining the fourth international spoligotyping database (SpolDB4) for classification, population genetics and epidemiology. *BMC Microbiol* 2006; 6: 23.
31. Dormans J, Burger M, Aguilar D, et al. Correlation of virulence, lung pathology, bacterial load and delayed type hypersensitivity responses after infection with different *Mycobacterium tuberculosis* genotypes in a BALB/c mouse model. *Clin Exp Immunol* 2004; 137: 460–468.
32. Hanekom M, van der Spuy GD, Streicher E, et al. A recently evolved sublineage of the *Mycobacterium tuberculosis* Beijing strain family is associated with an increased ability to spread and cause disease. *J Clin Microbiol* 2007; 45: 1483–1490.
33. Portevin D, Gagneux S, Comas I and Young D. Human macrophage responses to clinical isolates from the *Mycobacterium tuberculosis* complex discriminate between ancient and modern lineages. *PLoS Pathog* 2011; 7: e1001307.
34. Tsenova L, Ellison E, Harbacheuski R, et al. Virulence of selected *Mycobacterium tuberculosis* clinical isolates in the rabbit model of meningitis is dependent on phenolic glycolipid produced by the bacilli. *J Infect Dis* 2005; 192: 98–106.
35. van der Spuy GD, Kremer K, Ndabambi SL, et al. Changing *Mycobacterium tuberculosis* population highlights clade-specific pathogenic characteristics. *Tuberculosis* 2009; 89: 120–125.
36. Zhang M, Gong J, Yang Z, et al. Enhanced capacity of a widespread strain of *Mycobacterium tuberculosis* to grow in human macrophages. *J Infect Dis* 1999; 179: 1213–1217.
37. Pilli M, Arko-Mensah J, Ponpuak M, et al. TBK-1 promotes autophagy-mediated antimicrobial defense by controlling autophagosome maturation. *Immunity* 2012; 37: 223–234.
38. Albanna AS, Reed MB, Kotar KV, et al. Reduced transmissibility of East African Indian strains of *Mycobacterium tuberculosis*. *PloS One* 2011; 6: e25075.
39. Yorsangsukkamol J, Chaiprasert A, Prammananan T, et al. Molecular analysis of *Mycobacterium tuberculosis* from tuberculous meningitis patients in Thailand. *Tuberculosis* 2009; 89: 304–309.
40. Yorsangsukkamol J, Chaiprasert A, Palaga T, et al. Apoptosis, production of MMP9, VEGF, TNF-alpha and intracellular growth of M. tuberculosis for different genotypes and different pks5/1 genes. *Asian Pac J Allergy Immunol* 2011; 29: 240–251.
41. Kimura S, Noda T and Yoshimori T. Dissection of the autophagosome maturation process by a novel reporter protein, tandem fluorescent-tagged LC3. *Autophagy* 2007; 3: 452–460.
42. Ponpuak M, Delgado MA, Elmaoued RA and Deretic V. Monitoring autophagy during *Mycobacterium tuberculosis* infection. *Methods Enzymol* 2009; 452: 345–361.
43. Floto RA, Sarkar S, Perlstein EO, et al. Small molecule enhancers of rapamycin-induced TOR inhibition promote autophagy, reduce toxicity in Huntington's disease models and enhance killing of mycobacteria by macrophages. *Autophagy* 2007; 3: 620–622.
44. Yuk JM, Shin DM, Lee HM, et al. Vitamin D3 induces autophagy in human monocytes/macrophages via cathelicidin. *Cell Host Microbe* 2009; 6: 231–243.
45. Zullo AJ and Lee S. Mycobacterial induction of autophagy varies by species and occurs independently of mammalian target of rapamycin inhibition. *J Biol Chem* 2012; 287: 12668–12678.
46. Harris J, De Haro SA, Master SS, et al. T helper 2 cytokines inhibit autophagic control of intracellular *Mycobacterium tuberculosis*. *Immunity* 2007; 27: 505–517.
47. Hanekom M, Gey van Pittius NC, McEvoy C, et al. *Mycobacterium tuberculosis* Beijing genotype: a template for success. *Tuberculosis* 2011; 91: 510–523.
48. Lerena MC and Colombo MI. *Mycobacterium marinum* induces a marked LC3 recruitment to its containing phagosome that depends on a functional ESX-1 secretion system. *Cell Microbiol* 2011; 13: 814–835.
49. Terebiznik MR, Raju D, Vazquez CL, et al. Effect of *Helicobacter pylori*'s vacuolating cytotoxin on the autophagy pathway in gastric epithelial cells. *Autophagy* 2009; 5: 370–379.
50. Terebiznik MR, Vazquez CL, Torbicki K, et al. *Helicobacter pylori* VacA toxin promotes bacterial intracellular survival in gastric epithelial cells. *Infect Immun* 2006; 74: 6599–6614.
51. Hasilik A and Neufeld EF. Biosynthesis of lysosomal enzymes in fibroblasts. Synthesis as precursors of higher molecular weight. *J Biol Chem* 1980; 255: 4937–4945.
52. Kornfeld S. Lysosomal enzyme targeting. *Biochem Soc Trans* 1990; 18: 367–374.
53. Benes P, Vetvicka V and Fusek M. Cathepsin D—many functions of one aspartic protease. *Crit Rev Oncol Hematol* 2008; 68: 12–28.
54. Reed MB, Domenech P, Manca C, et al. A glycolipid of hypervirulent tuberculosis strains that inhibits the innate immune response. *Nature* 2004; 431: 84–87.
55. Satin B, Norais N, Telford J, et al. Effect of *Helicobacter pylori* vacuolating toxin on maturation and extracellular release of procathepsin D and on epidermal growth factor degradation. *J Biol Chem* 1997; 272: 25022–25028.
56. Merker M, Blin C, Mona S, et al. Evolutionary history and global spread of the *Mycobacterium tuberculosis* Beijing lineage. *Nat Genet* 2015; 47: 242–249.
57. Wang C, Peyron P, Mestre O, et al. Innate immune response to *Mycobacterium tuberculosis* Beijing and other genotypes. *PloS One* 2010; 5: e13594.

Available online at www.sciencedirect.com

ScienceDirect

Current Opinion in Cell Biology

Secretory autophagy

Marisa Ponpuak[1,2], Michael A Mandell[2], Tomonori Kimura[2], Santosh Chauhan[2], Cédric Cleyrat[3] and Vojo Deretic[2]

Autophagy, once viewed exclusively as a cytoplasmic autodigestive process, has its less intuitive but biologically distinct non-degradative roles. One manifestation of these functions of the autophagic machinery is the process termed secretory autophagy. Secretory autophagy facilitates unconventional secretion of the cytosolic cargo such as leaderless cytosolic proteins, which unlike proteins endowed with the leader (N-terminal signal) peptides cannot enter the conventional secretory pathway normally operating via the endoplasmic reticulum and the Golgi apparatus. Secretory autophagy may also export more complex cytoplasmic cargo and help excrete particulate substrates. Autophagic machinery and autophagy as a process also affect conventional secretory pathways, including the constitutive and regulated secretion, as well as promote alternative routes for trafficking of integral membrane proteins to the plasma membrane. Thus, autophagy and autophagic factors are intimately intertwined at many levels with secretion and polarized sorting in eukaryotic cells.

Addresses
[1] Department of Microbiology, Faculty of Science, Mahidol University, 272 Rama VI Road, Ratchathewi, Bangkok 10400, Thailand
[2] Department of Molecular Genetics and Microbiology, University of New Mexico Health Sciences Center, 915 Camino de Salud NE, Albuquerque, NM 87131, USA
[3] Department of Pathology, University of New Mexico Health Sciences Center, 915 Camino de Salud NE, Albuquerque, NM 87131, USA

Corresponding author: Vojo Deretic, Vojo (vderetic@salud.unm.edu)
URL: http://mgm.unm.edu/

Current Opinion in Cell Biology 2015, **35**:106–116

This review comes from a themed issue on **Cell organelles**

Edited by **Maya Schuldiner** and **Wei Guo**

http://dx.doi.org/10.1016/j.ceb.2015.04.016

Introduction

The majority of eukaryotic secreted proteins are endowed with N-terminal signal peptides, which authorize them to enter the endoplasmic reticulum (ER) and follow a well-defined secretory pathway via the Golgi apparatus for delivery to the extracellular space (Figure 1). However, an exclusive subset of purely cytosolic proteins, lacking signal peptides and thus not capable of entering the ER, are nonetheless actively secreted from the cells to perform their extracellular biological functions. This phenomenon, termed unconventional secretion (Figure 1), includes several distinct processes [1,2]. One form of unconventional secretion (secretory autophagy [3]) is associated specifically with the autophagy pathway defined by ATG factors that govern the biogenesis of autophagic membranes [4]. The ATG factors directing canonical autophagy include ULKs (mammalian paralogs of yeast Atg1, an upstream protein kinase), Beclins (mammalian paralogs of yeast Atg6, a key component of the lipid kinase VPS34, which generates phosphatidylinositiol 3-phosphate/PI3P), and LC3s and GABARAPs (mammalian paralogs of the yeast Atg8). Classically, the above factors result in the formation of double membrane autophagosomes, which in cooperation with cargo receptors such as p62/SQSTM1 [5], capture and eliminate cytoplasmic components. Conventionally, this occurs through degradation upon fusion of autophagosomes with lysosomes. In contrast to degradative autophagy, the autophagic machinery, through a shared but partially divergent pathway, may lead to secretion/expulsion of cytoplasmic constituents instead of their degradation. Either way, the cell gets rid of the captured cytoplasmic material, but the biological functions and repercussions are different.

The degradative canonical autophagy pathway, also referred to as macroautophagy, is classically considered together with microautophagy and chaperone-mediated autophagy as a collection of cytoplasmic self-digestion processes merging with lysosomes, whereby they carry out: (i) nutrient recycling functions at times of starvation by bulk digestion of the cytoplasm [6]; and (ii) cytoplasmic quality control functions [7] by removing a wide spectrum of substrates such as aggregation-prone or aggregated proteins [5,8], damaged organelles such as irreversibly depolarized mitochondria [9], and invading microbes [10]. These well-studied aspects of degradative autophagy render it an attractive target for disease treatments [11]. In contrast to degradative autophagy, it has become slowly but increasingly apparent that autophagy has other, sometimes biogenesis-associated functions as well as a role in unconventional secretion (secretory autophagy; Figure 2). Secretory autophagy exports a range of cytoplasmic substrates (Table 1) [2,12–15,16••,17•,18••,19,20•,21••]. This review primarily examines the developing concept of secretory autophagy including its cargo, biological functions, and the currently limited understanding of its regulation. We will furthermore provide a brief update on the

Figure 1

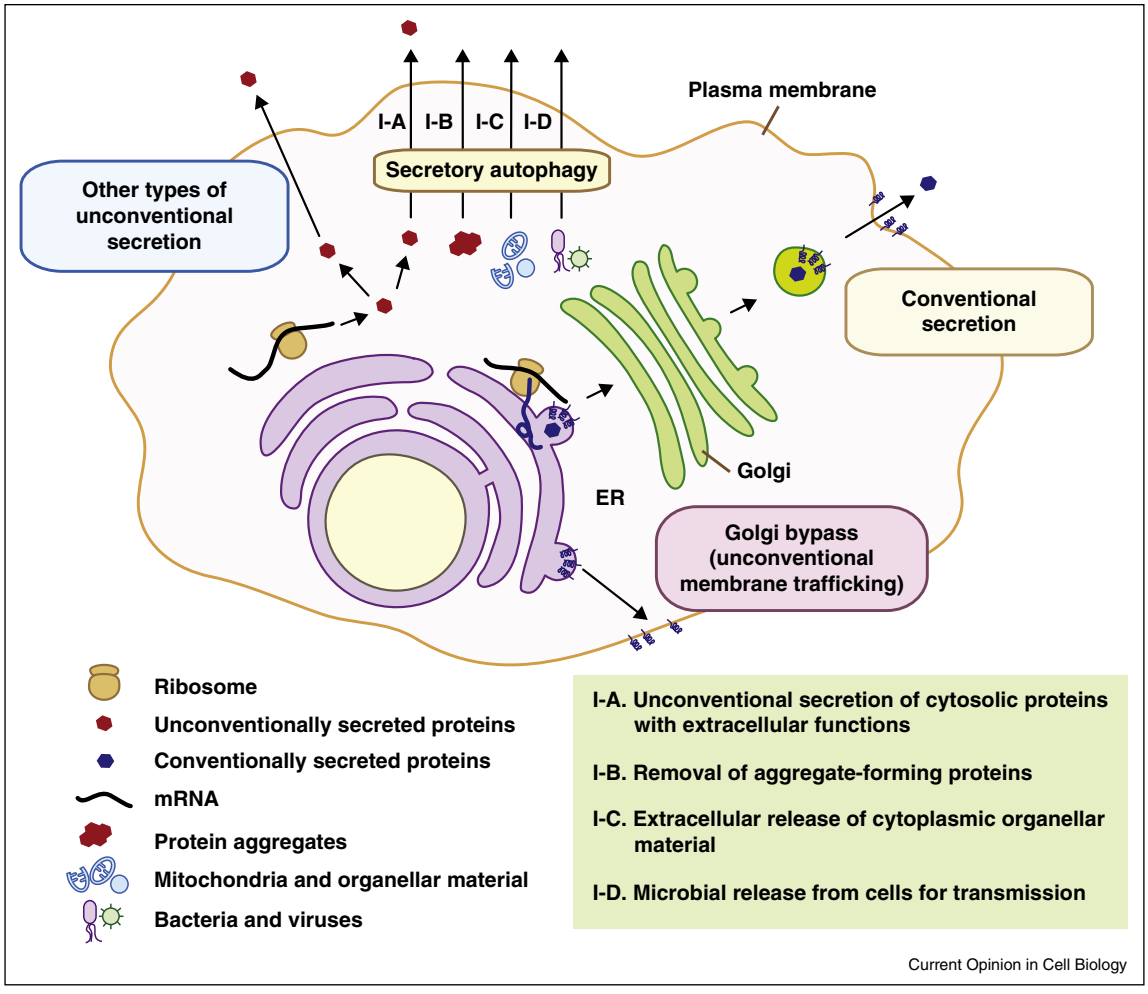

Conventional and unconventional secretion with emphasis on secretory autophagy. In conventional secretion, proteins possessing a signal peptide enter the lumen of the ER followed by the Golgi apparatus for secretion at the plasma membrane. In unconventional secretion, cytoplasmic proteins that lack a signal sequence and do not get delivered to the lumen of the ER are transported into the extracellular milieu via diverse unconventional secretory pathways, including secretory autophagy. For the latter, depicted are four subtypes (I-A to I-D) differentiated based on the substrates (see also Table 1).

complementary processes of autophagy intersections [15] with the conventional (constitutive and regulated) secretion as well as with vectorial membrane protein trafficking and polarized sorting in mammalian cells. Although these latter processes should not be confused with the *sensu stricto* secretory autophagy, they complete the picture of the multi-tiered overlaps between autophagy and secretion in eukaryotic cells.

Secretory autophagy as a form of unconventional protein secretion

One of the earliest examples of the unconventional secretion of a cytosolic protein is the non-lytic export from the mammalian cells of the cytosolic protein IL-1β, a proinflammatory cytokine with important biological roles in mammalian systems. IL-1β lacks a leader/signal peptide and resides in the cytosol as an inactive precursor; upon activation of the cytoplasmic protein platform termed the inflammasome [22], IL-1β undergoes proteolytic processing and is exported outside of the cells in membranous carriers first observed by Rubartelli *et al.* [23,24]. Export is important for IL-1β biological function, as only upon its secretion can IL-1β meet its destination — IL-1 receptors on other cells — thereby evoking pro-inflammatory signaling. The nature of the membranous carriers exporting IL-1β from the cells and the mechanism of the unconventional secretion processes involved have been a matter of debate. Recently, the secretion of IL-1β has been linked to the autophagy machinery [1,3,14]. These studies have been extended

and expanded by several groups [19,20•,25,26••]. This was made possible in part by the details of autophagy-assisted unconventional secretion uncovered in yeast through the power of genetics [12,13]. The yeast studies, although recently re-interpreted by one of the groups [27], have paved the way for reports on autophagic secretion in mammalian cells of a number of cytosolic proteins [3,14,19,20•,25,26••], in keeping with the earlier definition of a large repertoire secretome induced by starvation [28], a classical signal for induction of autophagy.

Mechanisms of secretory autophagy in yeast and mammalian cells

The studies in yeast [12,13] have identified that secretion of a substrate termed Acb1 depends on Atg genes controlling autophagosome formation, Golgi reassembly stacking protein (GRASP in mammals/Grh1 in yeast; known for its conserved role in unconventional secretion [1,29]), ESCRT proteins involved in endosomal multivesicular bodies (MVB) biogenesis and sorting, and SNAREs important for vesicle fusion at the plasma membrane [12,13].

In mammalian cells, secretory autophagy of IL-1β depends upon the autophagy factor Atg5, a GRASP homolog (GRASP55) also affecting general autophagy, and a small GTPase Rab8a, which regulates vectorial sorting to plasma membrane [14]. Rab8a has also been reported to regulate autophagic secretion of other cargo, including α-synuclein [17•], a major constituent of Lewy bodies, which are the hallmark protein aggregates associated with Parkinson's disease. Secretion of α-synuclein required autophagosome formation as demonstrated by the inhibitory effects of 3MA and siRNA-mediated knockdown of Atg5. Secretory autophagy of α-synuclein (a cytosolic cargo) was enhanced by inhibiting fusion of autophagosomes with lysosome using bafilomycin A1 [17•]. Likewise, downregulation of HDAC6, with accompanied increased in acetylation of microtubules and decreased autolysosomal fusion, increased α-synuclein secretion [17•]. Pharmacological inhibition of degradative autophagic flux, decrease of autophagosomal minus-end motility, and increase of plus end vectorial transport along microtubules may divert autophagosomal organelles (including amphisomes) from degradation into the secretory autophagy pathway. Depending on circumstances, both IL-1β (reviewed in [25]) and α-synuclein [30] can be substrates for autophagic degradation. Thus, degradative and secretory autophagy may in some cases diverge from common precursors, and fate of the cargo (degradation vs. secretion) determined by trafficking directly or via an intermediate toward the lysosomes or plasma membrane. In support of the aforementioned concept, a clear differences between the two pathways identified in yeast is that secretory autophagy requires a SNARE (Sso1) necessary for plasma membrane fusion whereas it is independent of the vacuole fusion SNARE complex (VAM7/VAM3) leading to degradation [12]. Analogous dichotomy is seen in mammalian cells: whereas Rab8a, a regulator of polarized sorting to the plasma membrane, was shown to be needed for secretory autophagy [14,17•], its closely related isoform Rab8b may be more important for maturation of the degradative autophagosome [31].

The similarity between secretory and degradative autophagosome formation extends to the discovery of a structure that is associated with secretory autophagy in yeast, the compartment for unconventional protein secretion (CUPS) [32], which morphologically resembles the mammalian omegasome, an ER-derived precursor structure that acts as a cradle for the generation of degradative autophagosomes [33]. Yeast GRASP re-localizes to CUPS under starvation conditions [32]. Both CUPS and omegasome can be induced by starvation [32,33] and their structures are similarly enriched in PI3P and Atg proteins. As CUPS has yet to be demonstrated in mammalian cells and omegasome has not been shown in yeast, whether these two structures are distinct or similar requires further investigation. In addition, whether GRASP, a marker for CUPS, can be found at the mammalian omegasome upon starvation is unknown and this may help resolve the identity of the two structures. If these two structures are the same, this would support the idea that the processes of autophagosome formation for secretory and degradative autophagy share the same set of precursor and Atg proteins and that the two pathways diverge at a later point in the pathway.

In contrast to the above simplistic model, which likens CUPS in yeast to omegasomes (precursors to autophagic organelles in mammals), a recent study in yeast argues that CUPS are distinct from autophagosomes [34]. Further details are now available on CUPS [34]: CUPS are formed by the fusion of at least two classes of membranes. One comes from early Golgi containing Grh1 (yeast equivalent of GRASP), Bug1, the membrane tethering factor Uso1, and the t-SNARE Sed5. The other membrane sources are vesicles coming from the late Golgi in a Sec7-dependent and Pik1-dependent manner. The fusion of these two sets of membranes is likely mediated by Sed5 and Uso1. CUPS then mature by addition of membranes from the endosomes by a Vps34-dependent process. More work in both mammalian and yeast systems is needed to determine whether precursors discussed above lead to functionally related (or different) compartments of relevance for secretory processes.

Based on the studies in yeast [12,13], the cytosolic secretory cargo may be engulfed into an autophagosome but may alternatively include MVB-like intermediates [1] (Figure 2). In mammalian cells, MVBs are affected by autophagic machinery since autophagosomes and MVBs interact to form hybrid structures referred to as amphisomes

Figure 2

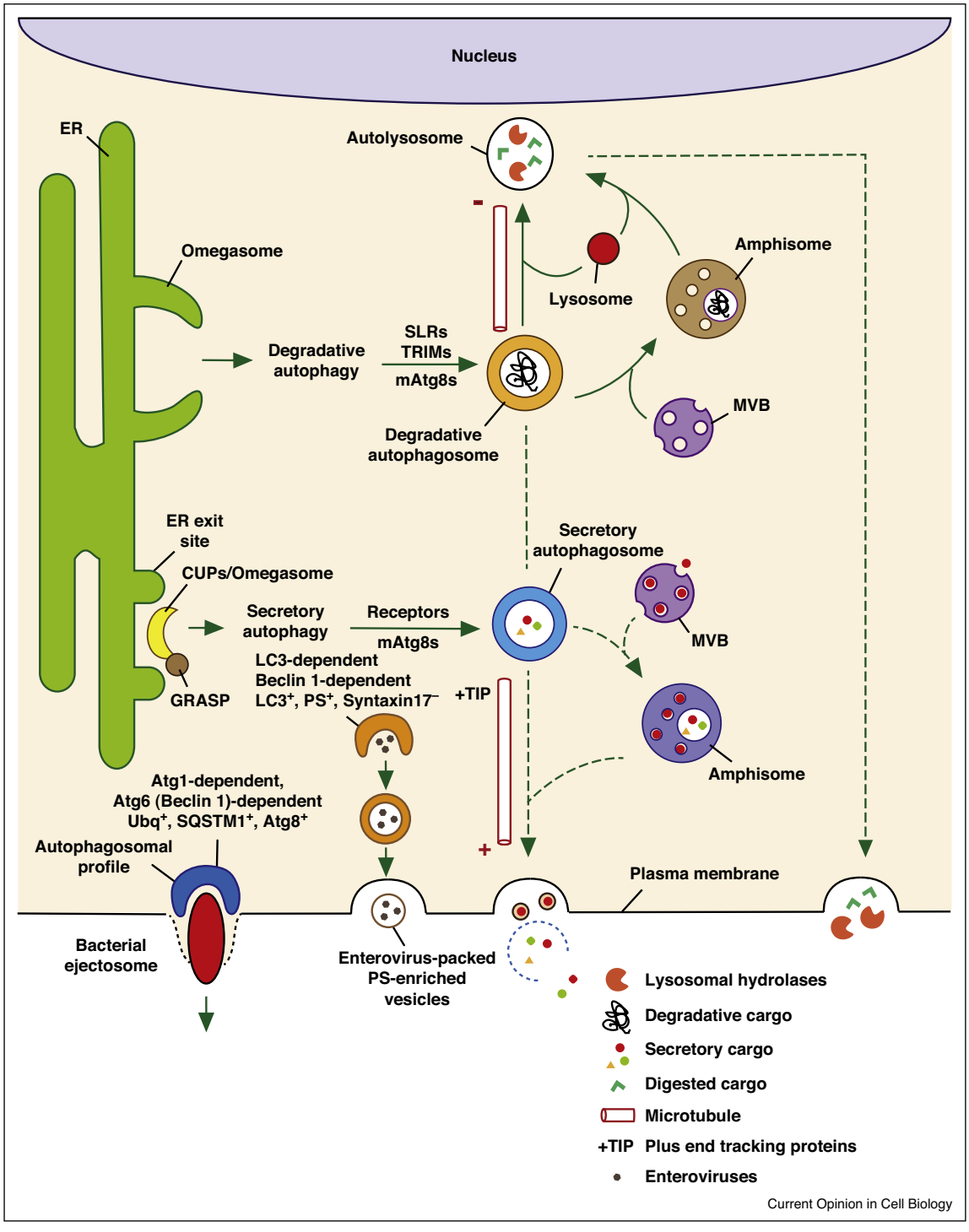

Proposed model for the divergent points of degradative versus secretory autophagy. At the ER exit sites, omegasomes (in mammalian cells) facilitate the formation of degradative autophagosomes, of which the elongation and closure require LC3B. The degradative cargo can be captured/delivered into the degradative autophagosomes via autophagy receptors such as SLRs and TRIMs. Upon closure, degradative autophagosomes display motility toward the minus end of the microtubules where they fuse with lysosomes resulting in the degradation of the engulfed contents by lysosomal hydrolases. Conversely in secretory autophagy, CUPS (in yeast) or their putative (see text for discussion) equivalents in mammalian cells that may be omegasomes located near ER exit sites marked by GRASP localization (as shown for CUPS) aid the formation of secretory autophagosomes. The specific members of mammalian Atg8s that facilitate this process and receptors that capture the cargo into secretory autophagosomes have not been defined. Secretory autophagosomes show vectorial motility toward the plus end of the microtubules and eventually fuse with the plasma membrane releasing their contents into the extracellular environment. The vectorial directionality

[35,36]. Autophagy could export cytosolic substrates directly or deliver them to an MVB intermediate for subsequent release via MVB–plasma membrane fusion. An analogous process has been observed in maturing reticulocytes in which LC3-positive MVB were shown to fuse with the plasma membrane *in vitro*, and similar vesicles were identified in peripheral blood [37•]. Indeed, several overlaps between the MVB-exosome pathway and autophagy exist [38].

Secretory autophagy: cargo selection

Unlike the well-characterized cargo selection process in degradative autophagy [39], nothing is known of how the secretory cargo is selected and engulfed by an autophagosome. The only clue so far comes from the fact that yeast Vps23 (TSG101 in mammals), a component of the endosomal sorting complex required for transport (ESCRT)-I in mammalian cells, is found at the CUPS [32]. As Vps23 is not essential for CUPS formation and as its known mammalian function is to sort ubiquitinated cargo into the MVB, Vps23 may function as a secretory autophagy receptor to capture the unconventional secreted protein substrates into the amphisome. Whether secretory autophagy substrates are ubiquitinated has not been elucidated. In addition, the involvement of other well-known autophagy receptors (e.g. p62, NBR1, NDP52, and optineurin), which facilitate the delivery of ubiquitinated autophagic substrates to degradative autophagosomes, remains unexplored, with the exception of SQSTM1 (the p62 *Dictyostelium* ortholog), which turned out to be present during but functionally dispensable for secretion of a particulate substrate termed ejectosome [21••]. In addition to these well-known autophagy receptors, the tripartite motif (TRIM) family of proteins has been recently reported as a new class of dual autophagic receptor — regulators [40] and it is possible that at least some member(s) of this protein family may act in secretory autophagy.

Secretory autophagy exports a range of cytosolic proteins in mammalian cells

Autophagic machinery is involved in unconventional secretion of the inflammatory cytokine IL-1β [3,14,19,20•,25,26••]. Moreover, autophagy facilitates active export (without a nonspecific permeabilization of the plasma membrane) of additional unconventionally secreted proteins, which encompass a broader range of cytosolic substrates [14,19,20•] (Table 1; section IA). Among the secretory autophagy cargo are IL-18 [14] and HMGB1 [14,41]. Similarly to IL-1β, IL-18 and HMGB1 do not contain a signal peptide and their secretion can be triggered by inflammasome activation [28]. IL-18 is a conventional inflammasome substrate, whereas HMGB1 is most likely indirectly associated [28]. However, secretory autophagy is not restricted to inflammasome substrates. Additional leaderless cytosolic proteins have been reported in the autophagy-dependent secretome, including galectins (galectin-3), cytoskeletal proteins (tubulin), and others such as annexin-I [20•].

Secretory autophagy of aggregation-prone proteins

Among the conventional cargo for degradative autophagosomes are protein aggregates [5]. Mirroring this, secretory autophagy may play a role in extracellular export of protein aggregates or aggregation-prone protein species (Table 1, I-B). Induction of autophagy in conjunction with inhibition of degradative autophagic flux induces secretory autophagy of α-synuclein species or aggregates associated with Parkinson disease [17•]. Secretion of α-synuclein may be associated with inter-neuronal transmission mechanisms of α-synuclein species and the spreading pattern of α-synuclein inclusion body disease throughout the nervous tissues.

In addition to α-synuclein aggregate expulsion, secretory autophagy has also been implicated in extrusion of amyloid beta (Aβ) peptide aggregates associated with Alzheimer's disease [18••]. By crossing amyloid precursor protein transgenic mice with neuron-specific Atg7-deficient mice, Nilsson *et al.* observed a paradoxical increase in intracellular Aβ aggregate accumulation in the perinuclear regions of neurons and a concurrent decrease in Aβ secretion and extracellular Aβ plaque formation [18••]. This neurotoxic phenotype, which could be further exacerbated through inhibition of autophagy by eventual extracellular amyloidosis due to the overall Aβ accumulation in neural tissues, resulted in impaired memory. Transduction of neurons isolated from these mice with Atg7 rescued their ability to release Aβ [18••]. Moreover, rapamycin (an autophagy inducer) increased whereas spautin-1 (an autophagy inhibitor) decreased secretion of Aβ from wild-type primary neurons [18••]. These data indicate a role of secretory autophagy in toxic

(Figure 2 Legend Continued) of secretory autophagic organelles may be controlled by +TIP (plus end tracking proteins). Note that both degradative and secretory autophagosomes may fuse with MVBs to generate amphisomes before fusion with lysosome or plasma membrane, respectively. Degradative and secretory autophagosomes may undergo interconversion or redirection in some instances, for example, when the same substrate can be secreted or degraded. Either way, the destiny of the contents is removal, whether by lysosomal degradation (degradative autophagy) or plasma membrane extrusion (secretory autophagy). At the bottom left, two recently described processes of autophagy-dependent nonlytic extracellular release of cytoplasmic microbes are depicted: Far left, bacterial ejectosome is represented with the associated autophagosomal profile cup shown to be important for providing membrane to prevent host cell lysis during bacterial ejection. The ejectosome-associated autophagosomal cup is positive for ubiquitin (Ubq), sequestosome 1 (SQSTM1), and Atg8 and its formation requires Atg1, 5, 6, and 7. To the right of bacterial ejectosome, enterovirus release (nonlytic) is depicted within phosphatidylserine-rich vesicles of autophagic origin that are formed within syntaxin 17-negative, LC3- and Beclin 1-dependent compartments. The examples depicted for autophagic secretion represent two extremes of a potential continuum — from delicate cargo of select proteins or their assemblies to large particulates and whole live microbes.

Table 1

Autophagy intersection with unconventional and conventional secretion and polarized protein sorting

Cargo	Methods[a,b]	Effects	Function[c]	References
Pathway I: Secretory autophagy				
I-A. Unconventional secretion of cytosolic proteins with extracellular functions				
Acb1	Analysis of yeasts lacking *Atg* genes; induction of autophagy by starvation but not with rapamycin	Autophagy induction enhanced and Atg factors required for Acb1 secretion	Necessary for yeast sporulation; in mammals, precursor to neuropeptides and role in metabolism	[12,13]
IL-1β	Pharmacological and starvation modulation of autophagy; knockdowns and knockouts of ATG factors and Rab8	Autophagy enhanced IL-1β secretion	Key pro-inflammatory cytokine processed by inflammasome	[14,19,20•,25,26••]
IL-18	Pharmacological and physiological modulation of autophagy	Autophagy enhanced IL-18 secretion	Inflammasome-processed cytokine with roles in cell mediated immunity and retinal health	[14]
HMGB1	Atg5 knockout; physiological modulation of autophagy without causing lysis	Autophagy enhanced and Atg5 was necessary for secretion of HMGB1	Damage-associated molecular pattern–inflammatory mediator	[14,41]
Galectin-3	Beclin 1 knockdown in β-glucan-stimulated cells via Dectin 1	Beclin 1 was necessary for secretion	A cytosolic β-galactoside-binding protein with roles in autophagy, cancer, heart disease and stroke	[20•]
Annexin I, tubulin	As above	As above	Proposed members of Dectin-induced secretome	[20•]
I-B. Removal of aggregate-forming proteins				
α-Synuclein	Inhibition of degradative autophagic flux; knockdown of *Atg5*; analysis of HDAC6 and Rab8	Inhibition of autophagic maturation enhanced α-synuclein release.	Inter-neuronal transmission of α-synuclein species (modified or aggregated) in Parkinson's disease	[17•]
Amyloid beta (Aβ)	Analysis of neuron-specific Atg7-deficient APP transgenic mice and pharmacological stimulation of autophagy	Increased intracellular Aβ accumulation	Alzheimer's disease pathology and memory impairment	[18••]
I-C. Extracellular release of cytoplasmic organellar material				
Mitochondria	Induction of autophagy; autophagic receptor NIX dependent clearance; ultrastructural analyses	Mitochondria removal from developing reticulocytes; release of mitochondrial components	Developmentally regulated clearance of mitochondria	[47,49]
Mixed organellar remnants	Detection of autophagic markers	Release of an $LC3^+$ compartment with organellar remnants (ER, Golgi, plasma membrane)	Final stages of reticulocyte development	[37•]
Autophagic organelles	Physiological and pharmacological modulation of autophagy	Extracellular export of autophagic vacuoles without cell membrane permeabilization	Linking secretory autophagy with caspase activation	[64]
Phagolysosomes	Purinergic stimulation and microtubule perturbation	Release of microbial material captured in autophagolysosomes	Possible immune adjuvant or alternative elimination mechanism	[48]
I-D. Microbial release from cells and transmission				
M. marinum	Genetic and cell biological analyses in the amoeba *Dictyostelium* as an infected host	Atg1-dependent, Atg6 (Beclin)-dependent, Atg7-dependent, but independent of SQSTM1 (p62 ortholog).	Intercellular spread of infection	[21••]
B. abortus	Genetic and cell biological analyses	ULK1-, Beclin 1-, ATG14L- and PI3-kinase dependent (but independent of ATG5, ATG16L1, ATG4B, ATG7, and LC3B).	Intercellular spread of infection	[51]
Poliovirus Enteroviruses	Genetic and pharmacological manipulation of autophagy and time lapse microscopy.	Virus released nonlytically within phosphatidylserine-rich vesicles of autophagic origin that are formed within lysosomal enzymes-negative syntaxin 17-negative, LC3 and Beclin 1-dependent compartments	Intercellular spread of infection	[16••,52,57••]

Table 1 (*Continued*)

Cargo	Methods[a,b]	Effects	Function[c]	References
Morbillivirus	Atg7 knockdown, chloroquine	Virus spread associated with syncytia formation	Spread of infection	[53]
Coxsackievirus	Analysis of extracellular microvesicles containing viruses	Released virus detected in LC3II$^+$ extracellular microvesicles.	Intercellular spread of infection	[54•]
Infleunza A virus	Viral M2 protein association with LC3	Plasma membrane translocation of LC3	Supporting alternative (filamentous) mode of budding	[56•].
Pathway II: Autophagy and regulated secretion				
Paneth cell granule contents	ATG16L1- and ATG5-deficient Paneth cells	Autophagy-deficient Paneth cells exhibit abnormalities in the granule exocytosis pathway	Crohn's disease intestinal abnormalities	[65]
Cathepsin K	Analysis of Atg5, Atg7, Atg4B, and LC3 in polarized secretion of lysosomal components	Atg defects impaired secretory lysosomal fusion and ruffled border formation	Osteoclast bone resorption and remodeling	[66]
Mast cell degranulation	Atg7 defective bone marrow-derived mast cells BMDMC	Impairment in degranulation by Atg7 BMDMC	Allergic disease and anaphylaxis reactions	[67]
von Willebrand factor (VWF)	Pharmacological inhibition, knockdowns of *Atg5*/*Atg7*, mice with endothelial-specific deletion of *Atg5*/*Atg7*	Atg5-deficient endothelium shows defective secretion of VWF from Weibel-Palade bodies	Platelet adhesion in blood vessel injury	[68••]
Otoconial core proteins	*Atg4b-null* mice and *Atg5-null* neonatal mice	Impaired secretion of otoconial (organic calcium carbonate crystals) core proteins.	Equilibrioception and balance disorders	[69]
Mucin	Effects of ATG factors on mucin secretion and effects of nonhematopoietic inflammasome on autophagy	Autophagosomal organelles enriched in NADPH oxidase enhance mucin secretion via ROS, and NLRP6 inflammasome controls autophagy	Goblet cell mucin secretion and control of intestinal microbiota	[70••,71•]
Pathway III: Autophagy and constitutive secretion				
IL-6	*Atg5* deletion	Autophagy enabled enhanced secretion during oncogene-induced senescence	Contributing to the senescence-associated secretory phenotype (SASP)	[58]
IL-8	*Atg5* deletion, Atg7 depletion, stimulation with tat-BECN1 peptide	Autophagy enhanced senescence associated IL-8 secretion	SASP and potential biomarkers	[58,19]
LIF, FAM3C, DKK3	Stimulation with tat-BECN1 peptide and depletion of *Atg7*.	Autophagy-augmented secretion	Potential biomarkers for autophagy in anti-cancer therapy	[19]
Pathway IV: Autophagy and plasma membrane protein sorting and organelle biogenesis				
ΔF508-CFTR	Depletion of *ATG* factors or pharmacological stimulation in *ΔF508 Cftr* mice and *ΔF508 CFTR* cystic fibrosis patients	Autophagy-assisted increase in ΔF508-CFTR cell surface expression	Rescuing CFTR function	[59,60•]
Mpl	Pharmacological stimulation and dominant negative expression of Atg5	Surface expression of immature Mpl linked to mutant Jak2 signaling	Potential role in myeloproliferative cancers	[61••]
Primary cilium	Genetic and cell biological analyses of multiple ATG, IFT, and centriolar satellite components	Autophagy initiates ciliogenesis on serum starvation but limits ciliary growth under nutrient-rich conditions.	Autophagy and ciliogenesis are regulating each other. Nutrition deprivation is a shared signal.	[62••,63••]

[a] The methods for monitoring secretory autophagy are diverse and await a unifying definition. However, one set of three common rules that can be applied at this point are: (i) that secretion is dependent on a subset of ATG factors; (ii) that the secretion of substrates is not due to cell lysis and parallel controls for nonspecific release of cytosolic proteins such as extracellular levels of LDH indicate that this is less in magnitude than the response of the bona fide secreted material; and (iii) that in cases where conditions do lead to eventual cell death that the secretion kinetically precedes cell death and wholesale cell membrane leakage.

[b] Of note, signaling pathways for secretory autophagy sometimes overlap with pathways of degradative autophagy, but in other cases additional stimuli are necessary.

[c] This column also contains disease and physiological context information that can give the reader a selection of the potential practical or clinical applications of secretory autophagy.

protein aggregate extrusion and protection against their intracellular accumulation.

Secretory autophagy and extracellular release of intracellular organellar contents

One distinct feature of autophagy is that large cytoplasmic objects such as organelles including surplus peroxisomes [42], excess mitochondria [43], depolarized mitochondria [9,44], damaged endosomes and lysosomes [45,46], or invading microbes [10] can be engulfed by autophagosomes. Some of the above autophagy targets, typically associated with degradative autophagy, can also become secretory autophagy cargo [43,47–49] (Table 1, I-C). The massive developmentally-regulated mitochondrial clearance during reticulocyte maturation depends on autophagy and can terminate either in degradation or in a readily observable exocytosis of the captured mitochondria [47]. This programmed process of mitochondrial release relies on the mitochondrial autophagic receptor Nix [47] and seems to differ from sporadic mitochondrial depolarization and Parkin-dependent mitophagy as an ongoing quality control process in most cells [44]. Nevertheless, mitochondrial material can be released from other cells in association with autophagy. Proteomic analysis of extracellular membranous material released upon starvation of endothelial cells shows enrichment of autophagy proteins (LC3 and Atg16L1) along with mitochondrial components (VDAC and COX4) [49]. In other instances, extracellular release of mitochondrial material [50] has been noted, although mechanisms have not been determined.

Autophagolysosomes and their content instead of being fully processed by degradation can be extruded from cells [48]. This is an active process dependent on stimulation of the purinergic receptor P2X7R with its agonist ATP and the associated microtubule rearrangement into radial extension from the centrosome toward the cell periphery [48]. The control of the divergence between continuation of degradation versus extrusion of the autophagocytosed material from cells remains to be fully analyzed and the specific biological functions of these phenomena remain to be understood.

Secretory autophagy in microbial egress and dissemination

Intracellular pathogens such as bacteria [21••,51] and viruses [16••,52,53,54•57••] can be released from infected cells in a variety of process assisted by the autophagic machinery (Table 1, I-D). A recent study with *Mycobacterium marinum* [21••] showed that autophagosomal organelles chaperone a structure termed the ejectosome [55], an actin-tail based apparatus enabling cytosolic bacteria to exit the host cell with the purpose of potentially contributing to microbial cell-to-cell spread (Figure 2). A functional (non-lytic to the host cell) ejectosome in *M. marinum*-infected amoeba *Dictyostelium* is seen [21••] as escorted by a distinct polar autophagic profile, which is Atg8 positive, ubiquitin-positive, and SQSTSM1 (an autophagic receptor)-positive. Although the host-sparing function of the ejectosome was SQSTM1-independent (thus indicating possible involvement of other unknown receptors) it was Atg5, Atg7 and Atg6 (Beclin)-dependent. Atg18 (a PI3P-recognizing autophagic regulator) and PI3P fluorescent probes colocalized with these profiles. Whereas the bacteria could still form an ejectosome and leave the host cell in Atg1-negative amoeba, the autophagic machinery was important to seal the plasma membrane and protect the host cell from leaking cytoplasm and undergoing death [21••]. Other forms of autophagy-assisted bacterial (*Brucella*) egress from infected cells without causing cell death have been reported [51]. Thus, autophagy enables non-lytic egress of bacteria from host cells. This may support spread of infection while avoiding excessive inflammatory signaling and immune clearance elicited by host's own alarmins released from necrotic cells.

Viral budding or release from cells can be assisted by ATG factors. The M2 protein of influenza contains a motif termed LIR (LC3 interacting region), which enables it to associate with LC3 at the plasma membrane to assist filamentous mode of viral budding [56•]. Autophagy assists other viruses, such as poliovirus and coxsackievirus B, in their egress from cells. Although classically poliovirus spreads by lysing host cells, autophagy has been proposed to support an alternative, non-lytic exit of the poliovirus [16••,52]. Using quantitative time-lapse microscopy, Bird *et al.*, demonstrated that poliovirus can be released from cells in tissue culture without cell lysis, a process augmented by autophagy induction and diminished by knockdown of the key autophagic membrane protein LC3 [16••]. This process was validated *in vivo* in a mouse model of polio infection [16••]. A significant new study [57••] has shown that enteroviruses (note: poliovirus is a prototypical enterovirus) are non-lytically secreted from cells in membrane-bound phosphatidylserine (PS)-positive vesicles originating from autophagosome-like organelles (Figure 2). The precursor compartments for these virus-laden secreted vesicles is enriched for PS and is LC3-positive, whereas their formation depends on LC3 and Beclin1 and can be stimulated by tat-Beclin 1 peptide [57••]. Cells can also shed nonpolio viruses such as coxsackievirus B in LC3-positive vesicles [54•], a phenomenon that may contribute to infection spread and avoidance of neutralizing antibodies.

Intersections between autophagy and conventional secretion

In addition to the secretory autophagy pathway discussed above that involves the secretion of leaderless proteins and possibly whole organelles and microbes via an autophagosome intermediate to the extracellular space (Table 1, pathway I), autophagy also affects three other general secretory and plasma membrane protein trafficking pathways in the cell (Table 1, pathways II–IV). In

pathway II, autophagy affects (probably via indirect mechanisms) the regulated secretion of cargo within pre-formed secretory granules. In pathway III, autophagy affects (selectively) the output for subsets of constitutively secreted proteins (Table 1, pathway III) [58]. The above pathways, recently covered in a review [15], are updated in Table 1. The pathway IV is addressed in the following section. Importantly, these pathways should not be confused with unconventional secretion but consist of (a) conventional (ER-to-Golgi-to plasma membrane) secretion of lumenal cargo (both regulated or constitutive) or (b) alternative pathways of trafficking of integral membrane proteins to the plasma membrane and organelle biogenesis at the plasma membrane.

Autophagic machinery in polarized membrane protein sorting and ciliogenesis

Autophagy has also been shown to be associated with the unconventional trafficking of proteins to the plasma membrane, first shown in the case of CFTR (Table 1, pathway IV) [59,60•]. Cell surface expression of ΔF508-CFTR, the most prevalent CFTR mutant associated with cystic fibrosis, can be restored in a GRASP-dependent manner [59]. In addition, expression of the autophagy protein Beclin 1 or treatment with the autophagy-inducer cystamine can increase ΔF508-CFTR cell surface expression *in vitro* and *in vivo* and reduce lung inflammation and mortality in the $Cftr^{F508del}$ homozygous mice [60•].

Mpl, the receptor for thrombopoietin and a major player in megakaryocytes differentiation and maturation, is another example of transmembrane protein being exported to the plasma membrane via unconventional trafficking pathways (Table 1, pathway IV) [61••]. While the fully glycosylated, mature, receptor follows the canonical ER-to-Golgi-to-membrane pathway, the unconventional, autophagy-related secretory pathway allows the core-glycosylated, immature, protein to reach the cell surface through a GRASP-dependent pathway. Aberrant Mpl intracellular trafficking has been linked to mutant Jak2 signaling associated with myeloproliferative neoplasms (progressive blood cancers). Mpl was observed to be loaded onto autophagic vesicles directly from the ER, as shown by high-resolution correlative light/electron microscopy technique [61••]. Pharmacological inhibition of autophagy or expression of mutant $Atg5^{K130R}$ led to a decrease cell surface expression of the ER form of Mpl. Complementing these observations, autophagic route for delivery of immature (core-glycosylated) Mpl was significantly activated by pharmacological induction of autophagy with rapamycin and by overexpression of GRASP55 [61••]. Thus, autophagy may provide a target in certain hematologic malignancies treatments.

Autophagy has other polarized sorting and plasma membrane organelle biogenesis roles. Starvation is a common signal for autophagy and biogenesis of the primary cilium, a sensory organelle continuous with but functionally delimited from the plasma membrane. Autophagy plays both a positive and a negative role in the formation and length of the primary cilium [62••,63••], whereas cilium can serve as a staging ground for autophagic machinery components [63••]. Autophagy helps initiate cilium formation under starvation conditions by reducing levels of OFD1, a protein that accumulates at the centriolar satellites where it inhibits ciliogenesis [63••]. Basal autophagy limits uncontrolled cilium growth under nutrient-rich conditions by diminishing intraflagellar transport protein IFT20 levels [62••]. Finally, signaling from the cilia regulates autophagy [62••]. Thus, not only does autophagy provide alternative trafficking routes for integral membrane proteins to reach the plasma membrane where they carry out their functions, but it also controls biogenesis of complex domains and organelles at the plasma membrane.

Concluding remarks

The concept of secretory autophagy, discovered less than half a decade ago, is still in its infancy. Although some progress has been made, new questions emerge whereas previously identified ones remain to be answered. What differentiates a secretory autophagosome from a degradative autophagosome? For instance, what aspects of the molecular machinery of secretory autophagy overlap with degradative autophagy, and how and where do the two mechanisms diverge? What are the molecular tags/signals that identify a secretory substrate and what are the receptors that bring it into the autophagosomes? Can cells switch between secretory and degradative autophagy modes for the same cargo? Is conversion into amphisome a mandatory sorting station before secretory autophagy can occur? What is the composition and biological function spectrum of the autosecretome, how does its composition change with physiological needs, and how does it influence cellular, tissue, and organismal functions? Many questions remain before we can define secretory autophagy as a specific pathway, but it is an attractive concept deserving further testing.

Acknowledgements

M.P. was supported by National Science and Technology Development Agency, Development and Promotion of Science and Technology Talents Project research grant 023/2557, Thailand Research Fund, Office of the Higher Education Commission, and Mahidol University. NIH grant GM085273 and ACS grant 126768-IRG-14-187-19 provided support for C.C. T.K. was supported in part by Manpei Suzuki Diabetes Foundation and Uehara Memorial Foundation. This work was supported by NIH grants AI042999 and AI111935 to V.D.

References and recommended reading

Papers of particular interest, published within the period of review, have been highlighted as:

- • of special interest
- •• of outstanding interest

1. Rabouille C *et al.*: **Diversity in unconventional protein secretion**. *J Cell Sci* 2012, **125**:5251-5255.

2. Zhang M, Schekman R: **Cell biology. Unconventional secretion, unconventional solutions**. *Science* 2013, **340**:559-561.

3. Jiang S *et al.*: **Secretory versus degradative autophagy: unconventional secretion of inflammatory mediators**. *J Innate Immun* 2013, **5**:471-479.

4. Mizushima N *et al.*: **The role of Atg proteins in autophagosome formation**. *Annu Rev Cell Dev Biol* 2011, **27**:107-132.

5. Rogov V *et al.*: **Interactions between autophagy receptors and ubiquitin-like proteins form the molecular basis for selective autophagy**. *Mol Cell* 2014, **53**:167-178.

6. Galluzzi L *et al.*: **Metabolic Control of Autophagy**. *Cell* 2014, **159**:1263-1276.

7. Kroemer G: **Autophagy: a druggable process that is deregulated in aging and human disease**. *J Clin Invest* 2015, **125**:1-4.

8. Frake RA *et al.*: **Autophagy and neurodegeneration**. *J Clin Invest* 2015, **125**:65-74.

9. Yamano K *et al.*: **Mitochondrial Rab GAPs govern autophagosome biogenesis during mitophagy**. *Elife* 2014, **3**:e01612.

10. Deretic V *et al.*: **Immunologic manifestations of autophagy**. *J Clin Invest* 2015, **125**:75-84.

11. Levine B *et al.*: **Development of autophagy inducers in clinical medicine**. *J Clin Invest* 2015, **125**:14-24.

12. Duran JM *et al.*: **Unconventional secretion of Acb1 is mediated by autophagosomes**. *J Cell Biol* 2010, **188**:527-536.

13. Manjithaya R *et al.*: **Unconventional secretion of *Pichia pastoris* Acb1 is dependent on GRASP protein, peroxisomal functions, and autophagosome formation**. *J Cell Biol* 2010, **188**:537-546.

14. Dupont N *et al.*: **Autophagy-based unconventional secretory pathway for extracellular delivery of IL-1beta**. *EMBO J* 2011, **30**:4701-4711.

15. Deretic V *et al.*: **Autophagy intersections with conventional and unconventional secretion in tissue development, remodeling and inflammation**. *Trends Cell Biol* 2012, **22**:397-406.

16. •• Bird SW *et al.*: **Nonlytic viral spread enhanced by autophagy components**. *Proc Natl Acad Sci USA* 2014, **111**:13081-13086.
An elegant demonstration of autophagy-dependent nonlytic release of poliovirus.

17. • Ejlerskov P *et al.*: **Tubulin polymerization-promoting protein (TPPP/p25alpha) promotes unconventional secretion of alpha-synuclein through exophagy by impairing autophagosome-lysosome fusion**. *J Biol Chem* 2013, **288**:17313-17335.
Secretory autophagy of α-synuclein may explain its spread in nervous tissues, of high relevance for Parkinson's disease.

18. •• Nilsson P *et al.*: **Abeta secretion and plaque formation depend on autophagy**. *Cell Rep* 2013, **5**:61-69.
An important aspect of Aβ biology in Alzheimer's disease is revealed in this study that shows that autophagy contributes to secretion of Aβ, and that when this is blocked (e.g. when autophagy is disabled), Aβ accumulates intracellularly where it can be toxic to the neurons.

19. Kraya AA *et al.*: **Identification of secreted proteins that reflect autophagy dynamics within tumor cells**. *Autophagy* 2015, **11**:60-74.

20. • Ohman T *et al.*: **Dectin-1 pathway activates robust autophagy-dependent unconventional protein secretion in human macrophages**. *J Immunol* 2014, **192**:5952-5962.
Expansion of autophagy-dependent secretome.

21. •• Gerstenmaier L *et al.*: **The autophagic machinery ensures nonlytic transmission of mycobacteria**. *Proc Natl Acad Sci USA* 2015, **112**:E687-E692.
An elegant morphological and molecular description of autophagy-assisted expulsion of live bacteria through the plasma membrane without causing cell lysis, which may aid infection spread without the inflammatory consequences that promote pathogen clearance.

22. Schroder K, Tschopp J: **The inflammasomes**. *Cell* 2010, **140**:821-832.

23. Rubartelli A *et al.*: **A novel secretory pathway for interleukin-1 beta, a protein lacking a signal sequence**. *EMBO J* 1990, **9**:1503-1510.

24. Muesch A *et al.*: **A novel pathway for secretory proteins?** *Trends Biochem Sci* 1990, **15**:86-88.

25. Piccioli P, Rubartelli A: **The secretion of IL-1beta and options for release**. *Semin Immunol* 2013, **25**:425-429.

26. •• Wang LJ *et al.*: **The microtubule-associated protein EB1 links AIM2 inflammasomes with autophagy-dependent secretion**. *J Biol Chem* 2014, **289**:29322-29333.
A mechanistic dissection of how secretory autophagosomes are vectored toward the plus end of microtubules.

27. Malhotra V: **Unconventional protein secretion: an evolving mechanism**. *EMBO J* 2013, **32**:1660-1664.

28. Keller M *et al.*: **Active caspase-1 is a regulator of unconventional protein secretion**. *Cell* 2008, **132**:818-831.

29. Kinseth MA *et al.*: **The Golgi-associated protein GRASP is required for unconventional protein secretion during development**. *Cell* 2007, **130**:524-534.

30. Webb JL *et al.*: **Alpha-Synuclein is degraded by both autophagy and the proteasome**. *J Biol Chem* 2003, **278**:25009-25013.

31. Pilli M *et al.*: **TBK-1 promotes autophagy-mediated antimicrobial defense by controlling autophagosome maturation**. *Immunity* 2012, **37**:223-234.

32. Bruns C *et al.*: **Biogenesis of a novel compartment for autophagosome-mediated unconventional protein secretion**. *J Cell Biol* 2011, **195**:979-992.

33. Axe EL *et al.*: **Autophagosome formation from membrane compartments enriched in phosphatidylinositol 3-phosphate and dynamically connected to the endoplasmic reticulum**. *J Cell Biol* 2008, **182**:685-701.

34. Cruz-Garcia D *et al.*: **Remodeling of secretory compartments creates CUPS during nutrient starvation**. *J Cell Biol* 2014, **207**:695-703.

35. Gordon PB, Seglen PO: **Prelysosomal convergence of autophagic and endocytic pathways**. *Biochem Biophys Res Commun* 1988, **151**:40-47.

36. Klionsky DJ *et al.*: **Autophagosomes, phagosomes, autolysosomes, phagolysosomes, autophagolysosomes. wait, I'm confused**. *Autophagy* 2014, **10**:549-551.

37. • Griffiths RE *et al.*: **Maturing reticulocytes internalize plasma membrane in glycophorin A-containing vesicles that fuse with autophagosomes before exocytosis**. *Blood* 2012, **119**:6296-6306.
Autophagy-dependent excretion of membrane remnants during reticulocyte maturation.

38. Baixauli F *et al.*: **Exosomes and autophagy: coordinated mechanisms for the maintenance of cellular fitness**. *Front Immunol* 2014, **5**:403.

39. Johansen T, Lamark T: **Selective autophagy mediated by autophagic adapter proteins**. *Autophagy* 2011, **7**:279-296.

40. Mandell MA *et al.*: **TRIM proteins regulate autophagy and can target autophagic substrates by direct recognition**. *Dev Cell* 2014, **30**:394-409.

41. Thorburn J *et al.*: **Autophagy regulates selective HMGB1 release in tumor cells that are destined to die**. *Cell Death Differ* 2009, **16**:175-183.

42. Nazarko TY *et al.*: **Peroxisomal Atg37 binds Atg30 or palmitoyl-CoA to regulate phagophore formation during pexophagy**. *J Cell Biol* 2014, **204**:541-557.

43. Ney PA: **Normal and disordered reticulocyte maturation**. *Curr Opin Hematol* 2011, **18**:152-157.

44. Youle RJ, Narendra DP: **Mechanisms of mitophagy**. *Nat Rev Mol Cell Biol* 2011, **12**:9-14.

45. Maejima I *et al.*: **Autophagy sequesters damaged lysosomes to control lysosomal biogenesis and kidney injury**. *EMBO J* 2013, **32**:2336-2347.

46. Chen X *et al.*: **Autophagy induced by calcium phosphate precipitates targets damaged endosomes**. *J Biol Chem* 2014, **289**:11162-11174.

47. Schweers RL *et al.*: **NIX is required for programmed mitochondrial clearance during reticulocyte maturation**. *Proc Natl Acad Sci USA* 2007, **104**:19500-19505.

48. Takenouchi T *et al.*: **The activation of P2X7 receptor impairs lysosomal functions and stimulates the release of autophagolysosomes in microglial cells**. *J Immunol* 2009, **182**:2051-2062.

49. Pallet N *et al.*: **A comprehensive characterization of membrane vesicles released by autophagic human endothelial cells**. *Proteomics* 2013, **13**:1108-1120.

50. Unuma K *et al.*: **Elimination and active extrusion of liver mitochondrial proteins during lipopolysaccharide administration in rat**. *Hepatol Res* 2013, **43**:526-534.

51. Starr T *et al.*: **Selective subversion of autophagy complexes facilitates completion of the Brucella intracellular cycle**. *Cell Host Microbe* 2012, **11**:33-45.

52. Jackson WT *et al.*: **Subversion of cellular autophagosomal machinery by RNA viruses**. *PLoS Biol* 2005, **3**:e156.

53. Delpeut S *et al.*: **Membrane fusion-mediated autophagy induction enhances morbillivirus cell-to-cell spread**. *J Virol* 2012, **86**:8527-8535.

54. • Robinson SM *et al.*: **Coxsackievirus B exits the host cell in shed microvesicles displaying autophagosomal markers**. *PLoS Pathog* 2014, **10**:e1004045.
This study reports viral egress in vesicles with autophagic properties.

55. Hagedorn M *et al.*: **Infection by tubercular mycobacteria is spread by nonlytic ejection from their amoeba hosts**. *Science* 2009, **323**:1729-1733.

56. • Beale R *et al.*: **A LC3-interacting motif in the influenza A virus M2 protein is required to subvert autophagy and maintain virion stability**. *Cell Host Microbe* 2014, **15**:239-247.
Autophagic factors (specifically LC3) assists an alternative mode of budding of the flu virus.

57. •• Chen YH *et al.*: **Phosphatidylserine vesicles enable efficient en bloc transmission of enteroviruses**. *Cell* 2015, **160**:619-630.
An exceptional new study showing that enteroviruses are released from cells without lysis by being packaged in LC3-positive autophagic precursors, whose formation depends on LC3 and Beclin 1, which do not acquire lysosomal properties (are negative for syntaxin 17) and are rich in phosphatidylserine.

58. Narita M *et al.*: **Spatial coupling of mTOR and autophagy augments secretory phenotypes**. *Science* 2011, **332**:966-970.

59. Gee HY *et al.*: **Rescue of DeltaF508-CFTR trafficking via a GRASP-dependent unconventional secretion pathway**. *Cell* 2011, **146**:746-760.

60. • Stefano DD *et al.*: **Restoration of CFTR function in patients with cystic fibrosis carrying the F508del-CFTR mutation**. *Autophagy* 2014, **10**:2053-2074.
Autophagy can be pharmacological modulated to improve trafficking of defective CFTR to the plasma membrane.

61. •• Cleyrat C *et al.*: **Mpl traffics to the cell surface through conventional and unconventional routes**. *Traffic* 2014, **15**:961-982.
Autophagy can assist trafficking of immature receptors to the plasma membrane resulting in oncogenic signaling.

62. •• Pampliega O *et al.*: **Functional interaction between autophagy and ciliogenesis**. *Nature* 2013, **502**:194-200.
Autophagy affects ciliogenesis as an example of autophagic contribution to formation of specialized domains and organelles on the plasma membrane.

63. •• Tang Z *et al.*: **Autophagy promotes primary ciliogenesis by removing OFD1 from centriolar satellites**. *Nature* 2013, **502**:254-257.
Study showing how autophagy promotes ciliogenesis at the plasma membrane.

64. Sirois I *et al.*: **Caspase activation regulates the extracellular export of autophagic vacuoles**. *Autophagy* 2012, **8**:927-937.

65. Cadwell K *et al.*: **A key role for autophagy and the autophagy gene Atg16l1 in mouse and human intestinal Paneth cells**. *Nature* 2008, **456**:259-263.

66. DeSelm CJ *et al.*: **Autophagy proteins regulate the secretory component of osteoclastic bone resorption**. *Dev Cell* 2011, **21**:966-974.

67. Ushio H *et al.*: **Crucial role for autophagy in degranulation of mast cells**. *J Allergy Clin Immunol* 2011, **127** 1267-1276 e1266.

68. •• Torisu T *et al.*: **Autophagy regulates endothelial cell processing, maturation and secretion of von Willebrand factor**. *Nat Med* 2013, **19**:1281-1287.
Autophagy intersection with regulated secretion in a medically highly important context.

69. Marino G *et al.*: **Autophagy is essential for mouse sense of balance**. *J Clin Invest* 2010, **120**:2331-2344.

70. •• Patel KK *et al.*: **Autophagy proteins control goblet cell function by potentiating reactive oxygen species production**. *EMBO J* 2013, **32**:3130-3144.
This study reports that autophagy intersects with regulated mucin secretion and that autophagosomes may enrich NADPH oxidase, which then provides reactive oxygen signals causing mucin secretion.

71. • Wlodarska M *et al.*: **NLRP6 inflammasome orchestrates the colonic host–microbial interface by regulating goblet cell mucus secretion**. *Cell* 2014, **156**:1045-1059.
This study reports that a nonhematopoietic inflammasome regulates autophagy to contribute to mucin secretion.

MALARIA JOURNAL

METHODOLOGY Open Access

A rapid and scalable density gradient purification method for *Plasmodium* sporozoites

Mark Kennedy[1], Matthew E Fishbaugher[1], Ashley M Vaughan[2], Rapatbhorn Patrapuvich[3], Rachasak Boonhok[3,4], Narathatai Yimamnuaychok[3], Nastaran Rezakhani[2], Peter Metzger[2], Marisa Ponpuak[4], Jetsumon Sattabongkot[3], Stefan H Kappe[2,5], Jen CC Hume[1] and Scott E Lindner[2*]

Abstract

Background: Malaria remains a major human health problem, with no licensed vaccine currently available. Malaria infections initiate when infectious *Plasmodium* sporozoites are transmitted by Anopheline mosquitoes during their blood meal. Investigations of the malaria sporozoite are, therefore, of clear medical importance. However, sporozoites can only be produced in and isolated from mosquitoes, and their isolation results in large amounts of accompanying mosquito debris and contaminating microbes.

Methods: Here is described a discontinuous density gradient purification method for *Plasmodium* sporozoites that maintains parasite infectivity *in vitro* and *in vivo* and greatly reduces mosquito and microbial contaminants.

Results: This method provides clear advantages over previous approaches: it is rapid, requires no serum components, and can be scaled to purify >10^7 sporozoites with minimal operator involvement. Moreover, it can be effectively applied to both human (*Plasmodium falciparum*, *Plasmodium vivax*) and rodent (*Plasmodium yoelii*) infective species with excellent recovery rates.

Conclusions: This novel method effectively purifies viable malaria sporozoites by greatly reducing contaminating mosquito debris and microbial burdens associated with parasite isolation. Large-scale preparations of purified sporozoites will allow for enhanced *in vitro* infections, proteomics, and biochemical characterizations. In conjunction with aseptic mosquito rearing techniques, this purification technique will also support production of live attenuated sporozoites for vaccination.

Keywords: Sporozoite, Purification, Plasmodium, Falciparum, Vivax, Yoelii, Humanized mouse model

Background

Plasmodium species, the aetiological agents of malaria, cycle between a mosquito vector and vertebrate host to complete its life cycle. Mammals become infected with malaria parasites when bitten by an infected *Anopheles* mosquito, which deposits the sporozoite form of the parasite into the host's skin (reviewed in [1]). Sporozoites then actively seek the host vasculature and upon invading it, passively migrate to the liver where they ultimately infect a hepatocyte and replicate within it. This liver stage of development (which lasts two days for rodent-infective species or six to eight days for human-infective species) results in the release of tens of thousands of red blood cell-infectious exoerythrocytic merozoites. These merozoites then initiate the blood stage of malaria infection that is associated with all clinical symptoms of the disease.

The characterization of sporozoite infectivity has often been limited by the presence of bacteria and yeast. Because of these contaminating microbes, the duration of many *in vitro* infections of permissive hepatocytes is often limited to only a few days. In addition, immunocompromised mice with humanized livers have recently been developed to provide an *in vivo* model of liver stage infections for both *Plasmodium falciparum* and *Plasmodium vivax* ([2,3], Mikolajczak *et al.*, *personal communication*). Infections of these mice with large numbers of unpurified sporozoites can also systemically introduce

* Correspondence: Scott.Lindner@SeattleBioMed.org
[2]Malaria Program, Seattle Biomedical Research Institute, 307 Westlake Avenue North, Suite 500, Seattle, WA 98109, USA
Full list of author information is available at the end of the article

large amounts of these microbes, which may negatively impact the health of these mice and affect the innate immune response against the parasite during the 6–8 day liver stage infection. These contaminants can similarly confound investigations of basic immunological responses of non-humanized mice against rodent malaria, as well.

Biochemical studies of sporozoites have also been hampered by relatively large amounts of residual mosquito debris compared to the parasite mass. For instance, proteomic studies of various *Plasmodium* species have used unpurified sporozoites and this has resulted in the identification of only a limited number of parasite-specific peptide hits, presumably due to the large number of contaminating mosquito-derived peptides [4-6]. Substantial reduction of mosquito proteins would substantially help such characterizations.

A previously published method of sporozoite purification requires that the parasites be first coated with bovine serum albumin (BSA) and then passed through ion exchange resin [7]. While this described procedure produces well-purified sporozoites, the fraction of sporozoites recovered is routinely low (30-40%) even with sporozoites obtained from isolated salivary glands (Lindner S., *unpublished results*). Moreover, this approach yields parasites coated with BSA, which is known to induce sporozoite apical organelle secretion and motility [8,9]. Another sporozoite purification method that employs BSA utilizes a discontinuous density gradient composed of diatrozoate sodium/Hypaque and several lengthy, high speed spins to purify sporozoites [10]. When injected into mice, these sporozoite preparations resulted in the death of significant numbers of the mice due to an immune response to BSA [11]. A revised protocol from the same authors that employed mouse serum in lieu of BSA did curtail mouse death, but did not reduce contaminating microbial burdens (ibid).

Ideally, an effective malaria vaccine will confer sterile protection prior to the onset of symptoms. The most promising subunit vaccine candidate, RTS,S, is currently in Phase 3 trials by GlaxoSmithKline but has shown only partial protection from subsequent infections [12]. Recent efforts have also focused on developing malaria vaccines comprised of live sporozoites attenuated by irradiation or genetic disruption, including the first trial testing syringe delivery of irradiated sporozoites [13-16]. These attenuated parasites are able to productively infect hepatocytes, but arrest at specific points within the liver stage of parasite development [17]. Interestingly, genetically attenuated parasites that arrest as late liver stage parasites (e.g. *pyfab b/f*$^{-}$ parasites) provide greater and broader CD8+ T-cell responses and higher levels of protection than do radiation attenuated parasites or early arresting genetically attenuated parasites (ibid). Further studies and large-scale implementation of these vaccine candidates would greatly benefit from the production of large numbers of sporozoites that have been purified away from mosquito-derived contaminants to facilitate their characterization and deployment.

To address all of the above problems, herein is described a discontinuous density gradient purification method that employs a dense layer composed of Accudenz dissolved in water. This strategy effectively removes mosquito debris and hemocoel lipids, does not require BSA or serum, greatly reduces bacterial contamination, and eliminates yeast contamination. Moreover, this approach is applicable across all species of *Plasmodium* tested, including rodent-infective *Plasmodium yoelii* and human-infective *P. falciparum* and *P. vivax* sporozoites. Importantly, this method is scalable, as $>10^7$ sporozoites can be routinely purified in a single gradient with excellent recovery rates. Lastly, this method is validated by demonstrating that these purified sporozoites are fully infectious in standard *in vitro* and/or *in vivo* infectivity assays for all three species. Taken together, this method provides a means to rapidly purify *Plasmodium* sporozoites for both basic research and vaccine production applications.

Methods

Accudenz column purification method

A 17% w/v solution of Accudenz (Accurate Chemical #AN7050) dissolved in distilled deionized water (ddH_2O, Mediatech #25-055-CM) was filter sterilized and stored at 4°C. A 3 ml Accudenz cushion was loaded in a 15 ml conical tube and the dissected sporozoite mixture (up to 1 ml) was gently layered on top of the cushion. The column was spun at 2,500 *g* at room temperature for 20 minutes (no brake) and the interface (±) was transferred to a new, clean microcentrifuge tube and spun at top speed in a microcentrifuge for three minutes. The supernatant was aspirated and the pelleted sporozoites were resuspended in RPMI 1640 or Schneider's insect medium and counted in a haemocytometer. Three or more biological replicates of all tested species of *Plasmodium* sporozoites (*Plasmodium yoelii*, *P. falciparum*, *P. vivax*) were tested to confirm sporozoite recovery.

Plasmodium yoelii sporozoite production

Six-to-eight week old female Swiss Webster ("SW") mice from Harlan (Indianapolis, IN) were used for production of wild-type *P. yoelii* 17XNL ("Py17XNL", a non-lethal strain) blood stage parasites. Animal handling was conducted according to Institutional Animal Care and Use Committee approved protocols at the Seattle Biomedical Research Institute. Py17XNL parasites were cycled between SW mice and *Anopheles stephensi* mosquitoes that had been reared by standard methods (as described in Methods in Anopheles Research available at www.

mr4.org). Infected mosquitoes were maintained on an 8% w/v dextrose solution in 0.05% w/v PABA water at 24°C and 70% humidity in 12 hour light/dark cycles. Mosquitoes were collected into sterile 70% v/v ethanol in ddH_2O, rinsed in sterile ddH2O and finally washed in sterile 1xPBS. Salivary glands were individually isolated by microdissection in sterile RPMI media 14–16 days post-blood meal from batches of 50–75 mosquitoes, and were placed in a microfuge tube containing sterile RPMI media. Sporozoites were then released by three rounds of manual grinding of salivary glands (50 grinds per round), with glands re-pelleted at 100 *g* for 1 minute between rounds. The sporozoite-containing mixture was applied to the gradient as described above.

Plasmodium falciparum sporozoite production

In vitro P. falciparum (NF54 strain) cultures were maintained in O+ erythrocytes grown in RPMI 1640 (25 mM HEPES, 2 mM L-glutamine) supplemented with 50 μm hypoxanthine and 10% A+ human serum in an atmosphere of 5% CO_2, 5% O_2, and 90% N_2. Gametocyte cultures were initiated at 5% haematocrit and 0.8-1% parasitaemia (mixed stages) and maintained for up to 17 days with daily media changes.

Non-bloodfed adult female *An. stephensi* mosquitoes three to seven days post-emergence were collected into mesh-topped, wax-lined pots each containing up to 300 mosquitoes. Gametocyte cultures were quickly spun down and the pelleted infected erythrocytes were diluted to 40% haematocrit with fresh A+ human serum and O+ erythrocytes. Mosquitoes were allowed to feed upon these cultures through Parafilm for up to 20 minutes. Following blood feeding, mosquitoes were maintained for up to 19 days at 27°C, 75% humidity and were provided with an 8% w/v dextrose solution in 0.05% w/v PABA water. Salivary gland sporozoites were isolated as described above by microdissection 14–19 days post-blood meal.

Plasmodium vivax sporozoite production

Blood samples from *P. vivax*-infected patients were collected at the Malaria Clinics (Kanchanaburi province, Thailand) in accordance with an approved human research protocol (protocol# TMEC 11–033, Faculty of Tropical Medicine, Mahidol University). Infected blood was heparinized and fed to five to seven-day old female *Anopheles dirus* mosquitoes using a membrane-feeding device [18]. Infected mosquitoes were maintained at 26°C, 75% humidity and were provided with a 10% w/v dextrose solution in water. Salivary gland sporozoites were isolated by microdissection as described above 15–18 days post-blood meal, but in batches of five mosquitoes at a time.

Measurement of the reduction of bacterial contaminants

Plasmodium yoelii salivary gland sporozoites were dissected from three independent mosquito cages and were resuspended at 2×10^5 sporozoites/1ml RPMI 1640 media. Sporozoites were either left untreated, or were incubated with 200 IU penicillin / 200 mg/ml streptomycin (Cellgro, Cat#30-002-CI) for 20 minutes at room temperature. Sporozoites from both conditions were then either left unpurified, or purified as described above. Sporozoites were pelleted, washed in RPMI 1640 to remove residual antibiotics, counted on a haemocytometer, serially diluted to 25000, 2500, 250, and 25 sporozoites in 100 μl RPMI 1640 and were plated on LB-agar plates. Plates were incubated at 37°C for 12–14 hours and colony-forming units per sporozoite plated were determined by manual counting.

Assessment of *in vivo P. yoelii* sporozoite infectivity

Plasmodium yoelii salivary gland sporozoites were isolated from mosquito salivary glands, and 10^3 or 10^4 sporozoites were injected intravenously ("iv") into the tail vein of SW mice. The time to blood stage patency (defined as >1 infected RBCs / 20,000 RBCs) was determined microscopically by Giemsa-stained thin blood smears. A one-day delay in the time to blood stage patency correlates with a 90% reduction in sporozoite infectivity [19]. Two biological replicates were measured for each condition.

Assessment of *in vitro P. vivax* and *P. falciparum* sporozoite infectivity

HC-04, a human hepatocyte cell line, was used to produce liver stage infections [20]. Cells (2.5×10^4) were seeded in each well of a 8-well chamber slides (LabTek, Campbell, CA) and incubated at 37°C with a complete medium (*P. vivax*: equal volumes of MEM and Ham's F12 (Gibco BRL); *P. falciparum*: DMEM) supplemented with 10% foetal bovine serum, 100 U/ml penicillin, and 100 μg/ml streptomycin. At 24 h, the medium was aspirated and replaced with 2×10^4 purified sporozoites in 250 μl of invasion medium (*P. vivax*: MEM: Ham's F12 supplemented with 10% human AB serum, 100 U/ml penicillin, 100 μg/ml streptomycin, and 0.25 μg/ml fungizone; *P. falciparum*: complete media as above). After a four hour incubation, the invasion medium was aspirated and 300 μl of fresh complete medium (as above) was added to the infected hepatocytes. The culture was maintained for up to four days with daily media changes prior to visualization by an IFA (see below).

Assessment of *in vivo P. falciparum* sporozoite infectivity

Female FRG NOD huHep mice with human chimeric livers (Yecuris Corp.) were infected with purified *P. falciparum*

sporozoites by intravenous tail vein injection as previously described [3]. Six and seven days post-infection, mice were injected intravenously with 400 μl of packed O+ human RBCs. Mice were sacrificed two hours after the second RBC injection, and the blood was collected by cardiac puncture and placed into *in vitro* culture under standard conditions. Additionally, livers were simultaneously harvested and processed for IFA (see below).

Indirect immunofluorescence assay (IFA)

Salivary gland sporozoites, *in vitro* and *in vivo* infected hepatocytes were processed for IFA essentially as described [21]. All sample types were stained at room temperature with phalloidin or the following appropriately diluted primary antibodies (rabbit anti-human fumaryl acetoacetate hydrolase (FAH, Yecuris), mouse anti-PfMSP1 (MR4), mouse anti-PfCSP (Clone 2A10), mouse anti-PvCSP210, mouse anti-PvCSP247, mouse anti-PbHsp70 (Clone 4C9) [22], Alexa Fluor- or FITC-conjugated secondary antibodies specific to mouse or rabbit IgG (Alexa Fluor 488, 594, Invitrogen; Dako), and 4′,6-diamidino-2-phenylindole (DAPI). Samples were covered with VectaShield (Vector Laboratories) and sealed under a coverglass slip. Fluorescent and DIC images were acquired using a DeltaVision Spectris RT microscope (Applied Precision) using a 40× or 100× oil objective and were deconvolved using the softWoRx software package, except for *P. vivax* liver stage parasites, which were acquired using a Nikon ECLIPSE 80i microscope with NIS-Elements F 3.0 software.

Flow cytometric quantification of sporozoite invasion

Infection of HC-04 hepatocytes by *P. falciparum* sporozoites was measured as described previously [23]. Briefly, 4×10^5 HC-04 cells were plated in each well of a 24-well plate one day prior to mock infection with dissection media or infection with 10^5 *P. falciparum* NF54 strain purified or unpurified sporozoites. Infection was allowed to proceed for 90 minutes, at which point hepatocytes were trypsinized, extensively washed, fixed, and permeabilized. Hepatocytes were blocked and then stained with an Alexa-Fluor 488-conjugated anti-PfCSP (2A10) to detect CSP-positive hepatocytes with a LSRII flow cytometer (Becton Dickinson) and FlowJo Software. Samples were normalized to the percent of hepatocytes infected by unpurified sporozoites (set at 100%).

Statistics

A measurement of the statistical significance of sporozoite infectivity *in vitro* was conducted by a standard student's t-test.

Results

Determination of critical purification parameters

After sporozoite isolation from mosquito midguts or salivary glands, many sporozoite investigations are then hampered by excessive amounts of mosquito debris, microbes such as bacteria and yeast, or both. It would, therefore, be beneficial to devise a purification method to simultaneously solve both problems that would require minimal operator involvement (<5 minutes), be simple (one step), be rapid (20 minutes) and be scalable (able to purify millions of sporozoites simultaneously). To this end, several commercially available chemicals commonly used to create density gradients were assessed for their ability to purify sporozoites, and Accudenz-based gradients were identified as the top performer. Gradients that used Accudenz as the dense layer consistently produced the highest recovery of purified sporozoites from the bilayer interface (*P. yoelii*: 80.4% ± 11.6; *P. falciparum* 81.3% ± 5.74; *P. vivax* 61.9 ± 6.86), and have been used to successfully purify as few as 10^5 sporozoites to over 2×10^7 sporozoites in a single gradient with comparable sporozoite recoveries (Additional file 1). The Accudenz gradient also performed well in removing both mosquito debris (which forms a pellet at the base of the tube) and lipids (which float to the top of the gradient) (Figure 1A). Microscopically, the purity of these sporozoite samples was excellent as well, with little to no contaminating material visibly remaining after centrifugation (Figure 1B).

During the optimization of this purification method, three major parameters were identified that affected sporozoite recovery: the solvent used to produce the Accudenz cushion, the final concentration of Accudenz in the dense layer, and the relative centrifugal force applied to the gradient. *Plasmodium falciparum* sporozoites were loaded onto cushions of Accudenz dissolved in either 2× phosphate buffer saline (PBS), 1×PBS, 0.5×PBS or distilled, deionized water (ddH_2O) and spun at 2,500 *g* for 20 minutes at room temperature (RT). A strong, dose-dependent negative effect on the percent recovery of sporozoites was observed with increasing concentrations of solutes present in PBS. In contrast, using ddH_2O as the solvent allowed for consistently high percentage recoveries of sporozoites, and was used for all subsequent experiments (Additional file 2). The optimal concentration of Accudenz for use in the dense layer (17%) was determined by testing a range of concentrations (5, 10, 17, 25% w/v in ddH_2O) with *P. falciparum* sporozoites (Additional file 3).

Additionally, using both sporozoite recovery and amounts of residual mosquito debris as metrics, various relative centrifugal forces (1,500 *g*, 2,000 *g*, 2,500 *g*, 3,000 *g*) were tested upon the gradient and it was determined that optimal recovery and purification was obtained at

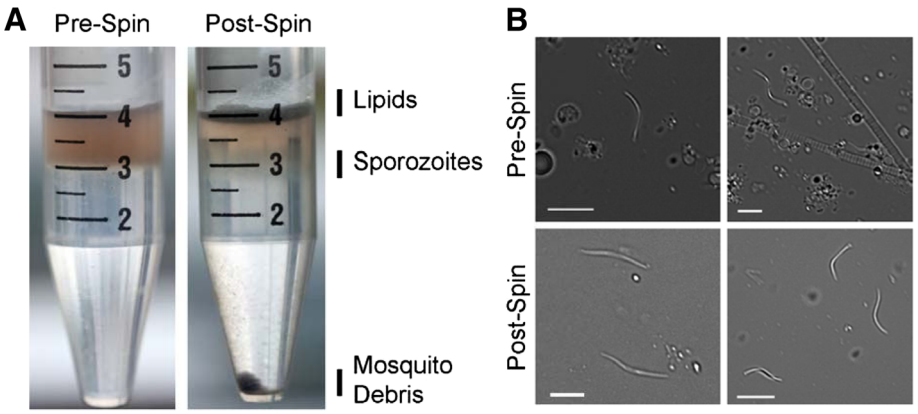

Figure 1 Accudenz density gradient purification of *Plasmodium* sporozoites. A. Photographs of a bilayer discontinuous Accudenz density gradient overlayed with *P. yoelii* sporozoites in RPMI before and after centrifugation. Mosquito debris pellets to the bottom of the gradient, mosquito lipids float to the top of the gradient, and sporozoites accumulate at the bilayer interface. **B**. Representative DIC images of unpurified and purified sporozoites before and after centrifugation show a significant reduction in mosquito material. Scale bar is 5 microns.

2,500 *g* (Additional file 4). Thus, the optimal conditions for sporozoite purification employ a 17% w/v Accudenz in ddH_2O cushion under the dissected sporozoite mixture (in either RPMI 1640 or Schneider's Medium), spun at 2,500 *g* for 20 minutes at room temperature.

Reduction/elimination of contaminating microbial burdens

Using these optimized purification conditions, it was determined if this method would significantly reduce the amounts of contaminating bacteria and yeast remaining with the purified sporozoites. To this end, *P. yoelii* salivary gland sporozoites were either left unpurified or were purified over an Accudenz cushion as described. Additionally, to test if pre-treatment of the sporozoites with antibiotics would further reduce the microbial burden, samples were incubated with penicillin/streptomycin or left untreated. Serial dilutions of sporozoites from each of these four conditions were plated on LB agar plates, the number of colony forming units (CFUs) per sporozoite was counted (Table 1). No significant reduction in CFUs was achieved by pre-treatment of sporozoites with antibiotics alone. In contrast, Accudenz purification greatly reduced bacterial contamination (97.5% + 0.757) associated with sporozoites, which was further affected by treatment with penicillin and streptomycin (99.0% + 0.252). In confirmation of this, an equal number of unpurified or purified *P. yoelii* (10^5), *P. falciparum* (10^5), or *P. vivax* (2×10^4) sporozoites were inoculated into complete DMEM or RPMI 1640 media in independent wells of 6-well tissue culture plates at 37°C with 5% CO_2. All wells containing unpurified sporozoites became overgrown (visible by eye and/or microscopically) with bacteria (within 1–2 days) or yeast (within 4 days, data not shown), whereas wells containing purified sporozoites routinely remained free from contamination for at least 1 week.

Purified *P. yoelii* sporozoites are fully infectious to mice

Having demonstrated that this method readily produces highly purified *Plasmodium* sporozoites, it was critical to next determine if these sporozoites remained infectious. This was first assessed by testing for any significant loss of infectivity with the rodent-infective *P. yoelii* malaria parasite, as this can be easily measured by the presence of a delay in the appearance of blood stage parasites

Table 1 Measurements of the reduction of bacterial contaminants by penicillin/streptomycin pre-treatment and Accudenz of *P. yoelii* sporozoites

	-	-	+	+	**Accudenz Purification**
	-	+	-	+	**Penicillin/Streptomycin**
Replicate 1	0.84	0.68	0.017 (98.0%)	0.0080 (99.0%)	
Replicate 2	1.2	2.1	0.040 (96.6%)	0.0080 (99.3%)	
Replicate 3	1.0	1.6	0.022 (97.8%)	0.012 (98.8%)	

Salivary gland sporozoites were resuspended in RPMI 1640, left untreated or treated with penicillin/streptomycin, and were left unpurified or were purified on an Accudenz discontinuous gradient. Sporozoites were pelleted and washed in RPMI 1640, and then serially diluted and plated on LB-agar plates. Total colony forming units per sporozoite are listed for three biological replicates. Percent reductions of residual bacterial burdens for purified sporozoites compared to unpurified sporozoites not treated with penicillin/streptomycin are listed in parenthesis.

(termed a "delay in blood stage patency") after the intravenous (iv) injection of salivary gland sporozoites. Using naïve outbred Swiss Webster (SW) mice, 10^3 or 10^4 unpurified or purified sporozoites were iv injected and the time to blood stage patency (defined as >1 Giemsa-positive, infected RBC per 20,000 RBCs on a thin blood smear) was measured. All mice infected with either purified or unpurified sporozoites developed blood stage patency at the same time point after infection (depending on the initial dose), indicating that no detectable loss of sporozoite infectivity (e.g. less than 10-fold) was produced by this purification method nor by sporozoite pre-treatment with penicillin/streptomycin (Table 2).

Purified *P. falciparum* sporozoites have no loss of infectivity *in vitro*

As purification of sporozoites over an Accudenz gradient significantly reduced the contaminating microbial burden found associated with sporozoites, it would also be important to determine if there was any effect upon the infectivity of *P. falciparum* sporozoites for hepatocytes *in vitro*. The human hepatocarcinoma cell line HC-04 was mock infected without sporozoites, or incubated with unpurified or purified sporozoites. Observations of infected hepatocytes by an indirect immunofluorescence assay (IFA) one day post-infection demonstrated no significant difference in parasite morphology with purified or unpurified sporozoites (Figure 2A). Moreover, while wells incubated with unpurified sporozoites readily became contaminated within two to three days, wells that received purified sporozoites remained contamination-free for the complete length of the assay (typically at least one week). Additionally, the fraction of infected hepatocytes was measured shortly after sporozoite infection (90 minutes) by using a recently published flow cytometric assay [23]. This assay allows precise quantifications of infection by analysing large numbers of cells (10^5) for the presence of the most abundant sporozoite protein, circumsporozoite protein (CSP).

Representative plots (Figure 2B) and a normalized graph of duplicate biological replicates (Figure 2C) of mock infected cells, or cells infected with unpurified or purified sporozoites indicate that no significant difference (measured by a student's t-test) in *P. falciparum* sporozoite infectivity exists between purified and unpurified parasites *in vitro*.

Table 2 Measurements of the time to blood stage patency indicate that there is no loss of infectivity with purified *P. yoelii* sporozoites

Type	Replicate #	# Sporozoites injected	# Mice infected	# Mice patent (Day of patency)
Unpurified	1	10,000	5	5 (3d)
	2	10,000	5	5 (3d)
	1	1,000	5	5 (4d)
	2	1,000	5	5 (4d)
Purified	1	10,000	5	5 (3d)
	2	10,000	5	5 (3d)
	1	1,000	5	5 (4d)
	2	1,000	5	5 (4d)

Salivary gland sporozoites were isolated from mosquitoes at 14d post-blood meal and injected intravenously into groups of five naïve Swiss Webster mice in duplicate. Time to blood stage patency (defined as >1 parasite per 20,000 RBCs) was determined microscopically by daily Giemsa-stained thin blood smears, and was identical for sporozoites pretreated with antibiotics or for those left untreated.

Purified *P. vivax* sporozoites retain infectivity *in vitro*

This purification technique was also tested to determine if it could be extended to *P. vivax* sporozoites, another major human-infective malaria species. Salivary gland sporozoites (both CSP210 and CSP247 parasite types [24]) were dissected from infected *Anopheles dirus* mosquitoes by standard methods, and were purified using standard optimized conditions. Consistently 55-69% of the input sporozoites were recovered with a comparable elimination of mosquito debris as with other species. Both the CSP210 and CSP247 types of purified *P. vivax* sporozoites were examined by IFA and found to retain normal morphology and antibody staining patterns (Figure 2D). The ability of purified and unpurified sporozoites to productively infect HC-04 hepatocytes *in vitro* was also tested. Mixed populations of CSP210 and CSP247 types of *P. vivax* sporozoites were allowed to infect and develop for four days, and were then observed by IFA. In both conditions, a comparable number of appropriately developing liver stage parasites were detected (94.2% ± 16.6, Figure 2E). This indicates that as with *P. yoelii* and *P. falciparum*, purified *P. vivax* sporozoites retain their infectivity for hepatocytes. Moreover, it was also observed that Accudenz purification routinely removed all traces of yeast contamination from the sporozoites, whereas unpurified sporozoites lead to the well becoming overgrown with yeast within 4 days. This sporozoite purification method should now enable long-term *in vitro* cultures, especially for the study of hypnozoites, to be routinely maintained contamination-free.

Purified *P. falciparum* sporozoites productively complete liver stage development in a humanized mouse model and transition to a sustainable blood stage infection

It has recently been shown that the FRG NOD huHep mouse, a human-liver chimeric mouse, can support complete *P. falciparum* liver stage development [3]. Additionally, these mice were competent to allow a liver stage to blood stage transition [3]. Since the FRG NOD huHep mouse is immunocompromised, it could be surmised that injection of these mice with purified sporozoites

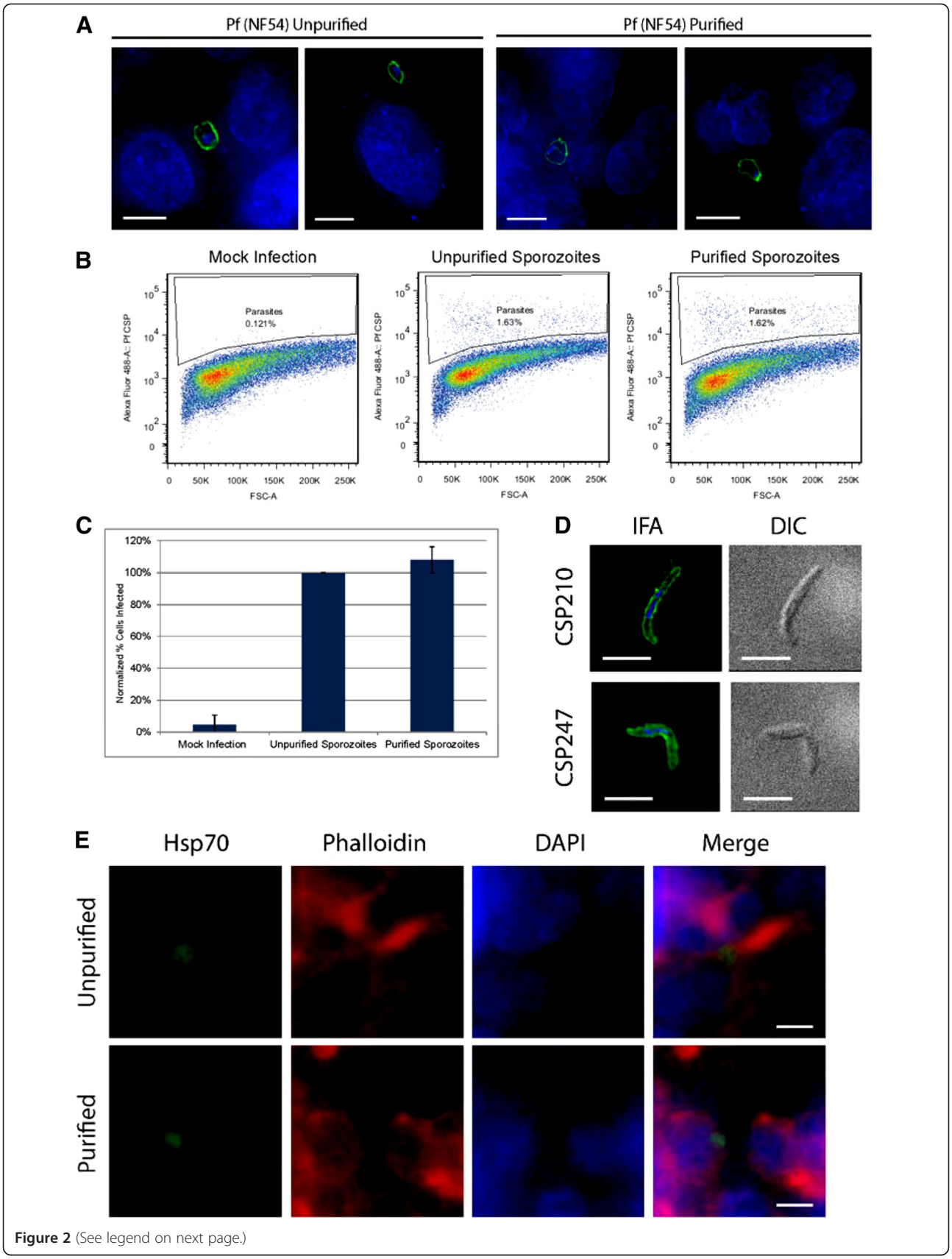

Figure 2 (See legend on next page.)

(See figure on previous page.)
Figure 2 Purified *P. falciparum* and *P. vivax* sporozoites remain infectious *in vitro*. A. HC-04 cells were infected with unpurified or purified P. falciparum sporozoites for 24 hours and were then subjected to an IFA (green: anti-PfCSP (2A10), blue: DAPI). Scale bar is 10 microns. **B**. Representative plots of sporozoite infectivity are provided from flow cytometric measurements of anti-Pf CSP antibody staining of HC-04 cells **C**. A graphical representation of two biological replicates of infections from (B) demonstrates that there is no infectivity defect of purified sporozoites. **D**. Purified *P. vivax* sporozoites were observed by IFA (green: anti-PvCSP 210 or anti-PvCSP247, blue: DAPI). No gross differences in parasite morphology were detected. Scale bar is 5 microns. **E**. HC-04 cells were infected with unpurified and purified *P. vivax* sporozoites for four days and developing liver stage parasites were observed by IFA (green: anti-PbHsp70, red: Phalloidin, blue: DAPI). No gross differences in parasite morphology were detected. Scale bar is 5 microns.

would reduce the bacterial and fungal burden on the mice, which could affect the health of the mice and possibly liver stage development. Therefore, two FRG NOD huHep mice were injected intravenously with 3×10^6 purified *P. falciparum* sporozoites. Mice were injected with human red blood cells as previously described and the mice were euthanized seven days after sporozoite infection [3]. The blood removed from the mice was transitioned into a *P. falciparum* asexual culture and indeed, a healthy *in vitro* asexual culture of transitioned *P. falciparum* blood stages was achieved. The livers were also removed from the euthanized mice, fixed and subjected to an IFA as previously described [25]. Using antibodies to parasite merozoite surface protein 1 (MSP1) and human fumaryl acetoacetate hydrolase (FAH) (present only in the human hepatocytes within the FRG NOD huHep mouse liver), as expected, mature liver stages were observed to be present in the livers of the inoculated mice (Figure 3). Thus, the purified *P. falciparum* sporozoites appear to behave no differently to the unpurified *P. falciparum* sporozoite in this *in vivo* assay of liver stage development and *ex vivo*/*in vitro* assay of liver stage to blood stage transition.

Discussion

This work describes and demonstrates that an Accudenz density gradient purification method of *Plasmodium* sporozoites produces parasites that remain viable and infective. A discontinuous gradient approach was favored over using a continuous gradient, as the former also acts to localize and concentrate sporozoites at the interface of the light and dense layers. This approach thus removes the requirement to collect and assess multiple samples for the presence of sporozoites, which is needed when using continuous gradients as sporozoites distribute throughout a larger portion of the gradient [26,27]. Moreover, this rapid and technically simple method successfully removes mosquito debris and lipids, as well as contaminating bacterial and fungal contaminants. Importantly, this is accomplished in the absence of serum or any serum components, which are known to induce sporozoite secretion and can cause immune responses in mice. Lastly, this approach was successfully scaled up and allowed the recovery of $>10^7$ sporozoites from a single density gradient. This purification method was validated for both rodent-infective and human-infective malaria species, as purified sporozoites perform identically to unpurified sporozoites by all *in vitro* and *in vivo* assays used to date.

Of special interest was the implementation of these purified sporozoites with humanized mouse models. Injection of purified sporozoites into the immunocompromised FRG NOD huHep mouse could be most beneficial due to the removal of contaminating bacteria and fungi which could cause inflammatory responses in

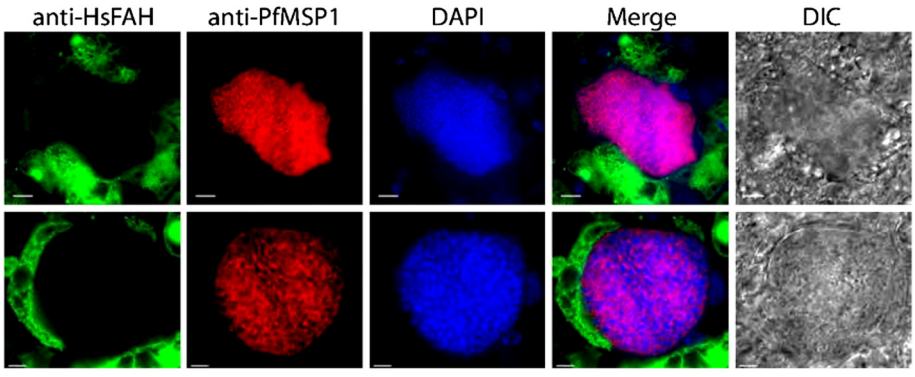

Figure 3 Purified *P. falciparum* sporozoites remain infectious to a humanized mouse. Two representative IFA panels of late liver stage *P. falciparum* parasites are shown using antibodies to human FAH (green), PfMSP1 (red) or with DAPI (blue). These images indicate that purified sporozoites are able to fully progress through liver stage development. Scale bar is 10 microns.

the mice and even an uncontrollable infection leading to their death. Inflammation could cause the death of *P. falciparum* liver stage parasites early after infection. If comparative studies were to be made on liver stage infectivity in the FRG huHep mouse model, purification of sporozoites would be vital to exclude the differing levels of microbial burden between sporozoite samples.

Also, because this method completely eliminated yeast contamination of *P. vivax* sporozoites, long-term *in vitro* assays should no longer be impacted by this contaminant. This is of particular interest for investigations of liver stage development of *P. vivax*. Not only will this enable easier characterization of the actively growing forms of the liver stage parasite, which take approximately 8 days to fully develop *in vivo*, but perhaps also studies of the poorly characterized "dormant forms" (termed hypnozoites) of the parasite. Hypnozoites are a major reservoir of viable parasites in infected individuals, which can persist for years and likely substantially hinder efforts to eradicate the disease.

In addition to the infectivity assays described here, it is anticipated that this purification method will greatly facilitate biochemical and molecular biological investigations that were hindered by the high amounts of microbial contamination and/or mosquito debris. For instance, previously reported proteomic efforts of sporozoites have been limited by contaminating mosquito proteins, which required large numbers of mass spectrometric runs to identify hundreds of parasite proteins. In contrast, recent proteomic efforts with purified sporozoites have overcome this limitation, producing the most comprehensive proteomes of this stage (~1,900-2,000 proteins), with >86% of proteins identified by multiple unique peptide hits (Lindner and Swearingen *et al.* submitted). Further investigations of sporozoite biology will no doubt benefit from these approaches as well.

Lastly, with the development of live attenuated sporozoites as potential malaria vaccines come several technical hurdles should a lead candidate be identified in clinical trials for large-scale implementation. One such hurdle is the effective removal of contaminating mosquito debris associated with the sporozoites. This density gradient purification method should meet several of the metrics required for this process (e.g. purity, infectivity, scalability), and may prove useful to streamline these efforts. When combined with aseptic mosquito rearing techniques, this method could make syringe administration of live attenuated sporozoite immunizations practical. All told, this novel, cross-species purification method holds great promise for accelerating both basic research of sporozoite biology and translational efforts to use the sporozoite medically.

Conclusions

Described in this study is a discontinuous density gradient method that rapidly and effectively purifies malaria sporozoites by greatly reducing contaminating mosquito debris and microbial burdens associated with parasite isolation. Moreover, the viability of these sporozoites was confirmed, and the application of this approach to commonly used *in vitro* and *in vivo* assays was demonstrated. Large-scale preparations of sporozoites purified by this approach will allow for enhanced *in vitro* infections, proteomics, and biochemical characterizations. Finally, this purification method, in conjunction with aseptic mosquito rearing techniques, will support production of live attenuated sporozoites that will be suitable for vaccination.

Additional files

Additional file 1: Representative pre- and post-purification sporozoite numbers tested in optimal conditions.

Additional file 2: The composition of the solvent used to produce the Accudenz gradient greatly affects sporozoite recovery.

Additional file 3: Representative pre- and post-purification sporozoite numbers tested with different accudenz concentrations.

Additional file 4: The relative centrifugal force applied to the Accudenz gradient greatly affects sporozoite recovery.

Abbreviations

BSA: Bovine Serum Albumin; IFA: Indirect Immunofluorescence Assay; FAH: Fumaryl Acetoacetate Hydrolase; CSP: Circumsporozoite Protein; MSP1: Merozoite Surface Protein 1; FITC: Fluorescein isothiocyanate; DAPI: 4′,6-Diamidino-2-Phenylindole; DIC: Differential Interference Contrast; PBS: Phosphate Buffer Saline; CFUs: Colony Forming Units; SW: Swiss Webster.

Competing interests

A provisional patent has been filed on this purification method on August 1st, 2012 (US Patent Application Number 61678541).

Authors' contributions

Developed purification method: MK, SEL; Assessed *P. yoelii* purification and infectivity: MK, MF; Assessed *P. falciparum* purification and infectivity: AMV, NR, PM, SEL; Assessed *P. vivax* purification and infectivity: RP, RB NY and SEL; Assessed reductions of microbial burden: MF; Provided project supervision: MP, JS, SHK, JCCH, SEL; Wrote the Manuscript and Analysed the Data: MK, AMV, JCCH, SEL. All authors read and approved the final manuscript.

Acknowledgements

We would like to thank Will Betz and Heather Kain for insightful discussions and technical assistance in developing this method. This work was supported by: Seattle Biomedical Research Institute's Global Health Biotechnology Center to J.C.C.H., Thailand Research Fund (TRF) and National Science and Technology Development Agency (NSTDA) to M.P., CDMRP Peer Reviewed Medical Research Program to J.S., US. Department of Defense Grants to J.S. and S.K. (W81XWH--11--2--0184), and a Ruth L. Kirschstein National Research Service Awards (F32GM083438) to S.E.L.

Author details

[1]Center for Mosquito Production and Malaria Infection Research, Seattle Biomedical Research Institute, 307 Westlake Avenue North, Suite 500, Seattle, WA 98109, USA. [2]Malaria Program, Seattle Biomedical Research Institute, 307 Westlake Avenue North, Suite 500, Seattle, WA 98109, USA. [3]Mahidol Vivax Research Center, Faculty of Tropical Medicine, Mahidol University, Bangkok,

Thailand. [4]Department of Microbiology, Faculty of Science, Mahidol University, Bangkok, Thailand. [5]Department of Global Health, University of Washington, Seattle, WA 98195, USA.

Received: 11 September 2012 Accepted: 21 November 2012
Published: 17 December 2012

References

1. Lindner SE, Miller JL, Kappe SH: **Malaria parasite pre-erythrocytic infection: preparation meets opportunity.** *Cell Microbiol* 2012, **14:**316–324.
2. Sacci JB Jr, Alam U, Douglas D, Lewis J, Tyrrell DL, Azad AF, Kneteman NM: ***Plasmodium falciparum*** **infection and exoerythrocytic development in mice with chimeric human livers.** *Int J Parasitol* 2006, **36:**353–360.
3. Vaughan AM, Mikolajczak SA, Wilson EM, Grompe M, Kaushansky A, Camargo N, Bial J, Ploss A, Kappe SHI: **Complete** ***Plasmodium falciparum*** **liver stage development in liver-chimeric mice.** *J Clin Invest* 2012, in press.
4. Carlton JM, Angiuoli SV, Suh BB, Kooij TW, Pertea M, Silva JC, Ermolaeva MD, Allen JE, Selengut JD, Koo HL, Peterson JD, Pop M, Kosack DS, Shumway MF, Bidwell SL, Shallom SJ, van Aken SE, Riedmuller SB, Feldblyum TV, Cho JK, Quackenbush J, Sedegah M, Shoaibi A, Cummings LM, Florens L, Yates JR, Raine JD, Sinden RE, Harris MA, Cunningham DA, *et al*: **Genome sequence and comparative analysis of the model rodent malaria parasite** ***Plasmodium yoelii yoelii*****.** *Nature* 2002, **419:**512–519.
5. Florens L, Washburn MP, Raine JD, Anthony RM, Grainger M, Haynes JD, Moch JK, Muster N, Sacci JB, Tabb DL, Witney AA, Wolters D, Wu Y, Gardner MJ, Holder AA, Sinden RE, Yates JR, Carucci DJ: **A proteomic view of the** ***Plasmodium falciparum*** **life cycle.** *Nature* 2002, **419:**520–526.
6. Lasonder E, Janse CJ, van Gemert GJ, Mair GR, Vermunt AM, Douradinha BG, van Noort V, Huynen MA, Luty AJ, Kroeze H, Khan SM, Sauerwein RW, Waters AP, Mann M, Stunnenberg HG: **Proteomic profiling of Plasmodium sporozoite maturation identifies new proteins essential for parasite development and infectivity.** *PLoS Pathog* 2008, **4:**e1000195.
7. Mack SR, Vanderberg JP, Nawrot R: **Column separation of** ***Plasmodium berghei*** **sporozoites.** *J Parasitol* 1978, **64:**166–168.
8. Kebaier C, Vanderberg JP: **Initiation of Plasmodium sporozoite motility by albumin is associated with induction of intracellular signalling.** *Int J Parasitol* 2010, **40:**25–33.
9. Vanderberg JP: **Studies on the motility of Plasmodium sporozoites.** *J Protozool* 1974, **21:**527–537.
10. Beaudoin RL, Strome CP, Mitchell F, Tubergen TA: ***Plasmodium berghei*****: immunization of mice against the ANKA strain using the unaltered sporozoite as an antigen.** *Exp Parasitol* 1977, **42:**1–5.
11. Pacheco ND, Strome CP, Mitchell F, Bawden MP, Beaudoin RL: **Rapid, large-scale isolation of** ***Plasmodium berghei*** **sporozoites from infected mosquitoes.** *J Parasitol* 1979, **65:**414–417.
12. Agnandji ST, Lell B, Soulanoudjingar SS, Fernandes JF, Abossolo BP, Conzelmann C, Methogo BG, Doucka Y, Flamen A, Mordmuller B, Issifou S, Kremsner PG, Sacarlal J, Aide P, Lanaspa M, Aponte JJ, Nhamuave A, Quelhas D, Bassat Q, Mandjate S, Macete E, Alonso P, Abdulla S, Salim N, Juma O, Shomari M, Shubis K, Machera F, Hamad AS, Minja R, RTS, S Clinical Trials Partnership, *et al*: **First results of phase 3 trial of RTS, S/AS01 malaria vaccine in African children.** *N Engl J Med* 2011, **365:**1863–1875.
13. Epstein JE, Tewari K, Lyke KE, Sim BK, Billingsley PF, Laurens MB, Gunasekera A, Chakravarty S, James ER, Sedegah M, *et al*: **Live attenuated malaria vaccine designed to protect through hepatic CD8(+) T cell immunity.** *Science* 2011, **334:**475–480.
14. Vaughan AM, Wang R, Kappe SH: **Genetically engineered, attenuated whole-cell vaccine approaches for malaria.** *Hum Vaccin* 2010, **6:**107–113.
15. Nussenzweig RS, Vanderberg J, Most H, Orton C: **Protective immunity produced by the injection of x-irradiated sporozoites of** ***Plasmodium berghei*****.** *Nature* 1967, **216:**160–162.
16. Butler NS, Vaughan AM, Harty JT, Kappe SH: **Whole parasite vaccination approaches for prevention of malaria infection.** *Trends Immunol* 2012, **33:**247–254.
17. Butler NS, Schmidt NW, Vaughan AM, Aly AS, Kappe SH, Harty JT: **Superior antimalarial immunity after vaccination with late liver stage-arresting genetically attenuated parasites.** *Cell Host Microbe* 2011, **9:**451–462.
18. Sattabongkot J, Maneechai N, Phunkitchar V, Eikarat N, Khuntirat B, Sirichaisinthop J, Burge R, Coleman RE: **Comparison of artificial membrane feeding with direct skin feeding to estimate the infectiousness of** ***Plasmodium vivax*** **gametocyte carriers to mosquitoes.** *AmJTrop Med Hyg* 2003, **69:**529–535.
19. Gantt SM, Myung JM, Briones MR, Li WD, Corey EJ, Omura S, Nussenzweig V, Sinnis P: **Proteasome inhibitors block development of Plasmodium spp.** *Antimicrob Agents Chemother* 1998, **42:**2731–2738.
20. Sattabongkot J, Yimamnuaychoke N, Leelaudomlipi S, Rasameesoraj M, Jenwithisuk R, Coleman RE, Udomsangpetch R, Cui L, Brewer TG: **Establishment of a human hepatocyte line that supports in vitro development of the exo-erythrocytic stages of the malaria parasites** ***Plasmodium falciparum*** **and** ***P. vivax*****.** *AmJTrop Med Hyg* 2006, **74:**708–715.
21. Miller JL, Harupa A, Kappe SH, Mikolajczak SA: ***Plasmodium yoelii*** **macrophage migration inhibitory factor is necessary for efficient liver-stage development.** *Infect Immun* 2012, **80:**1399–1407.
22. Tsuji M, Mattei D, Nussenzweig RS, Eichinger D, Zavala F: **Demonstration of heat-shock protein 70 in the sporozoite stage of malaria parasites.** *Parasitol Res* 1994, **80:**16–21.
23. Kaushansky A, Rezakhani N, Mann H, Kappe SH: **Development of a quantitative flow cytometry-based assay to assess infection by** ***Plasmodium falciparum*** **sporozoites.** *Mol Biochem Parasitol* 2012, **183:**100–103.
24. Arnot DE, Stewart MJ, Barnwell JW: **Antigenic diversity in Thai** ***Plasmodium vivax*** **circumsporozoite proteins.** *Mol Biochem Parasitol* 1990, **43:**147–149.
25. Vaughan AM, O'Neill MT, Tarun AS, Camargo N, Phuong TM, Aly AS, Cowman AF, Kappe SH: **Type II fatty acid synthesis is essential only for malaria parasite late liver stage development.** *Cell Microbiol* 2009, **11:**506–520.
26. Chen DH, Schneider I: **Mass isolation of malaria sporozoites from mosquitoes by density gradient centrifugation.** *Proc Soc Exp Biol Med* 1969, **130:**1318–1321.
27. Krettli A, Chen DH, Nussenzweig RS: **Immunogenicity and infectivity of sporozoites of mammalian malaria isolated by density-gradient centrifugation.** *J Protozool* 1973, **20:**662–665.

doi:10.1186/1475-2875-11-421
Cite this article as: Kennedy *et al.*: A rapid and scalable density gradient purification method for *Plasmodium* sporozoites. *Malaria Journal* 2012 **11**:421.